Dear Editor,

We have carefully gone through the comments of both reviewers and have made according changes to address these issues. The English language was improved and other necessary changes were made to improve the manuscript. Please see out point-by-point response to the reviewers and the revised manuscript as follows.

Response to reviewer #1

Thank you for your comments and suggestions. We have addressed all the issues that were raised and have made changes accordingly. We have also improved the English language and made other necessary changes. Please see our point-by-point response below.

General comments

This paper explores the factors driving the observed ozone changes at Mt. Waliguan Observatory (WLG) using basically backward trajectory analysis and chemistry-climate model hindcast simulations (GFDL-AM3). The paper also deals links of ozone variability at WLG with the QBO, NAO, the East Asian summer monsoon (EASM), and the sunspot cycle. Although the paper addresses very interesting topics (probably too many issues in a single paper), complementary to that addressed in the companion paper (Xu et al., 2016), in a region of enormous interest such as the Tibetan Plateau, and using valuable data from a global GAW station such as WLG, the paper suffers from significant weaknesses that must be addressed withmore credible and robust approaches.

The most important drawbacks are of methodological nature, and are briefly discussed below.

Specific comments:

1) The approach used for the backtrajectories dataset and climatology does not seem the most advisable to distinguish between ozone long-range transport from ozone produced by regional precursors. The use of the directions of only start-points (origin) of the trajectories into bins of 45°is a very weak approximation. Air masses normally move among sectors along their entire trajectory (especially those of 7 days duration). So, it seems more reasonable to use some index accounting for the time of residence of

the trajectory in each geographical sector. Bins of 45°seem to be too narrow for 7-day backtrajectories for which a great error / uncertainty in the geographical determination is associated.

RE: It is true that trajectories usually cross various sectors, which is why we analyzed both the 7day and 24h trajectory directions. The aim of using 7day direction is to look at the overall air-mass origin, while the 24h directions can show whether the air mass has changed its course before arriving at WLG. To better account for the other geographical sectors that the long trajectories might pass on their paths, instead of the direction of the t=-24h and t=-168h trajectory start-points, we now use the vector mean direction during the first 24h and 168h for each trajectory. The occurrence frequencies in each direction bin were recalculated and results turned out to be quite similar to that in manuscript.

We also took the advice of the reviewer and made a comparison using the PBL and free tropospheric residence time to do the analysis in Figure 2 and Table 1 (see Figs.1-2). Results turned out to be similar to those based on start-points. The use of the residence time has its advantage and disadvantage. We not only want to know where the air mass has been, but also when the air mass has been there, which is why we use the direction of the trajectory track points.

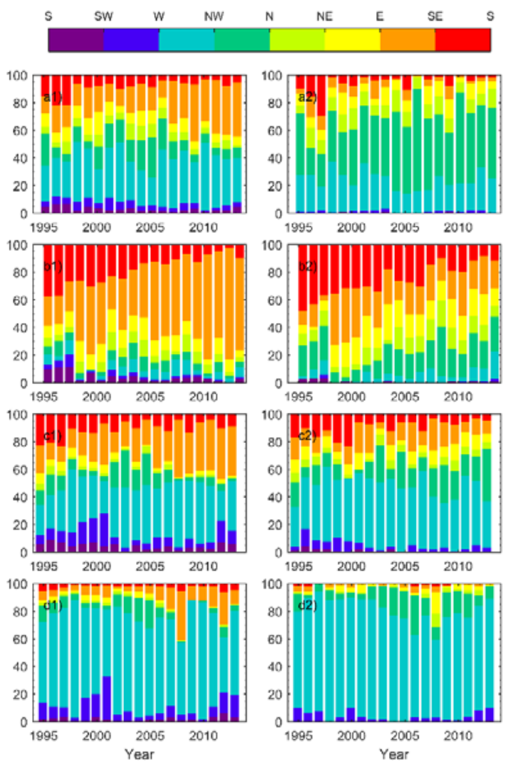

Figure 1 The average trajectory direction occurrence frequencies in a) spring, b) summer, c) autumn and d) winter of 1) t<24h and 2) t<168h.

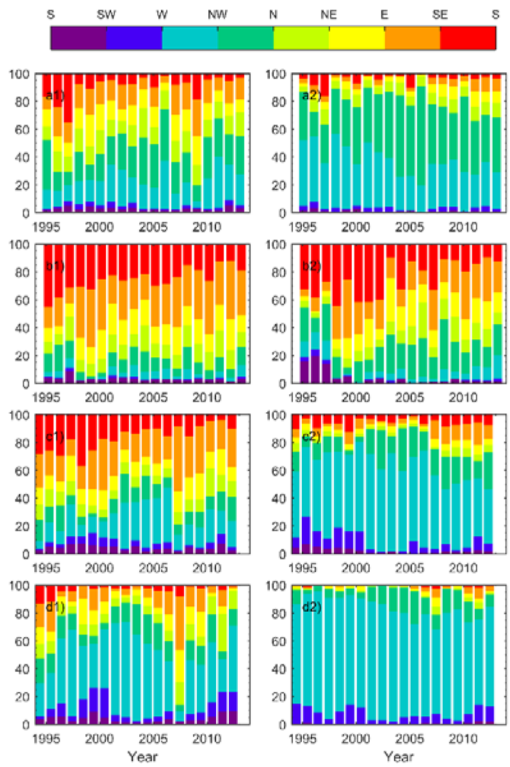

Figure 2 The 1) PBL and 2) free tropospheric trajectory residence time occurrence frequencies in a) spring, b) summer, c) autumn and d) winter.

We have redrawn Figures 2 and 3 using the statistics of average trajectory directions and updated the values in Tables 1 and 3 in the revised manuscript. We have added Figure S1 in the supplement to schematically show the way of obtaining average directions of the 168h and 24h trajectories. The 2nd paragraph in Section 2.2 has been modified as follows:

"To study the overall air-mass origin and to determine whether the air-mass collected pollutants from the nearby cities, the average direction of each trajectory relative to the WLG station is calculated both for the 168h and for the 24h trajectory (Figure S1). The 168h and 24h average directions relative to WLG are clustered into bins of 45° and the occurrence frequency in each bin is calculated."

2) The use of 1-day trajectories to estimate the impact of regional ozone sources and those of 7-day path (very long) as representative of ozone long-range transport are not well understood and not sufficiently justified. In fact, when the 1994-2013 climatology of air mass origins at WLG in the PBL and FT are depicted (Figure 1), the main patterns in the distribution of the air masses frequency is quite similar for both regions (PBL and FT). Indeed, that means that the discrimination between PBL and FT air masses has not been satisfactorily achieved.

RE: As already pointed out in previous studies (Ma et al., 2002; Xu et al., 2016), during daytime and nighttime the WLG site is mainly influenced by air from the PBL and FT, respectively, causing a daytime minimum and a nighttime maximum of the ozone concentration. And ozone in daytime and nighttime showed different trends, particularly in summer when daytime and nighttime ozone showed respective trends of 0.07 ppb/yr ($p=0.41$) and 0.22 ppb/yr ($p=0.04$) (see Xu et al., 2016). To understand this difference, we think it is necessary to investigate the impacts of air masses from the PBL and FT separately. Observations at WLG, a high mountain site (3.8km asl) with very little local emissions represent the large-scale atmospheric conditions. Even the PBL air mass should mostly be representing the background condition. In addition, air masses in the PBL and FT often move in similar directions, particularly when they are driven by large-scale circulations. These explain why there are similarities between the PSCF of PBL and FT air masses. Nevertheless, there are some differences between the PSCF of PBL and FT air masses, for example, the high PSCF of FT air masses in the northeast sector (Figs. 1a2 and 1b2), the high PSCF of PBL air masses over Nepal and Northern India (Fig. 1d1), the much larger extension for the PSCF of FT air masses than that of PBL air masses, etc. Therefore, the separation of the PBL and FT air masses does provide some more details about the potential sources of ozone at WLG.

We have revised the last paragraph of Section 2.2 as " Since ozone is a trace gas with a distinct vertical distribution, it is not enough to just determine the direction from which the air-mass came. The height of the air-mass is also crucial for interpreting the measured ozone concentrations. As discussed in previous studies (Ma et al., 2002;Xu et al., 2016), the WLG site is predominantly influenced by air from the planetary boundary layer (PBL) during daytime and from the free troposphere (FT) during nighttime, with ozone concentrations showing a daytime minimum and a nighttime maximum. Daytime and nighttime ozone at WLG show different trends, particularly in summer (0.07±0.18 ppb year-1for daytime and 0.22±0.20 ppb year-1 for nighttime; Xu et al., 2016). To investigate the impacts of air masses from the PBL and FT separately, the PBL height, which can be added in the Hysplit model along the trajectories, is used to judge whether the air-mass that arrived at WLG is representing the PBL or the FT. PBL trajectory sections are defined as the part of the trajectory that was continuously within the PBL before arriving at the station. Thus, PBL trajectory sections are usually close to the station. When the trajectory height exceeds that of the PBL, the rest of the trajectory is taken as the FT trajectory section. FT trajectory sections can also be close to the station, representing subsiding air from the FT near the station, however, most of them are located far away from the station."

Ma, J., Tang, J., Zhou, X., and Zhang, X.: Estimates of the Chemical Budget for Ozone at Waliguan Observatory, Journal of Atmospheric Chemistry, 41, 21-48, 10.1023/A:1013892308983, 2002.

Xu, W., Lin, W., Xu, X., Tang, J., Huang, J., Wu, H., and Zhang, X.: Long-term trends of surface ozone and its influencing factors at the Mt Waliguan GAW station, China – Part 1: Overall trends and characteristics, Atmospheric Chemistry and Physics, 16, 6191-6205, 10.5194/acp-16-6191-2016, 2016.

3) Nothing is said about the methodology used to determine the critical height of the back-trajectory in relation to the PBL height for each point of the airmass trajectory.

RE: The Hysplit model we used can add meteorology output (such as the PBL height, PBLH) along trajectories. The PBLH values along the trajectories are then compared with the trajectory height data, to determine whether the air mass is within the PBL or in the free troposphere. We have clarified this in Sect. 2.2 in the revised manuscript:

"To investigate the impacts of air masses from the PBL and FT separately, the PBL height, which can be added in the Hysplit model along the trajectories, is used to judge whether the air-mass that arrived at WLG is representing the PBL or the FT."

4) In page 8 Lines 5-13; The results are inconsistent and, in some cases, contradictory. Section 3.1 is plenty of inconsistencies such as the following in page 8 lines 16-18:"The t=-168h trajectory direction provides us information on the overall origin of the air-mass, while the trajectory direction calculated for t=-24h should be able to reveal if the airmass passed over nearby polluted regions before arriving at the station", while in lines 26-27, is said: "From the t=-168h trajectory direction frequencies, it can be seen that the anthropogenic influence is negligible in all seasons"

RE: Page 8 lines 5-13 has been modified as:

"During summer, when air-masses from the east occur most frequently(as will be shown in Figure 2), the entire eastern sector reveals low values of high ozone PSCF, hardly showing signs of anthropogenic influence on WLG. In other words, most air-masses from the east in summer are not associated with high ozone. High ozone PSCF occurs dominantly with trajectories from the NW or N. In autumn, in addition to NW or N, significant contributions of trajectories from the E, SE and S can also be discerned in the PBL trajectories, which suggest that high ozone is linked to air-masses coming from western China, central China and the northeastern part of the Tibetan Plateau, the southwestern part of Gansu province as well as north of China (east Mongolia). In the FT trajectories, high ozone concentrations were mainly linked to air-masses from western and central China. In addition, air masses over Gansu province, part of the Sichuan province and some parts of Russia also show high PSCF. In winter, the PBL trajectories show high ozone PSCF mainly in the NW sectors, however, the SW and N-NE sectors also revealed scattered high PSCF values (over some parts of Nepal, Northern India, Mongolia and Inner Mongolia). Aside from the NW sector, the FT trajectories display significantly high PSCF in the NE sector in the western half of Inner Mongolia."

Page 8 lines 26-27 has been rephrased as:

"From the 168h average trajectory direction frequencies, it can be seen that the anthropogenic influence is strongest in summer, followed by autumn, and almost negligible in winter."

5) Analyzing 24h and 7-day trajectories, how it is possible to say that "....with PBL airmasses dominating during the day and FT air-masses during the night, which led to a clear diurnal variation of high nighttime and low daytime ozone concentrations". This situation, which is very realistic, probably overturns all the assumptions made for the establishment of the methodology of FT and PBL backtrajectories.

RE: The conclusion "....with PBL air-masses dominating during the day and FT air-masses during the night, which led to a clear diurnal variation of high nighttime and low daytime ozone concentrations" was not drawn from the analysis of 24h and 7-day trajectories, it is the finding in studies by Ma et al. (2002) and Xu et al. (2016).

This conclusion is not in contradiction with the methodology used for the backtrajectories. Free-tropospheric air masses over WLG during nighttime might have come from the PBL of upwind locations, whereas PBL air masses during daytime might have also come from the free troposphere. The time of the day cannot provide enough information on the overall characteristics of the air mass, which is why we seek the aid of backtrajectories.

6) All of Section 3.1 should be reviewed using a consistent methodology.

RE: We thank the reviewer for the suggestion. We have carefully gone through and revised this section.

7) In Section 3.2 is difficult to support a joint analysis of point observations in WLG with simulations of GFDL-AM3 with a resolution of 200X200 km2.

RE: We respectfully disagree with the reviewer for this statement. Observations at the 3.8km altitude of WLG in the remote atmosphere of the Tibetan Plateau are representative of large-scale conditions that a 200x200 km^2 global model is expected to resolve. It is appropriate to compare observations at WLG with the model simulations sampled at 700 hPa. We have clarified this in Section 2.5 in the revised manuscript:

"The long-term ozone observational record at WLG provides an important test for the GFDL-AM3 model to represent the key processes driving year-to-year variability and trends of tropospheric ozone in the remote atmosphere of the Tibetan Plateau. For comparison with measurements at the 3.8 km altitude of WLG, the model is sampled at the grid box containing WLG and at the 700 hPa layer. This approach is appropriate because observations at Mt. WLG are representative of large-scale conditions with little influence from local urban emissions."

8) I do not see GFDL-AM3 captures the inter-annual variation of observed surface ozone anomaly, with the correlation coefficient ranging from 0.5 to 0.7 for spring, summer and autumn, as it is said.

RE: We have rephrased the discussion in the revised manuscript:

"GFDL-AM3 captures <u>some</u> inter-annual variation of observed surface ozone anomaly, with the correlation coefficient ranging from 0.5 to 0.7 for spring, summer and autumn. The correlations between the observed and modelled ozone anomaly are significant at the 90% confidence level in all seasons except winter. The model fails to reproduce the small observed ozone variability in winter."

9) The sentence "A stratospheric ozone tracer implemented in GFDL-AM3 (O3Strat; Sect. 2.5) indicates that the stratospheric influence can explain 23% (r=0.48) of the observed ozone interannual variability in spring (Fig.4a) but contributes little to observed variability in other seasons" is quite speculative.

RE: We have clarified the credibility of AM3 O3Strat to infer stratospheric influence, based on prior process-oriented evaluation with intensive field measurements available over the western United States:

"A stratospheric ozone tracer implemented in GFDL-AM3 (O_3Strat; Sect. 2.5) enables us to quantify the stratospheric contribution to variability and trends of ozone measured at WLG. Prior analysis of daily ozonesondes, water vapour, and lidar measurements indicates that variability in AM3 O_3Strat represents the episodic, layered structure of ozone enhancements in the free troposphere consistent with the observed characteristics of deep stratospheric intrusions (Lin et al., 2012b; Lin et al., 2015a; Langford et al., 2015). Sampling AM3 O_3Strat at WLG indicates that the stratospheric influence can explain 23% (r=0.48) of the observed ozone interannual variability at WLG in spring

(Fig.4a) but contributes little to observed variability in other seasons (r<0.1; Fig.4b-d)."

This conclusion is further supported by our model sensitivity simulations with time-varying and constant anthropogenic emissions (Fig.6 and related discussions in the text).

10) The trends on frequency of trajectories, by using only the geographical sector, where the starting point is 7 days before, it could give misleading results. However, potential trends in backtrajectories frequency constitutes a key point in the analysis and assessments of the paper.

RE: As mentioned in the response to comment 1, the trajectory directions of t=-168h have been replaced by the average directions during the traevelling, which should be more representative of the geographical sectors on the pathways of the trajectories. The trajectory frequency trends were recalculated and results turned out to be similar with those in the previous manuscript.

11) EACOt (page 11 Line 9) does not seem to have any bearing on the changing trend of ozone, according to Figure 5 and 6.

RE: We are not sure what the reviewer means. Emissions of EACOt do not change over time. We are using these COt tracers to bin modelled ozone according to the dominant influence of different continental air regimes in the BASE simulation, in which emissions of ozone precursors change over time. That sentence is rephrased:

"To evaluate the effect of pollution transport from Southeast and East Asia, we filter ozone in the AM3 BASE simulation with the East Asian CO tracer (EACOt; see Sect.2.5)."

12) In sections 3.2 and 3.3., it is difficult to understand why the authors have not used in-situ ancillary observations to distinguish the impact of direct ozone transport from that formed from precursors, and ozone from upper troposphere from pollution-derived ozone. Authors have used in a very limited way carbon monoxide (CO) in Section 3.3 (this does not appear in section 2.1 Data) but they have not crossed O3 and CO data to discriminate the O3 origin, but they have used the CO and backtrajectories trends (??). Authors might have also used water vapour mixing-ratio or absolute humidity to discriminate high ozone from upper levels. On the contrary, the authors have used rough simulations whose uncertainty is not known.

RE: The CO data used in the manuscript are monthly CO data from flask sampling and analysis. The time resolution of the data has limited its use. High resolution CO data would be much better to distinguish ozone measurements impacted by anthropogenic emissions and from those impacted by upper tropospheric/lower stratospheric air. Indeed, based on shorter period observations, Wang et al. (2006) were able to identify ozone measurements impacted by upper tropospheric/lower stratospheric air using the negative correlation between CO and ozone. In-situ observations of CO have been attempted at WLG using different techniques. Unfortunately, the coverage of qualified data is poor due to various technical problems. Therefore, we cannot use in-situ CO measurements in the analysis of the long-term ozone measurements (1994-2013). However, some reliable in-situ measurements of CO are available for recent years. We used these CO data to check the reliability of the model and found a significant correlation ($r=0.48$, $p<0.01$) between the measured CO and the modeled East Asian COtracer, which proves that the model is able to identify pollution transport from East Asia.

We tried using water vapor data to identify air mass from upper layers. However, the RH data from the WLG station show significant, uncorrectable biases during the period of 2004-2013, which influence the credibility of the analysis outcome. Hence, this part of the study was not brought into the manuscript.

We have added in Section 2.1 "We also use monthly CO data based on weekly flask sampling at 5 m above ground, obtained from the World Data Centre for Greenhouse Gases (http://ds.data.jma.go.jp/gmd/wdcgg/wdcgg.html), to infer changes of regional emissions near WLG. Using high frequency (e.g., minutes) in-situ observations of CO and water vapour would be ideal to diagnose the presence of stratospheric versus anthropogenic influences, however, continuous high-quality data are not available at WLG due to various technical challenges." in the revised manuscript.

Wang, T., Wong, H. L. A., Tang, J., Ding, A., Wu, W. S., and Zhang, X. C.: On the origin of surface ozone and reactive nitrogen observed at a remote mountain site in the northeastern Qinghai-Tibetan Plateau, western China, Journal of Geophysical Research: Atmospheres, 111,25 D08303, 10.1029/2005JD006527, 2006.

13) In section 3.3, again the methodological approach used in the backtrajectory sectors might result in wrong results since air masses pass over different ozone precursors sources along their paths. Considering the start-point (origin) of the trajectory is too simplistic.

RE: Indeed, if we want to consider all the sectors on the trajectory pathway, the use of trajectory directions has its limitations. However, we do not know the actual 4D distribution of ozone, hence considering all the sectors of the trajectory has no sense. Based solely on the ozone observations at WLG, using the backtrajectories to filter out air masses that might be influenced by anthropogenic emissions is the most direct method. As an improvement to the methodology, we already replaced the trajectory directions calculated from the start-point with average trajectory directions, which should be more representative of all the sectors on the trajectories. Results turned out to be quite similar with the previous ones.

14) In section 4.1 (Stratosphere-to-troposphere transport and jet characteristics) the methodology approach is also quite weak. The authors use model simulations, when they could also/instead in-situ water vapour mixing ratio at WLG to discriminate upper troposphere (rather than stratospheric air masses) with the help of PV at a near WLG level . Unfortunately, the example given for March 30, 2012 is also not good since the

values of O3 and PV do not correspond to upper troposphere air masses (and even less to stratospheric air masses). The 7 PVU at 250 hPa does not justify the impact of upper tropospheric air masses to WLG.

RE: We tried using water vapor data to identify air mass from upper layers, however, the RH data at the WLG station show significant errors during the period of 2004-2013, which influence the credibility of the analysis outcome. Hence, this part of the study was not brought into the manuscript. We clarify this in Sect. 4.1 of the revised manuscript:"Due to the transient, localized nature of stratospheric intrusions, diagnosing the presence of stratospheric influence in near-surface ozone requires precise, high-frequency (a few minutes), and co-located measurements of ozone, CO, water vapor and surface wind gust at remote sites (see Langford et al., 2015). These measurements are not available at WLG. Thus, we rely on a global model that has been previously shown to be able to represent deep stratospheric intrusions".

In the example given for March 30, 2012, we did not solely look at the PV at 250hPa over WLG to prove that it is an STT event. We made slight changes to Figure 12 to clarify the case (see Figure 3). 500hPa Geopotential height, the U wind cross-section were added and we have changed the color scales in Figure 12c-d to more clearly show this event of stratospheric intrusion. The isentropic PV filament is clearly depicted in Figure 3b. The high PV airmass was transported south to the midlatitudes by the strong northerly winds ahead of the ridge and behind the trough. The easterly airflow between 450hPa and 250hPa north of the fold and the subtropical jet south of the fold have brought the high PV airmass to the west to WLG (Figure 3c). Figure 3c clearly showing a tropopause fold over WLG, The high PV reached down to the surface layer at WLG station and correspondingly the transport of stratospheric high O_3 down to the surface can be detected in Figure 3d.

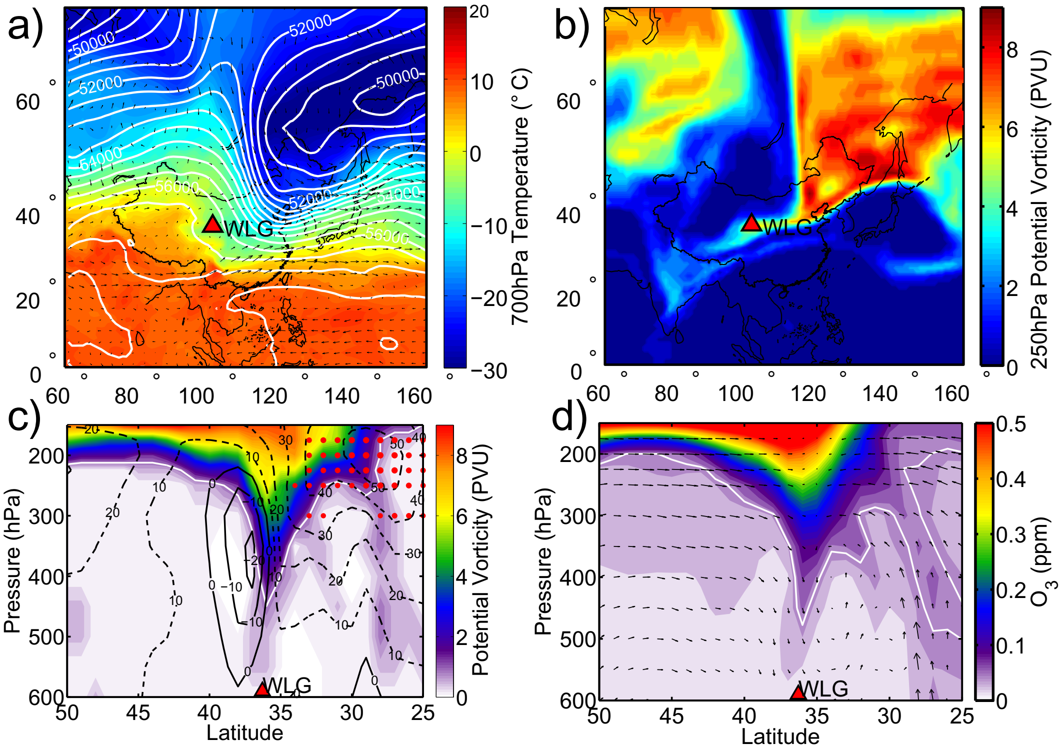

Figure 3 a) Map of 500hPa geopotential height (white contours), 700hPa temperature (shading) and wind field (black arrows); b) Map of 250hPa potential vorticity; c) the cross-section of potential vorticity along the 101.0E longitude line. The white line denotes the 1 PVU isoline, the black lines are U wind isolines (dashed lines for westerly winds and solid lines for easterly winds) and the red dots indicate the location of the subtropical jet stream (U wind>35m s-1); d) The cross-section of ozone mixing ratios, V wind and W wind vector along the 101.0E longitude line from the ECMWF reanalysis during an STT transport event on 30 Mar 2012. The while line denotes the 50-ppbv ozone contour.

Langford, A. O., Senff, C. J., Alvarez Ii, R. J., Brioude, J., Cooper, O. R., Holloway, J. S., Lin, M. Y., Marchbanks, R. D., Pierce, R. B., Sandberg, S. P., Weickmann, A. M., and Williams, E. J.: An overview of the 2013 Las Vegas Ozone Study (LVOS): Impact of stratospheric intrusions and long-range transport on surface air quality, Atmospheric Environment, 109, 305-322, 2015.

15) In section 4.1 an important conceptual issue it is not clear at all. The authors, when referring to STE air masses, mean to a quite jet or to baroclinic cut-off lows (or deep lows) associated to the position of the jet? It is difficult to conceive the direct impact and of a quite jet on surface ozone at WLG, and if it so, the authors should demonstrate this important result.

RE: In the case study of 30th Mar 2012, the STE was associated with a deep low, which, however, is not always the case. Typical baroclinic cut-off lows were hardly observed during the STT events in the springs of 1999 and 2012. The frequency of stratospheric intrusions has been found to be highest along the subtropical jet stream, where the tropopause break is located (e.g. Homeyer, 2012 and Sprenger et al., 2003). Tropopause folds are typically located to the north of the subtropical jetstream, hence the location of the jet stream directly influences the location of the STE event. If the jet is located

more to the south, the stratospheric ozone input might not reach WLG.
For the springs of 1999 and 2012, we calculated the average subtropical jet location (latitude) at the longitude of WLG for STE cases and non-STE cases (Table 1). Results show that the shift of the jet to the north pushes the location of the tropopause fold to the north, which then leads to STE processes over the WLG region. The difference in STE and Non-STE jet location passed the t-test at a 99% significance level.

Table 1 Average subtropical jet location (latitude) for STE cases and non-STE cases for the springs of 1999 and 2012

	Spring 1999		Spring 2012	
	avg	std	avg	std
STE	35.6	4.5	35.2	5.3
NO-STE	33.1	4.3	31.8	4.9

Homeyer, C. R.: Chemical and Dynamical Characteristics of Stratosphere-Troposphere Exchange, Atmospheric Sciences, Texas A&M University, 2012.
Sprenger, M. and Wernli, H.: A northern hemispheric climatology of cross-tropopause exchange for the ERA15 time period (1979-1993), J. Geophys. Res., vol. 108, no. D12, 8521, 2003.

16) Finally, the link between ozone at WLG with different modes of atmospheric circulation (section 4.2) is not justified or explained in all the cases. The authors limit themselves to presenting a series of statistical relationships, in some cases with very low and non-significant correlations, between ozone and climatic indexes, without necessarily having a causal relationship. Authors should decide whether to maintain this section with the degree of development they have so poorly achieved. If they maintain the section, it should be significantly improved, discarding those indices that clearly have no direct relation to the ozone observed in WLG.

RE: This paper is the part-2 of our study about long-term measurements of surface ozone at WLG. In the part-1 paper (Xu et al., 2016) ozone trends were obtained and the time-series of surface ozone at WLG was decomposed into five intrinsic mode functions (IMFs) with different periodicities. The IMFs did not contribute much to ozone trends but they are important in the interannual as well as seasonal variabilities. This paper aims to understand the factors driving the long-term trends and interannual variability. The major part of this paper focuses on the interpretation of the observed ozone trends. However, we think it is also necessary to understand the possible causes of the interannual variability. We tried this in the previous manuscript, but we did not show causal relationships. After careful consideration we decide to maintain this section but make necessary changes.

We have removed the materials about the NAO (Figure 15 and last paragraph in section 4.2 in previous manuscript) from this section. We have strengthened the analysis about the QBO and added more discussions in this section. We found that the QBO index was positively correlated with zonal and meridional wind over the areas west and north of China, suggesting increases in westerly and southerly winds over those areas when the QBO was in its positive phase. We also found similar positive correlations between the QBO index and air temperatures at different pressure levels, with a warming of 0.01–0.05 ℃ per unit increase in the QBO index. We think that these periodic changes in air circulations and temperature might have influenced the transport of ozone and its precursors and the photochemical conditions. Furthermore, we can see significant positive correlations of the QBO index with the 3-8 km TOST ozone columns over some areas west and north of China, over which the FT air can be transported to WLG. Therefore, we believe that the QBO can exert a small indirect influence on surface ozone at WLG through periodically changing dynamical and photochemical conditions over west and north of China.

The first paragraph of this section has been revised as follows:

" The time-series of surface ozone at WLG was decomposed into five intrinsic mode functions (IMFs) with different periodicities using the HHT analysis in combination with the empirical mode decomposition (EMD) (Xu et al., 2016). The 1st IMF shows high frequency, representing variations associated with synoptic systems. The 2nd IMF, with a periodicity of one year, represents seasonal variation and made the largest contribution to the variability of ozone. The other IMFs played minor roles in the variations of ozone. However, these IMFs are interesting because they are related to the 2–4-year, 7- year and 11-year periodicities found in the ozone data and contribute to the interannual variability of ozone at WLG. There are many oscillations within the atmospheric circulation with different periodicities, e.g. QBO with a quasi-2-year periodicity and ENSO with a 2 to 7-year periodicity (Xu et al., 2016). Here, we explore potential links of some atmospheric circulation oscillations to the variations of surface ozone at WLG (Xu et al., 2016). Since nighttime ozone concentrations at WLG are more representative of the free-tropospheric air condition, IMFs of the nighttime ozone data are applied in the following analysis. "

We have added "This suggests that surface ozone at WLG was indirectly linked to the QBO; however, the EMD analysis was not fully able to extract the QBO signal during 2003-2010 probably due to the interference of other signals or the abnormally long QBO period from 1998 to 2001. This link of surface ozone to the QBO cannot be explained by the finding of Ji et al. (2001) because surface ozone is independent of total column ozone and the GFDL-AM3 O3Strat is not correlated with the QBO index " at the end of second paragraph of section 4.2.

We have added the following text as an additional paragraph to this section:

" Although the QBO is an atmospheric oscillation in the stratosphere, its dynamical and chemical effects are not limited to the stratosphere but can propagate downward to the Earth's surface and upward to the mesosphere(Baldwin et al., 2001). Some mechanisms have been proposed to show how the QBO can change the large scale circulations and exert impacts the tropospheric winds, temperature, etc (e.g., Collimore et al., 2003; Kwan and Samah, 2003). To see the possibility of a QBO influence on surface ozone at WLG, correlations between the QBO index and zonal as well as meridional wind were calculated for different pressure levels. Figure 14 shows the correlation coefficients for the 500 hPa and 700 hPa levels. As can be seen in Figure 14, there is a large zone of positive correlation between the annual QBO index and zonal winds at both levels, extending from western Asia to central Asia to the middle of Russia. There is also a large zone of positive correlation between the annual QBO index and meridional winds at both levels, extending from the north of Indian Ocean to central Asia to Russia. These results suggest that when the QBO is in its positive phase, westerly and southerly winds over large areas west, northwest and north of China are increased. Similar zones of positive correlations exist also between the annual QBO index and air temperatures at different pressure levels, with a warming of 0.01–0.04℃ per unit increase in the QBO index (Figure S2). These periodic changes in air circulations and temperature might have influenced the transport of ozone and its precursors and the photochemical conditions. In fact, we can see significant positive correlations of the QBO index with the 3-8 km TOST ozone columns over some areas west and north of China (Figure 15). As the FT air over these areas can influence surface ozone at WLG through long-range transport (see Figure 1), we can expect a small signal in ozone at WLG that is related to the periodic changes in tropospheric ozone over areas west and north of China, caused indirectly by the QBO. The 3rd IMF reported in Xu et al. (2016) may be such a signal. There are other ways that the QBO influences the ozone distribution. For example, Hudson (2011) reported than the QBO can cause a few degrees of poleward movement of the subtropical jet streams and a shift of the subtropical front towards the pole. At present, it is not clear whether or not this mechanism influenced our ozone measurement. To better understand the QBO influence on surface ozone at WLG, a comprehensive modelling study is necessary, which is out of the scope of this paper."

Baldwin, M. P., Gray, L. J., Dunkerton, T. J., Hamilton, K., Haynes, P. H., Rande, W. J., Holton, J. R., Alexander, M. J., Hirota, I., Horinouchi, T., Jones, D. B. A., Kinnersley, J. S., Marquardt, C., Sato, K., and Takahashi, M.: The Quasi-Biennial Oscillation, Reviews of Geophysics, 39, 179–229, 2001.

Collimore, C.C., Martin, D.W., Hitchman, M.H., and Huesmann, A.: On the relationship between the QBO and tropical deep convection, Journal of Climate, 16, 2552-2568, 2003.

Kwan, K.F. and Samah, A.A.: A conceptual model relating the quasi-biennianl oscillation and the tropospheric biennial oscillation, International Journal of Climatology, 23, 347-362, 2003.

Xu, W., Lin, W., Xu, X., Tang, J., Huang, J., Wu, H., and Zhang, X.: Long-term trends of surface ozone and its influencing factors at the Mt Waliguan GAW station, China – Part 1: Overall trends and characteristics, Atmospheric Chemistry and Physics, 16, 6191-6205, 10.5194/acp-16-6191-2016, 2016.

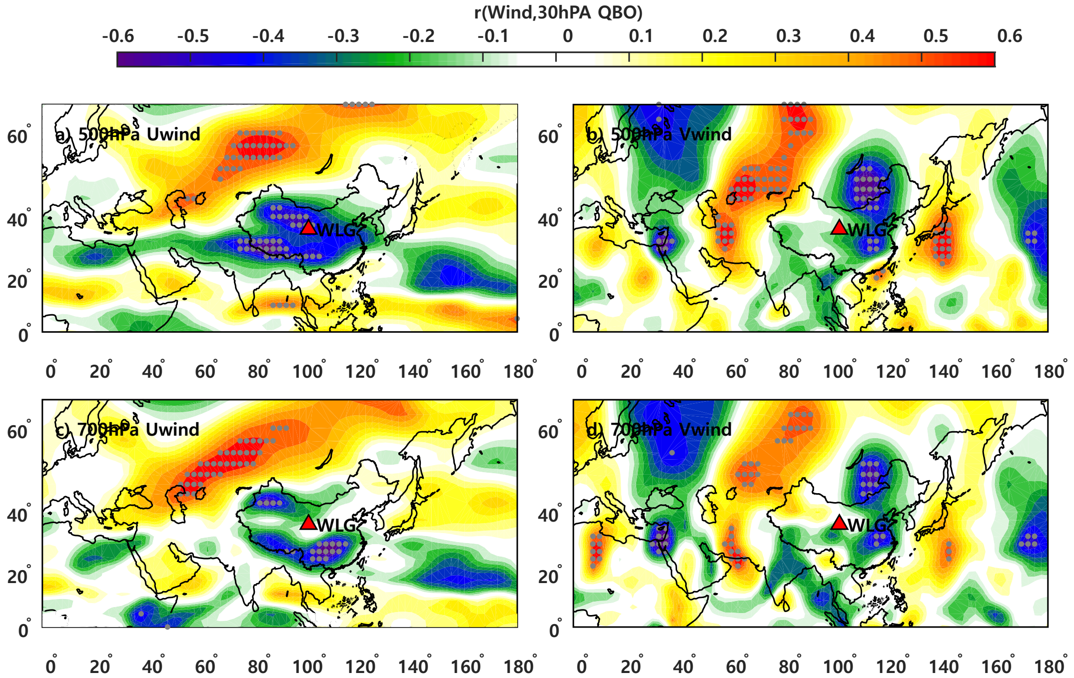

Figure 14 Correlation coefficients between the QBO index and zonal (a, c) and meridional (b, d) wind at 500 hPa and 700 hPa with grey dots indicating those that are significant ($p<0.05$). The red triangles indicate the position of WLG.

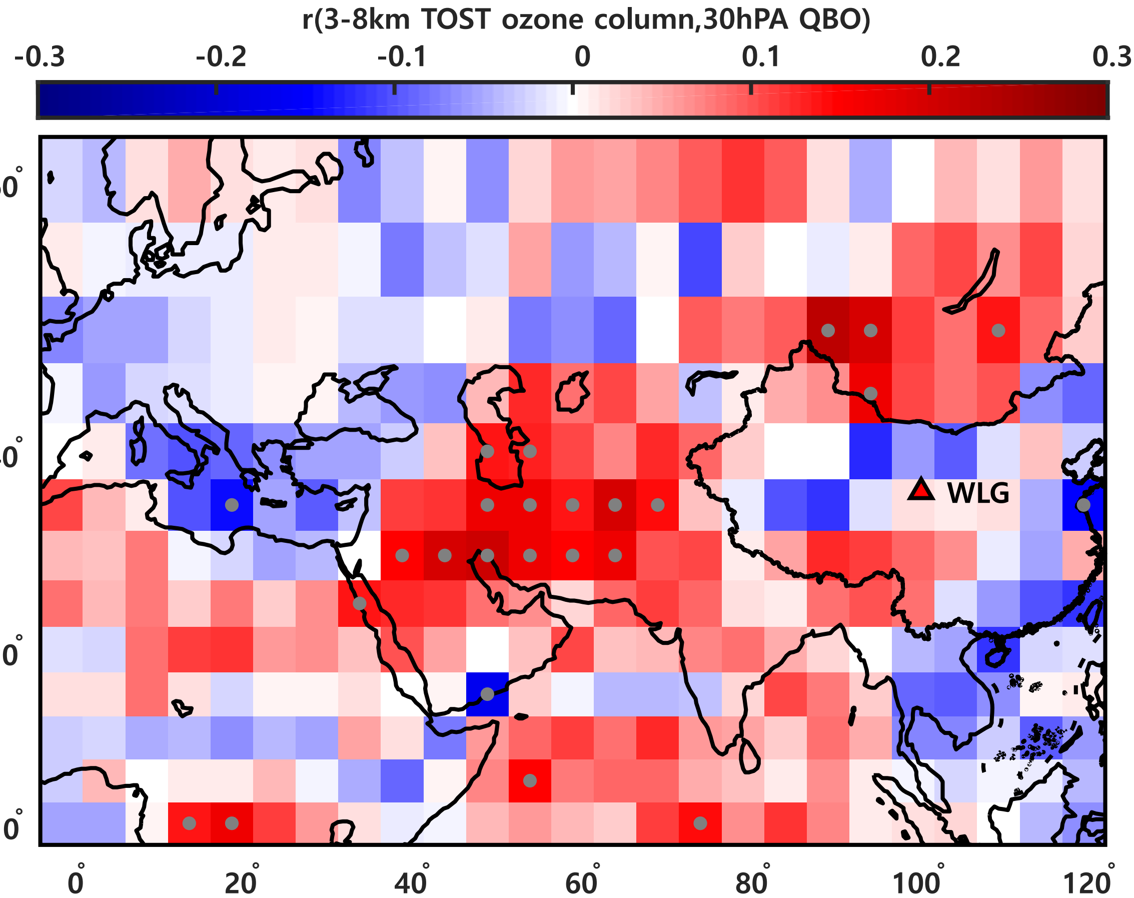

Figure 15 Correlation coefficients between the QBO index and the 3-8 km TOST ozone columns. Correlations for the grids with grey dots are significant ($p<0.05$)

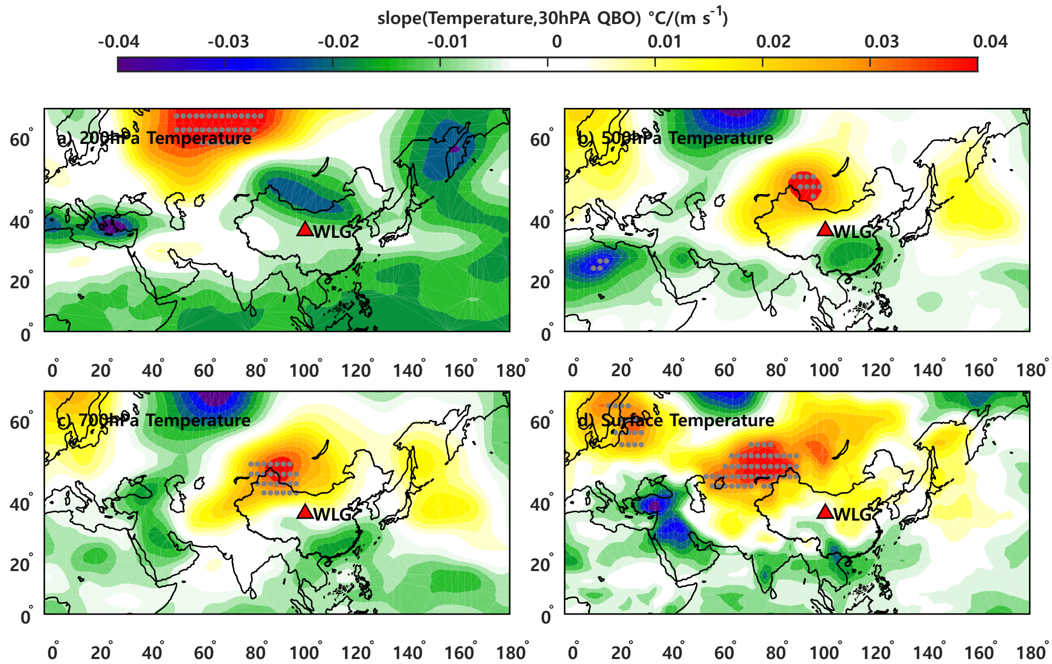

Figure S2 Regression slopes for the correlations between the QBO index and air temperatures at 200 hPa (a), 500 hPa (b), 700 hPa (c) and surface (d), with grey dots indicating the that are significantly correlated ($p<0.05$). The red triangles indicate the position of WLG.

Technical corrections

It does not make sense to go into details without having deeply addressed the changes proposed in the major comments. English should be significantly smoothed as it is difficult to understand the meaning of some sentences of the manuscript.

RE: We have tried to address the issues raised by both referees and improved the English language.

Response to reviewer #2

Thank you for your comments and suggestions. We have addressed all the issues that were raised and have made changes accordingly. We have also improved the English language and made other necessary changes. Please see our point-by-point response below.

General comments

This manuscript presents a detailed analysis on the interannual variability and long-term trends of surface ozone at the Mt. Waliguan (WLG) station for the period of 1994-2013. A number of approaches including backward trajectory, chemical transport model simulations, tropospheric ozonesonde dataset, correlations with multiple climate modes, and multi-variable regression are applied to address this issue. The results identify the importance of stratosphere-troposphere exchange to the observed ozone increases at WLG in spring, and increasing influences of anthropogenic pollution from Southeast Asia in summer.

This study provides valuable information to better understand the long-term changes of surface ozone at a background station in western China. I also feel difficult to follow while reading the manuscript, and I understand the attempts to combine together all these different approaches and difficulty in assessing their inconsistency quantitatively.

I have a few comments listed below for helping authors to clarify the manuscript.

Specific comments

1) Page 5, Line 5:

It is not clear how you clustered the trajectory directions into 45-degree bins. It shall be helpful to plot and define these bins on a figure, such as on a panel of Figure 1.

RE: Thank you for the suggestion. Instead of trajectory start-point direction we have calculated average trajectory directions, which have been used for clustering. To clarify the calculation process, we added the following example to show how the average 24h and 168h directions have been calculated as a supplement figure. The 45-degree bins were depicted along with the example.

We have made some changes in the second paragraph of section 2.2: "To study the overall air-mass origin and to determine whether the air-mass collected pollutants from the nearby cities, the average direction of each trajectory relative to the WLG station is calculated both for the 168h and for the 24h trajectory (Figure S1). The 168h and 24h average directions relative to WLG are clustered into bins of 45° and the occurrence frequency in each bin is calculated."

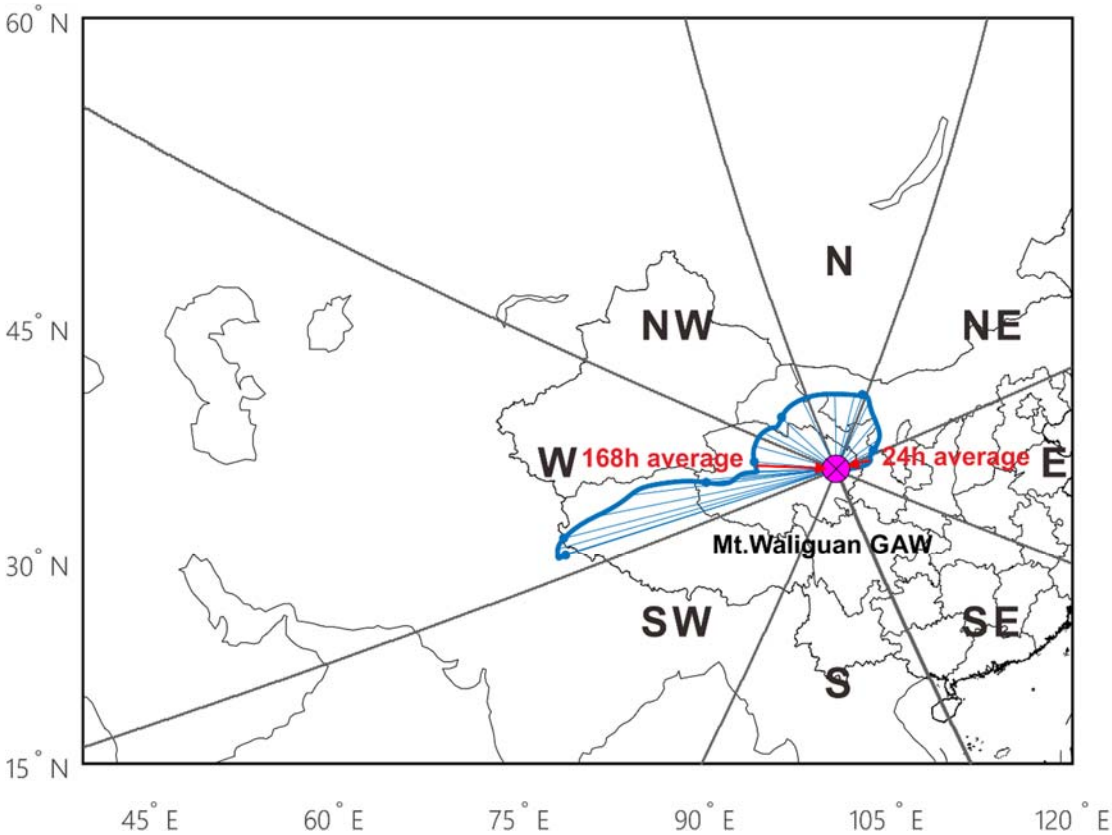

Figure 1 Schematic showing an example of the calculation process of 24h and 168h average trajectory directions and the 45-bins the trajectories were clustered into. The blue line shows a 7day trajectory example that bends from W to E, accounting for all the 168 hours, the average direction is westerly, while accounting only for the first 24 hours, the direction is easterly.

2) Page 8, Line 5:

For the statement "During summer, when air-masses from the east occur most frequently, the entire eastern sector reveals low PSCF", I suggest add "(as will be shown in Figure 2)" after "from the east occur most frequently", so that readers understand how you make the statement.

RE: Thank you for this suggestion. This sentence has been changed to "During summer, when air-masses from the east occur most frequently (as will be shown in Figure 2), the entire eastern sector reveals low values of high ozone PSCF, hardly showing signs of anthropogenic influence on WLG."

3) Page 8, Line 26:

Why do you state "the anthropogenic influence is negligible in all seasons except summer"? From Figure 1, we can also see high anthropogenic influences from Sichuan in spring and fall.

RE: Thank you for pointing out this. Page 8 lines 26-27 has been rephrased as:

"From the t=-168h average trajectory direction frequencies, it can be seen that the anthropogenic influence is strongest in summer, followed by autumn, and almost negligible in winter."

4) Page 11, Line 17-18:

You have argued above that the ozone trend in spring at WLG is driven by stratosphere troposphere-exchange. If so, shall we expect filtering for the East Asian anthropogenic influences, i.e., air masses with lower stratospheric influences, would show a lower trend? However, the results here show nearly no change in the springtime trend. Can you explain?

RE:We have explained this in the revised manuscript:

"We do not expect a decrease in springtime ozone when filtering the model for the East Asian anthropogenic influence, i.e., air masses with lower stratospheric influence, owing to the offsetting effects of increasing East Asian emissions."

5) Page 11, Line 20-30:

This section has showed that stratospheric influences explained two thirds of the ozone trend in spring. How about the rest one third? Would changes in anthropogenic emissions be the cause?

RE: Good suggestions. We have clarified in the revised manuscript:

"The stratospheric influence can explain two thirds of the total ozone increase at WLG in spring, with increases in Asian emissions contributing the rest one third"

6) Page 12, Sect. 3.3:

The TOST dataset are monthly averages from 1994 to 2012. Does that mean the dataset already account for ozone changes associated with increases in East Asian anthropogenic emissions? And then the direct tropospheric ozone transport as calculated in this section (Figure 8 and 9) has considered the tropospheric ozone changes associated with increases in precursor emissions. Please clarify.

RE: The TOST dataset is based on trajectory-mapped ozone soundings (Liu et al., 2013). The monthly averages of ozone in each grid should contain signals of background ozone and ozone produced with the grid from precursors emitted by anthropogenic and natural sources. Therefore, all the mean values in the TOST dataset already account for ozone changes associated with increases in East Asian (and other regions) anthropogenic emissions. One of the key issues in producing the TOST dataset was the impact of ozone production along the trajectories, which might cause errors in the mapped ozone data. A careful assessment indicates that the errors are mostly small and insignificant, as shown in Fig. 2 in Liu et al. (2013). Our approach of using TOST data is similar to the forward mapping in Liu et al. (2013), with the difference that we focus on the impacts on ozone in the WLG grid from the surrounding grids. Therefore, it is likely that the impact of ozone production along the trajectories on our results is small, as in the case of Liu et al. (2013).

To clarify this we have added the following two paragraphs in section 3.3:

"Different from the GFDL-AM3 FIXEMIS simulation discussed in Section 3.2, the TOST approach discussed in this section does not eliminate the impacts from increases in Asian anthropogenic emissions. The TOST dataset is based on trajectory-mapped ozone soundings (Liu et al., 2013). The monthly averages of ozone in each grid should contain signals of background ozone and ozone produced within the grid from precursors emitted by anthropogenic and natural sources. Therefore, mean values in the TOST dataset account for not only ozone changes due to transport but also ozone changes associated with varying global-to-regional anthropogenic and natural emissions."

"One of the key issues in producing the TOST dataset was the impact of ozone production along the trajectories, which might cause errors in the mapped ozone data. A careful assessment indicates that the errors are mostly small and insignificant (Liu et al., 2013). Our approach of using TOST data is similar to the forward mapping in Liu et al. (2013). Therefore, it is likely that the impact of ozone production along the trajectories during their residence time on our results is small, as in the case of Liu et al. (2013).As the bottom layer of the grid in which WLG resides is excluded in our calculations, direct impacts on our results from regional emissions in the grid containing WLG can be ruled out."

Liu, G., Liu, J., Tarasick, D. W., Fioletov, V. E., Jin, J. J., Moeini, O., Liu, X., Sioris, C. E., and Osman, M.: A global tropospheric ozone climatology from trajectory-mapped ozone soundings, Atmospheric Chemistry and Physics, 13, 10659-10675, 10.5194/acp-13-10659-2013,2013.

7) Page 13, Line 16-22:

In this paragraph, CO measurements at WLG are used to analyze the influences of anthropogenic emissions. The results show statistically significant increasing trends only in summer. How about the trend in autumn? The previous section showed that the ozone trend in autumn was driven by anthropogenic pollution, but this did not seem to be supported by the CO analysis. Can you please clarify? As for the contribution from precursor emissions, can the model simulation with fixed anthropogenic emissions provide a better estimate?

RE: The CO data used in the manuscript are monthly CO data from weekly flask sampling (at 5m height) and analysis. A study by Zhang et al. (2011) indicates that the concentration of CO at WLG is subject to influences of regional-scale pollution, particularly in summer. Therefore, our summer CO measurements are less representative of large-scale conditions. In Section 3.2 we study the impacts from anthropogenic emissions on a large-scale using GFDL-AM3 modeling. Our results are based on comparison of time-varying (BASE) and constant anthropogenic emissions (FIXEMIS).

8) Page 13, Line 23:

I feel confused about the discussion on ozone trends based on different trajectories in this paragraph. It reported the largest ozone trend associated with the SE direction, and the lowest trend with the NW direction. However, back on Page 9, Line 25-30,the trajectory analysis showed that the NW trajectories associated with high ozone concentrations had increasing occurrence frequencies, while the SE trajectory frequencies were decreasing. Are they consistent?

RE: These two results are not contradictory. The ozone concentrations associated with the NW trajectories are high in comparison to other sectors, but they show weak increasing trends, suggesting ozone coming from the NW have not changed much. The increase in NW trajectory frequency is what leads to the result that we experience these high ozone values more often, hence observe an increase in the ozone level. On the other side, ozone concentrations associated with the SE sector are not as high, but they show an increasing trend, highly possibly due to the change in precursor emissions in that sector.

9) Page 26, Table 5:

How do you estimate the ozone transported from East Asia, Europe, and North America? Please clarify.

RE: The GFDL model models CO-like-tracers from East Asia (EACOt), Europe (EUCOt) and North America (NACOt). For each month, we calculate the average ozone value associated with the upper 33 percentile EACOt, EUCOt, NACOt, to represent the ozone transported from East Asia ($O_{3,ea}$), Europe($O_{3,eu}$), and North America($O_{3,na}$). Then we use the East Asian Summer Monsoon Index (EASMI) to filter out those ($O_{3,ea}$,$O_{3,eu}$ and$O_{3,na}$) associated with the lower and upper 15 percentile of EASMI. The relative change induced by the East Asian Monsoon is then calculated with the equation: $(O_{3,\ EASMI<=15^{th}}-O_{3,EASMI>=85^{th}})/\bar{O}_3$.

We have clarified it in the revised manuscript by adding the above information to the header of Table 5.Thank you for pointing it out.

Some other comments

1) Page 3, Line 30:

“GOES-Chem” should be “GEOS-Chem”?

RE: Thank you, we have corrected this typo.

2) Page 8, Line 25:

“and least so in summer”. Need to remove “so”?

RE: Thank you for the correction, we have made according change in the revised manuscript.

3) Page 9, Line 19:

Here alpha is used to denote statistical significance, while in a few other places, such as Page 10, Line 12, ‘p’ is used. Please make them consistent.

RE: Thank you for the suggestion, we have made it consistent throughout the manuscript.

We have tried to address the issues raised by both referees and improved the English language. We have also made other changes where necessary. The title of this paper has been changed to “Long-term trends of surface ozone and its influencing factors at the Mt. Waliguan GAW station, China – Part 2: The roles of anthropogenic emissions and climate variability”.

Long-~~termtrends~~term trends of surface ozone and its influencing factors at the Mt. Waliguan GAW station, China – Part 2: ~~Exploring the~~The roles of anthropogenic emissions~~,~~ and climate~~, and their variation mechanism~~ variability

Wanyun Xu[1], Xiaobin Xu[1], Meiyun Lin[2], Weili Lin[3], ~~Jie Tang[3],~~ David Tarasick[4], Jie Tang[5], Jianzhong Ma[1], Xiangdong Zheng[1]

[1]State Key Laboratory of Severe Weather &Key Laboratory for Atmospheric Chemistry, Institute of Atmospheric Composition, Chinese Academy of Meteorological Sciences, Beijing, 100081, China
[2]NOAA Geophysical Fluid Dynamics Laboratory and Program in Atmospheric and Oceanic Sciences in Princeton University, Princeton, New Jersey 08540, USA
[3]College of Life and Environmental Sciences, Minzu University of China, Beijing, ~~10081~~100081, China
[4]Science and Technology Branch, Environment and Climate Change Canada, 4905 Dufferin Street, Downsview, Ontario, M3H 5T3, Canada
[5]Meteorological Observation Center, China Meteorological Administration, Beijing, 100081, China

Correspondence to: Xiaobin Xu (xuxb@camscma.cn)

Abstract

Interannual variability and long-term trends of tropospheric ozone are both ~~of~~ environmental and climate concerns. Ozone measured at Mt. Waliguan Observatory (WLG, 3816 m asl) on the Tibetan Plateau over the period 1994-2013 has increased significantly by 0.2-0.3 ppbv year^{-1} during spring and autumn, but shows a much smaller trend in winter and no significant trend in summer. Here we explore the factors driving the observed ozone changes at WLG using backward trajectory analysis, chemistry-climate model hindcast simulations (GFDL-AM3), a trajectory-mapped ozonesonde dataset and ~~various~~several climate indices. A stratospheric ozone tracer implemented in GFDL-AM3 indicates that stratosphere-to-troposphere transport (STT) can explain ~70% of the observed springtime ozone increase at WLG, consistent with an increase in the NW air mass frequency inferred from the trajectory analysis. Enhanced STT associated with the strengthening of the mid-latitude jet stream contributes to the observed high-ozone anomalies at WLG during the springs of 1999 and 2012. During autumn, observations at WLG are more heavily influenced by polluted air masses originated from Southeast Asia than in the other seasons. Rising Asian anthropogenic emissions of ozone precursors is the key driver of increasing autumnal ozone observed at WLG, as supported by the GFDL-AM3 model with time-varying emissions, which captures the observed ozone increase (0.26±0.11 ppbv year^{-1}). AM3 simulates a greater ozone increase of 0.38±0.11 ppbv year^{-1} at WLG in autumn under conditions with strong transport from Southeast Asia and shows no significant ozone trend in autumn when anthropogenic emissions are held constant in time. During summer, WLG is mostly influenced by easterly air masses but these trajectories do not extend to the polluted regions of eastern China and have decreased significantly over the last two decades, which likely explains why summertime ozone measured at WLG shows no significant trend despite ozone increases in Eastern China. Analysis of the Trajectory-mapped Ozonesonde dataset for the Stratosphere and Troposphere (TOST) and trajectory residence time reveals

increases in direct ozone transport from the eastern sector during autumn, which adds to the autumnal ozone increase. We further examine the links of ozone variability at WLG to the QBO, the East Asian summer monsoon (EASM) and the sunspot cycle. Our results suggest that the 2-3 year, 3-7 year and 11 year periodicities are linked to QBO, EASMI and the sunspot cycle, respectively. A multivariate regression analysis is performed to quantify the relative contributions of various factors to surface ozone concentrations at WLG. Through an observational and modelling analysis, this study demonstrates the complex relationships between surface ozone at remote locations and its dynamical and chemical influencing factors.

1 Introduction

Ozone in the troposphere is a potent greenhouse gas, an air pollutant detrimental to human health and vegetation, and the primary source of hydroxyl radicals, which play a critical role in atmospheric chemistry. The long-term variation of ozone is both of environmental and climate concern. Therefore, it is important to trace the long-term variations of ozone at different locations and understand the causes of such variations. Continuous long-term observations of surface ozone have been made only at a few representative sites in China. The Mt. Waliguan (WLG) station~~,~~ (36º17' N, 100º54' E, 3816 m asl), established in 1994, is situated in the northeastern part of the Tibetan Plateau, where population is ~~scarce~~sparse and industries hardly exist. It is one of the baseline stations in the Global Atmosphere Watch (GAW) program of the World Meteorological Organization (WMO) and the only one in the hinterland of the Eurasian continent with surface ozone measurement of longer than two decades. The long-term trend and periodicity of surface ozone at WLG during 1994-2013 are reported in the companion paper ~~(Xu et al., 2016)~~(Xu et al., 2016). Significant increasing trends have been detected in spring and autumn, while observations show no significant trend during summer when ozone is at its seasonal maximum. Here we investigate the mechanisms controlling the seasonal ozone trends measured at WLG using backward trajectory analysis and multi-decadal hindcast simulations (1980-2014) conducted with the Geophysical Fluid Dynamic Laboratory chemistry-climate model (Lin et al., 2014; 2015a; 2017).

With ~~the~~ rapid economic development in Eastern China,~~ the~~ anthropogenic emissions of ozone precursors have been increasing during the past two decades ~~(van der A et al., 2006;Kurokawa et al., 2013 ;Itahashi et al., 2014)~~(van der A et al., 2006;Kurokawa et al., 2013 ;Itahashi et al., 2014). Specifically, emissions of NO_x over Eastern China have tripled since 1990 (e.g. Lin et al., 2017). Increasing levels of surface and free tropospheric ozone have been detected at several locations in eastern China, e.g. in the North China Plain ~~(Ding et al., 2008;Wang et al., 2012;Ma et al., 2016;Sun et al., 2016b;Wang et al., 2017a)~~(Ding et al., 2008;Wang et al., 2012;Ma et al., 2016;Sun et al., 2016;Wang et al., 2017), in the Yangtze River Delta ~~(Xu et al., 2008)~~(Xu et al., 2008) and in the Pearl River Delta~~(Wang et al., 2009;Lin et al., 2017)~~(Wang et al., 2009;Lin et al., 2017). Rising Asian anthropogenic emissions of ozone precursors have been implicated in raising free tropospheric and surface ozone levels over the western U.S. during spring ~~(Verstraeten et al., 2015;Lin et al., 2015b;Lin et al., 2017)~~(Verstraeten et al., 2015;Lin et al., 2015b;Lin et al., 2017)~~. A recent study by Lin et al. (2017)~~. A recent study by Lin et al. (2017) shows that a tripling of NO_X emissions in Asia contributed up to 50-65% of the observed springtime ozone increases at western U.S. rural sites during 1988-2014, outpacing ozone decreases resulting from U.S. domestic NO_X emission controls. A few case studies have documented the influence of anthropogenic pollution from eastern and central China on ozone at WLG during the summer season ~~(Wang et al., 2006b;Xue et al., 2011)~~(Wang et al., 2006b;Xue et al., 2011)~~. Whether~~, but whether the growth in East Asian anthropogenic ozone precursor emissions has contributed to the long-term trend of surface ozone at WLG ~~needs to be~~has not yet been examined.

~~Asides~~Aside from regional precursor emissions and long-range horizontal transport ~~(Wang et al., 2006a;Lal et al., 2014)~~(Wang et al., 2006a;Lal et al., 2014), the concentration of surface ozone has many other influencing factors. For instance, surface ozone concentrations at high-elevation sites can also be ~~raised~~increased by the downward transport of ozone-rich air from the stratosphere during deep convection and stratosphere-to-troposphere exchange (STE) events ~~(Bonasoni et al., 2000;Stohl et al., 2000;Lefohn et al., 2012;Jia et al., 2015;Ma et al., 2014;Langford et al., 2009;Langford et al., 2015;Lin et al., 2012a;Lin et al., 2015a)~~(Bonasoni et al., 2000;Stohl et al., 2000;Lefohn et al., 2012;Jia et al., 2015;Ma et al., 2014;Langford et al., 2009;Langford et al., 2015;Lin et al., 2012a;Lin et al., 2015a).Studies based on short-term measurements suggested that surface ozone at WLG is influenced by STE events in spring ~~(Zheng et al., 2011)~~(Zheng et al., 2011) and sometimes during summer ~~(Ding and Wang, 2006)~~(Ding and Wang, 2006). The extent to which STE influences observed year-to-year variability and decadal trend of ozone at WLG has not been previously investigated.

Changes in large-scale atmospheric circulation patterns can modulate long-range transport of ozone pollution in the troposphere as well as stratosphere-to-troposphere ozone exchange. ~~The large~~Large-scale physical and dynamical processes including the El Niño–Southern Oscillation (ENSO), the North Atlantic Oscillation (NAO), the Quasi Bi-annual Oscillation (QBO) and the solar cycle ~~(Creilson et al., 2003;Ziemke et al., 2005;Oman et al., 2013;Sioris et al., 2014)~~(Creilson et al., 2003;Ziemke et al., 2005;Oman et al., 2013;Sioris et al., 2014) have been found to significantly affect stratospheric and tropospheric ozone variability. Based on the good correlation between the ENSO index and tropospheric column ozone (TCO) over tropical latitudes, ~~Ziemke et al. (2010)~~Ziemke et al. (2010) created a so-called "Ozone ENSO Index" (OEI). Over northern mid-latitudes, strong El Niño events enhance long-range transport of Asian ozone pollution towards the eastern North Pacific and the southwestern U.S. by modulating the strength and position of the subtropical jet stream ~~(Lin et al., 2014)~~(Lin et al., 2014). Some studies ~~(Zeng and Pyle, 2005;Langford, 1999;Koumoutsaris et al., 2008;Voulgarakis et al., 2011)~~(Zeng and Pyle, 2005;Langford, 1999;Koumoutsaris et al., 2008;Voulgarakis et al., 2011) ~~suggested~~suggest that the change in dynamics after El Niño events can promote~~ the~~ cross-tropopause ozone exchange and lead to a rise in global mean tropospheric ozone burden. However, ~~Lin et al. (2015a)~~Lin et al. (2015a) ~~found~~find that El Niño events lead to enhancements in upper tropospheric ozone but this influence does not reach surface air. ~~Over western U.S. high elevation regions prone to deep stratospheric intrusions, Lin et al. (2015b)~~Over high elevation regions prone to deep stratospheric intrusions in the western U.S., Lin et al. (2015b) ~~found~~find that the increased frequency of deep tropopause folds that form in upper-level frontal zones following strong La Niña winters exerts a stronger influence on springtime ozone levels at the surface than the El Niño-related increase in lower stratospheric to upper tropospheric ozone burden.

Similar to the western US, the Tibetan Plateau has been identified as a preferred region for deep stratospheric intrusions ~~(Škerlak et al., 2014)~~(Škerlak et al., 2014). Prior studies show that the QBO, ENSO and sunspot cycle influence ~~the~~ total ozone over the Tibetan Plateau ~~(Ji et al., 2001;Huang et al., 2009;Ningombam, 2011;Zou et al., 2001)~~(Ji et al., 2001;Huang et al., 2009;Ningombam, 2011;Zou et al., 2001). The mechanisms controlling the interannual variability of jet stream characteristics, STE and their influences on lower tropospheric ozone measured at WLG are poorly characterized. In addition, China is ~~largely~~strongly influenced by the East Asian summer monsoon (EASM). Past studies have pointed out that the EASM influences ozone concentrations in this region through altering the transport of anthropogenic pollution ~~(Derong et al., 2013;Liu et al., 2009;Liu et al., 2011)~~(Derong et al., 2013;Liu et al., 2009;Liu et al., 2011). Using the GEOS-CHEM global chemical transport model, ~~Yang et al. (2014)~~Yang et al. (2014) ~~reported~~report a positive interannual correlation between the EASM and the Tibetan surface ozone concentration. Their results were not evaluated with actual observations of surface ozone.

In this work, we aim to advance knowledge on the factors driving interannual variability and long-term trends of ozone at WLG over the past three decades. Sect. 2 briefly describes observational data, model simulations and analysis approach. In Sect. 3, we first discuss the links of surface ozone at WLG to air mass origin, including their seasonal to interannual variability (Sect. 3.1). We then use the GFDL-AM3 model hindcast simulations to interpret the influences of changes in meteorology, STE and anthropogenic emissions on ozone measured at WLG in winter, spring, summer and autumn (Sect. 3.2~~). The~~)and the impact of direct ozone transport versus precursor transport ~~is also discussed~~ (Sect. 3.3). Sect. 4 examines the relationship between atmospheric dynamics and surface ozone at WLG, including the influence of STE, EASM and the sunspot cycle. An empirical model is obtained for the normalized monthly level of surface ozone at WLG using the multivariate regression technique and used to explain the observed ozone trends.

2 Data and Methodology

2.1 Data

Ozone concentration, UV and meteorological parameters were measured at the Mt. Waliguan site (WLG, 36º17’ N, 100º54’ E, 3816 m asl) in Qinghai Province, China. Ozone concentrations at a 5-min resolution from Aug. 1994 to Dec. 2013 were averaged into hourly, daily and monthly ~~resolutions~~timescales, with a data completeness of 75% required for each averaging step. ~~In-situ observations of CO have been attempted at WLG using different techniques. Unfortunately, the coverage of qualified data is poor due to various technical problems. Therefore, monthly CO data the World Data Centre for Greenhouse Gases (http://ds.data.jma.go.jp/gmd/wdcgg/wdcgg.html) are used in this study. The monthly CO data are from weekly flask sampling at 5 m above ground and posterior analysis. The~~ Hilbert-Huang Transform (HHT) analysis was performed ~~respectively~~ using the monthly average daytime and nighttime ozone data~~.~~, respectively. Further details on the site, measurements, the daytime and nighttime data subsets and the HHT calculations can be found in Part I of our study ~~(Xu et al., 2016)~~(Xu et al., 2016). In this paper, the results of the HHT analysis are further associated with the sunspot number (SSN), the QBO and the EASM index ~~(Li and Zeng, 2002)~~(Li and Zeng, 2002) to investigate the influence of various climate oscillations on surface ozone at WLG. The SSN data are from Sunspot Index and Long-term Solar Observations (http://www.sidc.be/silso/datafiles). The QBO index is based on the 30 hPa Singapore zonal wind and available from the U.S. National Oceanic and Atmospheric Administration~~/Physical Sciences Division (NOAA/PSD)~~ at https://www.esrl.noaa.gov/psd/data/climateindices/. The EASM index ~~can be~~is acquired from ~~http://ljp.gcess.cn/dct/page/65577~~http://ljp.gcess.cn/dct/page/65577. We also use monthly CO data based on weekly flask sampling at 5 m above ground, obtained from the World Data Centre for Greenhouse Gases (http://ds.data.jma.go.jp/gmd/wdcgg/wdcgg.html), to infer changes of regional emissions near WLG. Using high frequency (e.g., minutes) in-situ observations of CO and water vapour would be ideal to diagnose the presence of stratospheric versus anthropogenic influences, however, continuous high-quality data are not available at WLG due to various technical challenges.

2.2 Backward Trajectory Analysis

The HYSPLIT model (version 4) from NOAA Air Resources Laboratory ~~(Draxler and Hess, 1997;Draxler and Hess, 1998;Draxler, 1999)~~(Draxler and Hess, 1997;Draxler and Hess, 1998;Draxler, 1999) is used for the trajectory analyses, using three different meteorological datasets from NCEP. The NCEP Global Reanalysis Data with a spatial resolution of 2.5°,the NCEP FNL operational data in 1.0° resolution and the NCEP GDAS (Global Data Assimilation System) operational forecast data in 1.0° resolution are used for 1994-1996,1997-2006 ~~and2007~~and 2007-2013, respectively. All the ~~reanalysis~~ meteorology data have a temporal resolution of 6-h. The trajectory endpoint is set to 36.28º N and 100.90º E with a height of 100 m above the ground level. The 168h (7 days) backward trajectories are calculated at a 6-h interval from 1st Aug. 1994 to 31st Dec. 2013. To study the overall air-mass origin and to determine whether the air-mass collected pollutants from ~~the~~ nearby cities, the average direction of each trajectory relative to the WLG station is calculated both for the 168h and for the 24h trajectory (Figure S1). The 168h and 24h average directions relative to WLG are clustered into bins of 45° and the occurrence frequency in each bin is calculated.

Since ozone is a trace gas with a distinct vertical distribution, it is not enough to just ~~determining~~determine the direction ~~of where~~from which the air-mass came ~~from~~. The height of the air-mass is also ~~very~~ crucial for interpreting the measured ozone concentrations. As ~~already pointed out~~discussed in previous studies ~~(Ma et al., 2002;Xu et al., 2016)~~(Ma et al., 2002;Xu et al., 2016), ~~during daytime and nighttime~~ the WLG site is ~~mainly~~predominantly influenced by air from the planetary boundary layer (PBL) during daytime and from the free troposphere (FT~~), respectively, causing~~) during nighttime, with ozone concentrations showing a daytime minimum and a nighttime maximum~~ of the ozone concentration. And ozone in daytime and~~. Daytime and nighttime ~~showed~~ozone at WLG show different trends, particularly in summer ~~when daytime and nighttime ozone showed respective trends of~~ (0.07±0.18 ppb year^{-1} ~~(p=0.41)~~for daytime and 0.22±0.20 ppb year^{-1} ~~(p=0.04) (see~~for nighttime; Xu et al., 2016). To investigate the impacts of air masses from the PBL and FT separately, the PBL height, which can be added in the Hysplit model along the trajectories, is used to judge whether the air-mass that arrived at WLG is representing the PBL or the FT. PBL trajectory sections are defined as the part of the trajectory that was continuously within the PBL before arriving at the station. Thus, PBL trajectory sections are usually close to the station. When the trajectory height exceeds that of the PBL, the rest of the trajectory is taken as the FT trajectory section. FT trajectory sections can also be close to the station, representing subsiding air from the FT near the station, however, most of them cover the sections that are located far away from the station.

2.3 Potential source contribution function analysis

The potential sources of high ozone are studied using the potential source contribution function (PSCF) analysis method, which has been widely applied to detect possible source regions (Ara Begum et al., 2005;Lucey et al., 2001;Zhou et al., 2004)(Ara Begum et al., 2005;Lucey et al., 2001;Zhou et al., 2004). The PSCF analysis is performed both on PBL and on FT trajectories to detect differences in source region distributions in the PBL and in the FT or above.

The PSCF on the grid (i,j) is defined as:

$$PSCF = m(i,j)/n(i,j), \quad (1)$$

where $n(i,j)$ is the residence time of all the trajectories and $m(i,j)$ is the residence time of a subset of trajectories in the grid cell (i,j). Each trajectory is associated with ozone concentrations that were measured at its arrival time. The 75th percentile of all the ozone concentrations at WLG is calculated and the residence time in each grid cell $m(i,j)$ of the subset of trajectories that is associated with ozone concentration higher than the 75th percentile value is counted.

Abnormally high PSCF values may be produced for certain gridsgrid cells with small $n(i,j)$ values, which would bear large uncertainties. To avoid such uncertainties, a weighting factor $W(n_{ij})$ is introduced, which was originally proposed by Zeng and Hopke (1989)Zeng and Hopke (1989):

$$W(n_{ij}) = \begin{cases} 1.0, & n_{ij} > \overline{n_{ij}} \\ 0.7, & 0.1 \cdot \overline{n_{ij}} < n_{ij} \leq \overline{n_{ij}} \\ 0.4, & 0.05 \cdot \overline{n_{ij}} < n_{ij} \leq 0.1 \cdot \overline{n_{ij}} \\ 0.2, & n_{ij} \geq 0.05 \cdot \overline{n_{ij}} \end{cases}, \quad (2)$$

where $\overline{n_{ij}}$ is the average number of n_{ij}.

2.4 Calculation of direct ozone transport contribution

A Trajectory-mapped Ozonesonde dataset for the Stratosphere and Troposphere (TOST) was generated from the ozone sounding records by trajectory mapping by Liu et al. (2013)Liu et al. (2013).The dataset has a spatial resolution of 5°×5°×1km (latitude, longitude and altitude). A subset from the TOST, the global three-dimensional (3-D) monthly average tropospheric ozone from 1994 to 2012 is applied in this paper to calculate the contribution of direct tropospheric ozone transport to the ozone trends at WLG. The 3-D tropospheric ozone data are in monthly intervals. A 3-D backward trajectory residence time within the same grids and with the same time interval as that of the tropospheric ozone data is calculated based on the backward trajectory analysis results in sect. 2.3. Assuming that ozone is nearly conserved on the transport pathway (i.e., ozone and production and loss are negligible), the contribution of O_3 in each grid cell to that of WLG during each month is calculated using the trajectory residence time as a weighting factor:

$$O_{3,contrib}(t,i) = \frac{O_3(t,i) \times T(t,i)}{\sum_{i=1}^{n} T(t,i)}, \quad (3)$$

where $O_3(t,i)$ and $T(t,i)$ respectively stand for the ozone concentration and the trajectory residence time at time t in grid cell i, while n stands for the total number of ~~grids~~grid cells.

To obtain the monthly time-series of total direct tropospheric ozone transport contribution to ozone at WLG, the 3-D ozone contribution climatology of all the ~~grids~~grid cells is summed up (eq. 4). The bottom layer of the grid cell in which WLG resides is excluded from the summation.

$$O_{3,contrib,tot} = \sum_{i=1}^{n} O_{3,contrib}(t,i) \quad (4)$$

The variation trend of $O_{3,contrib}(t,i)$ and $O_{3,contrib,tot}$ is calculated for the entire period of 1994-2013 and separately for each season. For display, $O_{3,contrib}(t,i)$ and its trend is integrated over height. $O_{3,contrib,tot}$ is used in the multivariate regression as $O_{3,trop}$ in Sect 2.6.

2.5 Modelling of stratospheric and anthropogenic contributions

The GFDL-AM3 global chemistry–climate model was used to make hindcast simulations of ozone and related tracers at ~200x200 km^2 horizontal resolution over the 1980-2014 period ~~(Lin et al., 2015a;Lin et al., 2015b;Lin et al., 2014;Lin et al., 2017)~~(Lin et al., 2015a;Lin et al., 2015b;Lin et al., 2014;Lin et al., 2017). The model is nudged to the NCEP/NCAR reanalysis zonal and meridional winds using a pressure-dependent nudging technique~~(Lin et al., 2012b)~~(Lin et al., 2012b). Two AM3 simulations are used in this study: one with both meteorology and anthropogenic emissions varying from 1980 to 2014 (BASE) and the other with anthropogenic emissions (including methane) held constant in time (FIXEMIS). To quantify the stratospheric influence on surface ozone, a stratospheric ozone tracer (O_3Strat) is defined relative to a dynamically varying tropopause and is subjected to chemical and depositional loss in the same manner as odd oxygen of tropospheric origin ~~(Lin et al., 2015a)~~(Lin et al., 2015a). Carbon-monoxide-like tracers for East Asia (EACOt), Europe (EUCOt) and North America (NACOt) are implemented to investigate the impact of circulation changes on hemispheric pollution transport~~(Lin et al., 2014)~~(Lin et al., 2014).These CO-like tracers have a 50-day exponential lifetime and are simulated with surface emissions held constant in time from each of the three northern mid-latitude source regions. Comparison with available observations from the mid-1990s to the 2000s at a suite of sites across Asia shows that GFDL-AM3 captures 65-90% of the observed ozone increases in Asia ~~(Lin et al., 2017)~~(Lin et al., 2017). The long-term ozone observational record at WLG provides an important test for the GFDL-AM3 model to represent the key processes driving year-to-year variability and trends of tropospheric ozone in the remote atmosphere of the Tibetan Plateau. For comparison with measurements at the 3.8 km altitude of WLG, the model is sampled at the grid box containing WLG and at the 700hPa layer. This approach is appropriate because observations at Mt. WLG are representative of large-scale conditions with little influence from local urban emissions.

2.6 Multivariate regression of surface ozone at Waliguan

Multivariate regression is applied to obtain an empirical model to explain the relationship and contribution of the various influencing factors to the surface ozone concentration at WLG. The regression model takes on the following form:

$$O_3 = \alpha(t) + \sum_{i=1}^{n} \beta_i(t) \cdot factor_i(t) \tag{5}$$

Where $\alpha(t)$ is a third order harmonic function used to interpret the background variation signal of surface ozone:

$$\alpha(t) = a_0 + \sum_{j=1}^{3} a_{1,j} \cdot cos\big(2\pi j(t - t_0)\big) + a_{2,j} \cdot sin\big(2\pi j(t - t_0)\big) \tag{6}$$

and $\sum_{i=1}^{n} \beta_i(t) \cdot factor_i(t)$ stands for the total contribution of the n influencing factors used in the regression model. $\beta_i(t)$ is a first order harmonic function, which can be expressed as:

$$\beta_i(t) = b_{i,0} + b_{i,1} \cdot \cos\big(2\pi(t - t_0)\big) + b_{i,2} \cdot \sin\big(2\pi(t - t_0)\big) \tag{7}$$

The coefficients $b_{i,1}$ and $b_{i,2}$ allow for the time-dependent intensification or attenuation of the influences of factors. Since our data start in the year of 1994, t is calculated as:

$$t = year + (month - 1)/12 - 1994 \tag{8}$$

3 Key drivers of long-term ozone trends at WLG

3.1 Climatology and interannual variability of air mass origin at WLG

Based on past studies, which were mostly focused on summertime ozone at WLG, high ozone concentrations were mostly linked to downward transport, instead of horizontal transport of anthropogenic pollution ~~(Zhu et al., 2004;Ma et al., 2005;Wang et al., 2006b;Xue et al., 2011)~~(Zhu et al., 2004;Ma et al., 2005;Wang et al., 2006b;Xue et al., 2011). Westerly trajectories were commonly associated with downward transport events and high ozone concentrations, whereas easterly trajectories carried air masses with signals of anthropogenic pollution and lower ozone concentrations. Anthropogenic impact was attributed mostly to the two big cities, Xining and Lanzhou, which are located both to the east of WLG, however, central and eastern China could also have potential impacts ~~(Wang et al., 2006b;Xue et al., 2011)~~(Wang et al., 2006b;Xue et al., 2011).

Since ozone and its precursors are usually inhomogeneously distributed, both the horizontal direction and vertical height of the air-mass origin may the local concentration of ozone at WLG. As already pointed out in previous studies ~~(Ma et al., 2002;Xu et al., 2016)~~(Ma et al., 2002;Xu et al., 2016), during daytime and nighttime the WLG site is mainly influenced by air from the PBL and FT, respectively, causing a daytime minimum and a nighttime maximum of the ozone concentration. And ozone in daytime and nighttime showed different trends, particularly in summer when daytime and nighttime ozone showed respective trends of 0.07±0.18 and 0.22±0.20 ppb year^{-1} (~~p=0.41) and 0.22 ppb year^{-1} (p=0.04) (see~~ Xu et al., 2016). To locate the origin of high surface ozone concentrations at WLG and understand the ozone difference between daytime and nighttime, it is necessary to investigate the respective impacts of air masses from the PBL and FT. ~~Affect the local concentration of ozone at WLG.~~ To locate the origin of high surface ozone concentrations at WLG, a PSCF analysis (section 2.3) was performed separately for the PBL and FT trajectories. Figure 1Figure 1 displays the ozone PSCF of the PBL and FT trajectories in spring, summer, autumn and winter from Aug. 1994 to Dec. 2013. For the PBL as well as the FT trajectories, the NW sector is most frequently accompanied by high ozone concentrations (higher than 75^{th} percentile ozone concentration), which is a common phenomenon existing in all seasons.

During spring, Sichuan province, which is southeast to WLG, displays significantly high ozone PSCF both in the PBL and FT trajectories, which is possibly an evidence for long range transport of ozone and/or its precursors from Sichuan to WLG. During summer, when air-masses from the east occur most frequently (as will be shown in Figure 2), the entire eastern sector reveals low values of high ozone PSCF, hardly showing signs of anthropogenic influence on WLG. In other words, most air-masses from the east in summer are not associated with high ozone. High ozone PSCF occurs dominantly with trajectories from the NW or N. In autumn, in addition to NW or N, significant contributions of trajectories from the E, SE and S can also be discerned in the PBL trajectories, which suggest that high ozone is linked to air-masses coming from western China, central China and the northeastern part of the Tibetan Plateau, the southwestern part of Gansu province as well as north of China (east Mongolia). In the FT trajectories, high ozone concentrations were mainly linked to air-masses from western and central China. In addition, air masses over Gansu province, part of the Sichuan province and some parts of Russia also show high PSCF. In winter, the PBL trajectories show high ozone PSCF mainly in the NW directionssectors, however, the SW and N-NE sectors also revealed scattered high PSCF values (over some parts of Nepal, Northern India, Mongolia and Inner Mongolia). Aside from the NW sector, the FT trajectories display significantly high PSCF in the NE sector in the western half of Inner Mongolia.

To evaluate the impact of different air-masses, we need to find out which air-masses are influencing WLG and evaluate the relative importance of the different air-masses during different seasons. Figure 2Figure 2 depicts the 24 and 168 hours average trajectory direction occurrence frequencies for spring, summer, autumn and winter, respectively. The 168h average trajectory direction provides us information on the overall origin of the air-mass, while the 24h average trajectory direction should be able to reveal if the air-mass passed over nearby polluted regions before arriving at the station.

From the 168h average trajectory direction occurrence frequencies (Figure 2(Figure 2 a2-d2), it can be seen that WLG is under the major influence of western and north-western air-masses throughout the year, with air-masses from the east only playing a significant role during summer, which is in accordance with previous studies (e.g. Zhang et al. (2011)Zhang et al. (2011)). Hence, the WLG site is overall very clean and highly representative of a background state. Trajectories from the east (including NE, E and SE) take up on average 20%, 65%, 31% and 6% of all the trajectory directions during spring, summer, autumn and winter, respectively. The NW trajectories at t=-168h are most frequent in spring (44%) and least frequent in winter (12%), while western trajectories are most dominant in winter (77%) and least in summer (6%).

From the 168h average trajectory direction frequencies, it can be seen that the anthropogenic influence is strongest in summer, followed by autumn, and almost negligible in winter. However, the 24h average trajectory direction frequencies show significantly larger portions of easterlyeastern trajectories and smaller percentages of northwesterlynorthwestern trajectories (Figure 2a1(Figure 2a1-d1), implying that a significant port of air-masses originating from the northwest of WLG often bendedbend over to the east 24h before arriving at WLG. Trajectories24-hour trajectories from the east (including NE, E and

SE) take up on average 40%, 76%, 30% and 15% of all the trajectory directions during spring, summer, autumn and winter, respectively. Air-mass trajectories originating from the far northwest bending to the east before their arrival at WLG may ~~catch~~entrain pollutants if they travel over the large cities. The large occurrence frequency of ~~easterly~~eastern trajectories in the endpoints within the last 24h suggests that anthropogenic influences on WLG during spring and autumn should not be neglected.

It is also worth noting from ~~Figure 2~~Figure 2 that the trajectory direction frequencies were far from constant throughout the two decades from 1994 to 2013. There was large interannual variability. Some directions show significant variation trends in their occurrence frequencies, which will be discussed later ~~on~~ in this section.

The air-mass direction analysis shows that the WLG site is under the influence of different air-masses from different horizontal directions. Apart from that, the WLG site is also under the control of distinct air-masses from different layers throughout the day, with PBL air-masses dominating during the day and FT air-masses during the night, which led to a clear diurnal variation with high nighttime and low daytime ozone concentrations ~~(Ma et al., 2002;Xu et al., 2016)~~(Ma et al., 2002;Xu et al., 2016). STE events were also held responsible for the injection of stratospheric ozone into the troposphere, leading to elevated surface ozone concentrations ~~(Bonasoni et al., 2000;Ding and Wang, 2006;Stohl et al., 2000;Tang et al., 2011;Lefohn et al., 2012;Jia et al., 2015;Ma et al., 2014;Lee et al., 2007;Liang et al., 2008)~~(Bonasoni et al., 2000;Ding and Wang, 2006;Stohl et al., 2000;Tang et al., 2011;Lefohn et al., 2012;Jia et al., 2015;Ma et al., 2014;Lee et al., 2007;Liang et al., 2008).

Changes in atmospheric circulations might lead to variations in the occurrence frequencies of air-masses from different directions shown in ~~Figure2.~~Figure 2. Due to the high dependence of local surface ozone concentrations on the air-mass origin, a significant change in atmospheric circulation may lead to changing local concentrations of surface ozone at WLG. To investigate this kind of impact, average 24h and 168h trajectory directions are used to uncover whether there were secular changes in the occurrence frequency of different directions. ~~Table 1~~Table 1 lists the variation trends (k, slopes of linear regression) of trajectory direction occurrence frequencies in different seasons. The bold numbers in the table are the variation trends that are statistically significant ($p<0.05$). From the168h results it can be noted that, the NW trajectories gained frequency in the two decades between 1994 and 2013 and the increasing trend is statistically significant in spring (1.34 % year^{-1}) and autumn (0.91 % year^{-1}), which would amount to total increases of 26.8% and 18.2=% by the end of the two decades. As is discussed in the PSCF analysis, the NW trajectories are associated with high ozone concentrations during all seasons (Figure 1) and thus an increase in ~~its~~their occurrence frequency would lead to an increase in surface ozone concentration at WLG. The SE trajectories are also often accompanied by high ozone concentrations, representing possible transport of ozone precursors that are of anthropogenic sources from Sichuan, Southeast China and Southeast Asian countries to WLG. However, the SE trajectories have been significantly decreasing in spring, summer and autumn, with the strongest decrease found in summer (-1.87 % year^{-1}), suggesting that changes in air mass origin alone cannot explain the seasonal ozone trends measured at WLG.

Table 1 shows an increasing trend in the occurrence frequency of E trajectories in the 24h average directions, but not in the 168h average directions. This indicates that, more trajectories from other directions were turning over to the east of WLG 24h before their arrival at the site. During spring and autumn, only an increase in the 168h NW trajectories was found, while during summer, increases were both found in the 168h W and NE trajectories, these increases are highly possibly linked to the increase in 24h E trajectories. The SE 24h trajectories~~ at in the 24h~~, however, show significant decreasing trends in spring, summer and autumn, with the strongest decrease in summer. This is consistent with the 168h results, suggesting that the entire SE air-mass transport pathway decreased in frequency.

Since the NW direction is often linked to high ozone concentrations according to the PSCF and a significant increase in 168h trajectory occurrences from that direction has been detected, a more detailed examination on that part of the trajectories is ~~highly~~ necessary. ~~After careful examination, it was found that the trajectories starting off in the NW direction mostly bended to the W and E direction or stayed on the NW path. Figure 3~~Figure 3 displays the occurrence frequency of 168h average trajectories in the NW ~~direction~~sector that turned to the E, NW and W ~~direction~~sector in the last 24h, with the lines indicating the according decadal linear variation trends. It can be seen that, more and more NW trajectories ~~bended~~bent to the E ~~direction~~sector before arriving at WLG, with significant trends in all seasons and ~~a~~the largest increasing slope in spring. The trajectories originating from the NW and staying on the NW path throughout the transport process take up a relatively smaller proportion compared to the other two pathways and do not show any significant variation trends throughout the two decades. Trajectories turning to the W ~~direction~~sector are most common and they are gaining in frequency in spring, autumn and winter, with autumn showing the largest increasing slope (0.79 % $year^{-1}$). Trajectories staying in the NW and those bending to the W are more likely to keep their original air-mass properties and may therefore show higher ozone concentrations than the air-masses turning to the E ~~direction~~sector. Our previous work (Xu et al., 2016) shows that the largest ozone increase occurs in autumn, followed by spring, and the increasing trend in summer is not significant. This may be partly explained by the fact that the 168h NW trajectory frequency increase is not as large in summer as in spring and autumn and more NW trajectories are turning to the E ~~direction~~sector (low ozone) during summer than in the other seasons.

3.2 Impacts of stratospheric exchange versus regional anthropogenic emission trends

We next examine a suite of GFDL-AM3 simulations designed to isolate the response of ozone to changes in meteorology, stratospheric exchange and anthropogenic emission trends. ~~Figure 4~~Figure 4 shows year-to-year variation and long-term trends of observed and modelled ozone at WLG, as well as the modelled stratospheric contribution (O_3Strat), for the four seasons over the period 1980-2014. GFDL-AM3 captures some inter-annual variation of observed surface ozone anomaly, with the correlation coefficient ranging from 0.5 to 0.7 for spring, summer and autumn. The correlations between the observed and modelled ozone anomaly are significant at the 90% confidence level in all seasons except winter. The model fails to reproduce the small observed ozone variability in winter. The modelled ozone trends during 1994 to 2013 are 0.30±0.10 ppbv $year^{-1}$ for spring, 0.25±0.10 ppbv $year^{-1}$ for summer, 0.26±0.11 ppbv $year^{-1}$for autumn, and 0.13±0.16 ppbv $year^{-1}$ for winter. Compared with the observed ozone trends, the modelled spring, summer and winter trends are slightly overestimated, while the autumn trend is slightly underestimated, but the overall increasing trend is well reproduced by the model.

A stratospheric ozone tracer implemented in GFDL-AM3 (O_3Strat; Sect. 2.5) enables us to quantify the stratospheric contribution to variability and trends of ozone measured at WLG. Prior analysis of daily ozonesondes, water vapour, and lidar measurements indicates that variability in AM3 O3Strat represents the episodic, layered structure of ozone enhancements in the free troposphere consistent with the observed characteristics of deep stratospheric intrusions (Lin et al., 2012b; Lin et al., 2015a; Langford et al., 2015). Sampling AM3 O_3Strat at WLG indicates that the stratospheric influence can explain 23% (r=0.48) of the observed ozone interannual variability at WLG in spring (Fig.4a) but contributes little to observed variability in other seasons (r<0.1; Fig.4b-d). AM3 O_3Strat shows ~~a significant~~an increasing trend of 0.19±0.18 ppbv year^{-1} ($p<0.05$) over the 1994-2013 period during spring, which can explain 59% of the simulated and 70% of the observed total surface ozone trend, indicating the importance of STT on raising springtime surface ozone measured at WLG over the past two decades (Fig.4a). The largest stratospheric influences are found in the springs of 1999 and 2012 when O_3Stratshows an enhancement coinciding with the observed high-ozone anomaly ~~(Figure 4a).~~(Figure 4a). We will further discuss the mechanisms driving these ozone enhancements in Sect. 4. During the other seasons, in contrast, O_3Strat reveals insignificant trends at the 95% confidence level and shows weak correlations with the observed ozone (Fig.4b-d). These results indicate that ozone from STT is the dominant contributor to the modelled increase in springtime ozone at WLG but it cannot explain the observed significant ozone increases in autumn.

To evaluate the effect of pollution transport from Southeast and East Asia, we filter ozone in the AM3 BASE simulation with the East Asian CO tracer (EACOt; see Sect.2.5). Following the approach of Lin et al. (2015b; 2017) for western U.S. sites, we use EACOt to identify days when WLG is strongly influenced by polluted airflow from Southeast Asia (including China) (i.e., EACOt greater than its 67th value during each season). Figure 5 shows the trends of ozone from observations, the BASE simulations and the simulated ozone trends under conditions with strong transport from Southeast Asia ($O_{3,EA}$) for the four seasons. During autumn, the simulated trend of ozone increases to 0.38±0.11ppbv year^{-1} under the dominant influence from Southeast Asian air masses, compared to 0.26±0.11 ppbv year^{-1} from the BASE simulation and 0.28±0.12 ppbv year^{-1} from observations (Fig.5c). Similar increases are found for summer when the model is filtered for the East Asian influence (Fig.5b). In contrast, the simulated ozone trend at WLG during spring shows little change from the BASE simulation when filtered for the Southeast Asian influence (Fig.5a), supporting our previous conclusion that the stratospheric influence is an important driver of springtime ozone trends measured at WLG (Fig.4a). We do not expect a decrease in springtime ozone when filtering the model for the East Asian anthropogenic influence, i.e., air masses with lower stratospheric influence, owing to the offsetting effects of increasing East Asian emissions.

To separate the influences of changes in transport patterns and anthropogenic emission trends, we compare trends of seasonal mean ozone at 700 hPa simulated by GFDL-AM3 with time-varying (BASE) and constant anthropogenic emissions (FIXEMIS) over 1995-2014 ~~(Figure 6).~~(Figure 6). With both emissions and meteorology varying, AM3 BASE simulates increasing free tropospheric ozone trends of as large as 1 ppbv year^{-1} throughout Southeast Asia and Northern Asia for both spring and autumn (Fig.6a and 6c). With emissions held constant in time, AM3 FIXEMIS shows very weak and insignificant ozone trends in Southeast Asia below 30N latitude (Fig.6b and 6d). During spring, however, FIXEMIS simulates significant ozone increases of 0.2 ppbv year^{-1} extending from Siberia to Northeastern China and to the subtropical Pacific Ocean (Fig.6b). This finding is consistent with our time-series analysis that increasing ozone in the Northwest flow from STT contributes to raising springtime ozone at WLG (Fig.3a and Fig.4a). The stratospheric influence can explain two thirds of the total ozone increase at WLG in spring, with increases in Asian emissions ~~and probably also air masses from the NW sector (Table 2)~~ contributing the rest one third. During autumn, AM3 shows strong ozone increases across the Asian continent in the BASE simulation but simulates little overall ozone trends (<0.05 ppbv year^{-1} around WLG) in FIXEMIS (Fig.6c versus 6d), indicating that the observed autumnal ozone increase at WLG reflects the influence from increases in regional anthropogenic precursor emissions in Southeast Asia as opposed to changes in air mass origin.

In summary, the AM3 modelling results clearly show that the spring and autumn increases in WLG surface ozone are governed by different processes. Observed increases in springtime ozone at WLG over the 1994-2013 period are linked to decadal variability in stratospheric ozone input in the northwest airflow, while the autumnal increase of ozone at WLG results from pollution transport from Southeast Asia, where NO_x emissions have increased markedly over the last two decades. Notably, surface ozone increases during autumn in AM3 BASE are most pronounced over the subtropical southeast Asian regions (south of 35°N; Fig.7a), consistent with the observed surface ozone increase at Hong Kong in South China during autumn (Wang et al., 2009). The model shows somewhat decreasing surface ozone trends in the North China Plain during autumn (Fig.7a), consistent with observations at Shangdianzi near Beijing and Linan near Shanghai (data not shown), indicating a NO_x-saturated ozone production. This north-to-south transition from NO_x-saturated to NO_x-sensitive O_3 production regimes during non-summer seasons has also been observed over the eastern U.S. ~~(Lin et al., 2017)~~(Lin et al., 2017). Increasing ozone produced from regional anthropogenic emissions in Southeast Asia during autumn is lofted into the FT via deep convection and mid-latitude storms and is further transported in southern and southwesterly airflow towards WLG (Fig. 7b). This interpretation is consistent with one previous modeling study showing that WLG is more heavily influenced by pollution transported from Southeast Asia in autumn than in spring ~~(Liu et al., 2002)~~(Liu et al., 2002).

3.3 Impacts of background ozone transport versus local precursor emissions

~~Ozone is a secondary air pollutant and has a lifetime of several weeks in the FT, which make it complicated to explain the origin of the measured ozone concentration. Local photochemical production can enhance O_3 at WLG, if higher levels of O_3 precursors are transported to the site. However, due to the nonlinear relationship of ozone to NO_x and VOC emissions, O_3 can be titrated under high NO_x conditions, resulting in a decrease in concentration. Estimates of the chemical budget suggest that O_3 at WLG was net destroyed under the conditions in July of 1996(Ma et al., 2002). O_3 levels in eastern China are high and have been on the rise during the past two decades(Ding et al., 2008;Wang et al., 2012;Ma et al., 2016;Xu et al., 2008;Wang et al., 2009;Wang et al., 2017b;Sun et al., 2016a), hence there the direct transport of ozone plumes within the troposphere will also have an impact on the ozone trend at WLG. In this section the impacts of direct ozone transport versus that of ozone precursors are discussed.~~

The impact of direct troposphericWe next examine the impacts of local photochemical production versus large-scale background ozone transport to WLG. The impact of direct ozone transport on ozone trends at WLG are studied by combining the 3-D TOST data from (Liu et al., 2013)(Liu et al., 2013) with the back trajectory analysis (section 2.4). Different from the GFDL-AM3 FIXEMIS simulation discussed in Section 3.2, the TOST approach discussed in this section does not eliminate the impacts from increases in Asian anthropogenic emissions. The TOST dataset is based on trajectory-mapped ozone soundings (Liu et al., 2013). The monthly averages of ozone in each grid should contain signals of background ozone and ozone produced within the grid from precursors emitted by anthropogenic and natural sources. with the back trajectory analysis results (section 2.4). Therefore, mean values in the TOST dataset account for not only ozone changes due to transport but also ozone changes associated with varying global-to-regional anthropogenic and natural emissions.

The seasonal average distribution of ozone contribution to WLG through direct tropospheric transport during 1994-2013 is shown in Fig. 8. It can be noted that the distribution varies with season. Spring shows a major contributionFor winter and spring, the TOST analysis indicates major contributions from the western edge of the Tibetan Plateau and a small contribution from Central China to the east of WLG (Fig. 8a). Large contributions from the northwestern to the eastern sector are found in summer, including contributions from Mongolia, Inner Mongolia, Central and Eastern China, where high ozone levels can be observed during summertime. AutumnDuring autumn, WLG is strongly influenced by transport from Central and Eastern China and less by the NW sector, while winter. This finding is underconsistent with the strong influence of transport from the western sectorAM3 attribution results that increases in East Asian anthropogenic emissions contribute to raising autumnal ozone measured at WLG.

Fig. The9 shows the trends of the ozone transport contribution in different seasons were calculated and are depicted in based on the TOST analysisFig. 9. Spring shows a significantly increasing contribution from the north-to-northwest of WLG and significantly decreasing contribution from the western sector, where the average contribution in spring is largest (see Fig. 8a). Statistically significant increases with small slopes were found in Central Asia and East Europe during summer and winter (Fig.9b, d). Significant increasing trends in ozone contribution with relatively large slopes (>0.5 ppbv year^{-1}) can be seen in Central and Eastern China during autumn, while slower increases exist in the western, north western and northern sectors.

TheTable 2 summarizes the total contribution of direct ozone transport to WLG ozone concentration can be calculated for each month and the total and seasonal trend is calculated and listed in Table 2.The overall trend (0.28±0.30 ppbv year^{-1}) and that inseason for the annual mean. The rate of ozone change derived from the TOST dataset for spring (0.27±0.30 ppbv year^{-1}) and summer (0.16±1.11 ppbv year^{-1}) agreeagrees well with the observed trends those derived from in situ observations at WLG (Xu et al., 2016), however, theythe trends derived from the TOST datasets are not statistically insignificant at (p<0.1).significant. This suggests that while important, the transport contribution is highly variable, or that the uncertainty in this calculation method is large. The autumn trend from TOST (0.56±0.54 ppbv year^{-1}) is much larger than the observed trend (0.28±0.11 ppbv year^{-1})and has passed the 90% significance test, and is relatively significant (p<0.1), indicating that tropospheric ozone transport has significantly elevated the level of autumn ozone at WLG. No trend was detected in winter, indicating that the ozone trend observed at WLG during winter was not caused by cannot be attributed to tropospheric ozone transport.

It is noted that the contribution of direct ozone transport to WLG ozone trend is not independent of impacts from the increases of anthropogenic emissions as discussed in section 3.2. The TOST dataset is based on trajectory-mapped ozone soundings (Liu et al., 2013). The monthly averages of ozone in each grid should contain signals of background ozone and ozone produced within the grid from precursors emitted by anthropogenic and natural sources. Therefore, all the mean values in the TOST dataset already account for ozone changes associated with increases in East Asian (and other regions) anthropogenic emissions. One of the key issues in producing the TOST dataset was the impact of ozone production along the trajectories, which might cause errors in the mapped ozone data. A careful assessment indicates that the errors are mostly small and insignificant (Liu et al., 2013). Our approach of using TOST data is similar to the forward mapping in Liu et al. (2013), with the difference that we focus on the impacts on ozone in the WLG grid from the surrounding grids.). Therefore, it is likely that the impact of ozone production along the trajectories during their residence time on our results is small, as in the case of Liu et al. (2013). As the bottom layer of the grid in which WLG resides is excluded in our calculations, direct impacts on our results from regional emissions in the grid containing WLG can be ruled out.

Influences from increasing anthropogenic precursor emissions should mostly come from the east of WLG. In Sect 3.1, an increase in trajectories originating in the NW and turning to the E has been found, while the SE trajectories significantly decreased. Under these circumstances, how does the rapid economic development and increased ozone precursor emissions of the cities to the east of WLG influence its ozone level?

Since CO has a relatively longer lifetime among the primary trace gas pollutants, it can be used to check whether WLG is influenced by the increasing anthropogenic emissions to its east. Figure 10 displays the variationLocal photochemical production can enhance O_3 at WLG, if higher levels of O_3 precursors are transported to the site. Here we use monthly CO measurements at WLG to infer changes in ozone precursor emissions in cities nearby WLG. Figure 10 displays the trend of observed seasonal average surface CO at WLG during spring, summer, autumn and winter, respectively. A statistically significant trend could increase (1.07 ppbv $year^{-1}$) is only be found in summer, where CO shows a linear increasing slope of 1.07 ppbv $year^{-1}$.. Since summer is the season when WLG is mostly influenced by easterly air-masses, the rising CO level is most likely the result of growing anthropogenic emissions in the regionscities to the east of WLG. UsingNote that trends in CO as a tracer forlevel reported here likely reflect changes in anthropogenic pollution, it is clear that WLG is to a certain extent influenced by the growing primary air pollutant emissions to its eastin the cities near WLG rather than changes in anthropogenic emissions in Eastern China.

To investigate the relative importance of the influence from the growing emissions east of WLG, the trajectories and the associated ozone concentrations were grouped into four groups (SW, NW, NE and SE) according to the t=-24h trajectory directions. The trends and the according confidence intervals of the monthly average ozone concentrations associated with different air-mass origins were calculated using the seasonal Mann-Kendall trend analysis and listed in Table 3. It can be noted that, the ozone associated with all trajectory directions showed statistically significant upward trends during 1994 to

2013 at a confidence level of 95%. The eastern sectors (NE and SE) display larger slopes than the western sectors (NW and SW). The largest ozone trend was associated with the SE direction, reaching 0.26 (0.19-0.34), 0.35 (0.26-0.44), 0.28 (0.21-0.35) ppbv year^{-1} respectively for the all-day, daytime and nighttime data subsets. The smallest ozone trend was associated with the NW direction, reaching 0.13(0.08-0.19), 0.14 (0.07-0.19), 0.11 (0.06-0.19) ppbv year^{-1} respectively for the all-day, daytime and nighttime data subsets. This indicates that easterly trajectories, which are more likely to be influenced by anthropogenic emissions of ozone precursors, are associated with larger ozone trend than westerly trajectories, ~~confirming~~suggesting that anthropogenic influence from the east is also leading to the increase of ozone at WLG.

In all, the increase in ozone at WLG is both influenced by direct tropospheric ozone transport and rising precursor emissions in the eastern sector. The increase in direct transport of ozone to WLG only led to a significant rise in autumnal ozone, which supports the conclusions from the modelling study in Sect. 3.2.

4 Atmospheric dynamics and ozone variability at WLG

4.1 Stratosphere-to-troposphere transport and jet characteristics

Due to the transient, localized nature of stratospheric intrusions, diagnosing the presence of stratospheric influence in near-surface ozone requires precise, high-frequency (a few minutes), and co-located measurements of ozone, CO, water vapor and surface wind gust at remote sites (see Langford et al., 2015). These measurements are not available at WLG. Thus, we rely on a global model that has been previously shown to be able to represent deep stratospheric intrusions~~.~~ (Lin et al., 2012a;Lin et al., 2015a).

The highest ozone concentrations at WLG during spring were observed in 1999 and 2012, coinciding with the largest stratospheric ~~influences~~influence simulated in the GFDL-AM3 model (Fig.4a). In contrast, the springs of 1998 and 2007 experienced lower observed ozone and simulated stratospheric influence. In this section we investigate the links of these ozone anomalies to changes in the structure of the jet stream. The top panels of Figure 11 show time series of observed daily surface ozone and modelled O_3Strat at WLG from March to May in 1999 and 2012, with the STT ozone transport events marked as the pink shades. During STT events, peaks are found both in observed surface ozone and modelled O_3Strat, accompanied mostly by enhancements in PV and ozone in the ERA-interim data, as illustrated for March 30, 2012 (Figure 12). A low pressure system ~~sits~~sat over Northeast China on March 30, 2012 ~~(Figure 12a).~~(Figure 12a). The WLG observatory was located ahead of a strong high pressure ridge and behind the low pressure trough. The strong northerly airflow behind the low pressure system and ahead of the ridge led to the transport of a high PV airmass to the south, which is clearly visible on the 250hPa PV field ~~(Figure 12b~~(Figure 12b). A filament of high PV bends to the west and reaches up to 7 PVU over WLG. The midlatitude jetstream (U wind >35 m s^{-1}; red dots in Fig.12c) extended up to 33°N, with a tropopause fold found to its north. Easterly airflows can be detected north of the tropopause fold, which together with the subtropical jet stream has forced the high PV airmass to bend to the west at the latitude of WLG, directly influencing the STE process over WLG. The cross-section of ozone from ECMWF shown in ~~Figure 12d~~Figure 12d displays a similar contour shape to the PV cross-section and strong downward winds over WLG, indicating downward intrusions of stratospheric ozone into the troposphere.

Analysis of 200hPa zonal wind anomalies from the NCEP reanalysis indicates strengthening of the midlatitude jet stream across the Tibetan Plateau during the springs of 1999 and 2012, with the centre of the jet stream shifted to the north towards WLG compared to the 1994-2013 mean state (Fig.11b). These circulation anomalies facilitate the formation of tropopause folding and transport of stratospheric ozone into the FT above WLG, consistent with frequent STT events as identified by GFDL-AM3 O_3Strat (Fig.11a). For comparison, the strength of the jet stream across the Tibetan Plateau was weakened during the springs of 1998 and 2007, leading to weaker stratospheric influence at WLG. In particular, the location of the subtropical jet was shifted to the south far away from WLG in spring 1998 following a strong El Nino winter. These interpretations are consistent with the findings of Lin et al. (2015a), who showed frequent stratospheric intrusions and high surface ozone events during the springs of 1999 and 2012 when the polar jet stream was unusually contorted over the western United States. Stratospheric intrusions over the subtropics are found most frequently along the subtropical jet stream, where the tropopause break is located (e.g. Homeyer et al., 2012 and Sprenger et al., 2003).Tropopause folds are typically located to the north of the subtropical jetstream, hence the location of the jet stream directly influences the location of the STE event. If the jet ~~is~~were located more to the south, the stratospheric ozone input might not reach WLG. For the springs of 1999 and 2012, the average subtropical jet locations (latitude) at the longitude of WLG for STE cases are respectively 2.5 and 3.4 degree more north than those for non-STE cases. This supports the view that the shift of the jet to the north pushes the location of the tropopause ~~fold~~folding to the north, which then leads to STE processes over the WLG region.

4.2 Modes of atmospheric circulation

The time-series of surface ozone at WLG was decomposed into five intrinsic mode functions (IMFs) with different periodicities using the HHT analysis in combination with the empirical mode decomposition (EMD) ~~(Xu et al., 2016)~~(Xu et al., 2016). The 1st IMF shows high frequency, representing variations associated with synoptic systems. The 2nd IMF, with a periodicity of one year, represents seasonal variation and made the largest contribution to the variability of ozone. The other IMFs played minor roles in the variations of ozone. However, these IMFs are interesting because they are related to the 2－4-year, 7- year and 11-year periodicities found in the ozone data and contribute to the interannual variability of ozone at WLG. There are many oscillations within the atmospheric circulation with different periodicities, e.g. QBO with a quasi-2-year periodicity and ENSO with a 2 to 7-year periodicity~~.~~ ~~(Xu et al., 2016)~~(Xu et al., 2016). Here, we explore potential links of some atmospheric circulation oscillations to the variations of surface ozone at WLG ~~(Xu et al., 2016)~~(Xu et al., 2016). Since nighttime ozone concentrations at WLG are more representative of the free-tropospheric air condition, IMFs of the nighttime ozone data are applied in the following analysis.

Previous studies concluded that column ozone over the Tibetan Plateau bears a QBO signal with the same phase as the tropical stratospheric wind QBO, which is caused by the increase and decrease in tropopause height over the Plateau region, as the tropical stratospheric winds shift from easterly to westerly (Ji et al., 2001)(Ji et al., 2001). The 3rd IMF of the nighttime surface ozone data reveals a periodicity closest to that of the QBO index. The comparison between the QBO index and the 3rd IMF is displayed in Figure 13.Figure 13. It can be discerned that, the normalized 3rd IMF and the QBO index show a positive correlation during nighttime ($r=0.29$, $p<0.01$). The peaks and valleys coincide well with each other during 1994-2002 and 2011-2013. During 2003-2010, the QBO index displays four peaks, while the 3rd IMF only shows two peaks. This suggests that surface ozone at WLG was indirectly linked to the QBO; however, the EMD analysis was not fully able to extract the QBO signal during 2003-2010 probably due to the interference of other signals or the abnormally long QBO period from 1998 to 2001. This link of surface ozone to the QBO cancannot be explained by the finding of Ji et al. (2001) because surface ozone is different fromindependent of total column ozone and the GFDL-AM3 O_3Strat is not correlated with the QBO index.

Although the QBO is an atmospheric oscillation in the stratosphere, its dynamical and chemical effects are not limited to the stratosphere but can propagate downward to the Earth's surface and upward to the mesosphere (Baldwin et al., 2001)(Baldwin et al., 2001).. Some mechanisms have been proposed to show how the QBO can change the large scale circulations and exert impacts on the tropospheric winds, temperature, etc. (e.g., Collimore et al., 2003; Kwan and Samah, 2003). To see the possibility of a QBO influence on surface ozone at WLG, correlations between the QBO index and zonal as well as meridional wind were calculated for different pressure levels. Figure 14 shows the correlation coefficients for the 500 hPa and 700 hPa levels. As can be seen in Figure 14, there is a large zone of positive correlation between the annual QBO index and zonal winds at both levels, extending from western Asia to central Asia to the middle of Russia. There is also a large zone of positive correlation between the annual QBO index and meridional winds at both levels, extending from the north of Indian Ocean to central Asia to Russia. The results suggest that when the QBO is in its positive phase, westerly and southerly winds over large areas west, northwest and north of China are increased. Similar zones of positive correlations exist also between the annual QBO index and air temperatures at different pressure levels, with a warming of 0.01–0.04℃ per unit increase in the QBO index (Figure S2). These periodic changes in air circulations and temperature might have influenced the transport of ozone and its precursors and the photochemical conditions. In fact, we can see significant positive correlations of the QBO index with the 3-8 km TOST ozone columns over some areas west and north of China (Figure 15). As the FT air over these areas can influence surface ozone at WLG through long-range transport (see Figure 1), we can expect a small signal in ozone at WLG that is related to the periodic changes in tropospheric ozone over areas west and north of China, caused indirectly by the QBO. The 3rd IMF reported in Xu et al. (2016) may be such a signal. There are other ways that the QBO influences the ozone distribution. For example, Hudson (2011)For example, Hudson (2011) reported than the QBO can cause a few degrees of poleward movement of the subtropical jet streams and a shift of the subtropical front towards the pole. At present, it is not clear whether or not this mechanism influenced our ozone measurement. To better understand the QBO influence on surface ozone at WLG, a comprehensive modelling study is necessary, which is out of the scope of this paper.

The EASM, ENSO and other circulation-related factors might influence surface ozone at WLG through the change of the precipitation or thevia STE processes. However, these influencing factors are often coupled with each other and a direct relationship between surface ozone observations and these factors might be hard to determine.

The correlation coefficients between surface ozone concentrations, precipitation and the EASM index (EASMI) for June, July and August is listed in ~~Table 4.~~Table 4. Only during July, a significant negative correlation (r=-0.59, significant at a 99% confidence level) could be detected between the ozone concentration and the EASMI, which coincides with the significant correlation between the precipitation rate and the EASMI (r=-0.47, significant at a 95% confidence level). However, no significant relationship was found between ozone and precipitation, indicating that the precipitation might not be the only or the most dominant process through which the EASM influences ozone.

To investigate the possible impact of the EASM on the STT processes at WLG, the average location of the subtropical jetstream for the top and bottom 15 percentile EASMI cases and the correlation coefficients between the 200hPa zonal wind and the EASMI in June, July and August from 1990 to 2015 were calculated and are displayed in ~~Figure 16a1-c1).~~Figure 16a1-c1). The jetstream location (dashed and solid black lines in Figure 16a1) near WLG does not change in June for strong (EASMI>85th) and weak (EASMI<15th) EASM years, however, a significant positive correlation band between the zonal wind and the EASMI is found over WLG along the subtropical jet, indicating that during strong EASM years, the subtropical jetstream strengthens as well. In July and August, the subtropical jetstream shifts north away from WLG during strong EASM years and shifts to the south towards WLG during weak ones. In ~~july~~July, the jetstream during weak EASM years is associated with significant negative correlation between zonal wind speed and EASMI, indicating that the jet gains strength during weak EASM years. The shift in subtropical jetstream location leads to changes in STT, which is confirmed by the ~~simulations~~simulation results of the stratospheric contribution ~~(Table 5).~~(Table 5). The modelled monthly O_3Strat data were associated with the EASMI, to filter out O_3Strat for weak and strong monsoon years. Results reveal that, O_3Strat concentrations during weak monsoon years are 10%, 19% and 27% higher than those during strong monsoon years in June, July and August, respectively.

The EASM can also change the atmospheric circulation and thus change transport processes over WLG. The average 500 hPa geopotential height distribution is shown in ~~Figure 16a2~~Figure 16a2-c2 and the locations where the geopotential height ~~are~~is significantly correlated to the EASMI are marked by + and – signs according to the sign of the correlation coefficients. It can be seen that, WLG is located behind a ridge, which is why WLG is often governed by northwesterly air flows. The center of the western Pacific subtropical high pressure belt shifts northwards during June to August. At the same time a strong low pressure system forms over India and reaches its strongest state in July. The location of the convergence belt between the Indian low and the subtropical high seems to ~~be most in~~ favour ~~of~~ transport from eastern China during July. Strong negative correlation exists between the EASMI and the 500hPa geopotential height to the south of WLG during June to August, while in July the negative correlation exists mostly to the east of the Indian low. The negative correlation in July suggests that the subtropical high is enhanced during July in weak monsoon years, without weakening the Indian low. This is probably the cause of an increased ozone concentration (6%) associated with high EACOt during weak monsoon cases in comparison to strong monsoon cases during July (Table 5). Additionally, increased ozone concentrations are also observed in those associated with high NACOt (4%) during July. June and August both display decreased ozone concentrations associated with the high EACOt and NACOt during weak monsoon years.

In summary, weak monsoon years ~~are in~~ favour ~~of the~~ STT ozone transport, especially during July and August, and the circulation pattern during weak monsoon years favours the horizontal transport of ozone to WLG during July, which ~~resulted~~results in ~~the overall effect of~~a strong negative correlation between the EASMI and the ozone concentrations in July. These results are in ~~contradiction with the modelling study by Yang et al. (2014)~~contrast with the modelling study by Yang et al. (2014), which suggested that summer ozone concentrations over the Tibetan Plateau were positively correlated to the EASMI.

4.3 The impact of solar activities

It is well known that changes in incoming solar ultraviolet radiation can cause solar cycle signals of ozone in the stratosphere ~~(Maycock et al., 2016)~~(Maycock et al., 2016). A solar cycle signal was also found in the tropospheric ozone column data over the Tibetan Plateau ~~(Huang et al., 2009)~~(Huang et al., 2009), with an increase of 4% in tropospheric ozone from solar minimum to solar maximum. Here, we investigate the impact of solar activities on surface ozone trends at WLG by comparing the normalized 1-year running average SSN with the normalized daytime and nighttime 5^{th} IMF of monthly average ozone that were obtained in our previous study ~~(Xu et al., 2016)~~(Xu et al., 2016). Results are displayed in ~~Figure 17,~~Figure 17, which shows that both the daytime and nighttime 5^{th} IMF are positively correlated to the SSN, with daytime ($r=0.70$, $p<0.01$) showing a better correlation than nighttime ($r=0.43$, $p<0.01$). During the 1994-2013 period, there were two valleys of the SSN respectively in 1996 and 2008 and two broad peaks respectively during 2000-2002 and 2012-2014. The occurrence time of the two valleys in the daytime 5^{th} IMF agrees well with that of the SSN, while the first peak shows a delay of 1-2 years. The nighttime 5^{th} IMF displays both delayed valley in 1997 and peak in 2004.

The positive correlation between the 5^{th} IMF and the SSN explains the 11-year periodicity found in the ozone data. Solar activity led to surface ozone variations within the range of ±0.5 ppbv over the period of 1994 to 2013 (see Fig. 6 in Xu et al., 2016). Both our result and that of Huang et al. (2009) indicate a positive impact of solar maximum on the ozone level. ~~However, Chandra et al. (1999)~~However, Chandra et al. (1999) obtained a 12.6% reduction in tropospheric column ozone over the tropics from solar minimum to solar maximum. They attributed this reduction to tropospheric ozone photochemistry under the condition of low NOx and high relative humidity, modulated by changing UV radiation related to solar cycle. ~~Both meteorological and photochemical conditions~~The opposite effect would be expected in the high-NOx regime over the Tibetan ~~Plateau differ from those over the tropics. Therefore, it is not surprise to see the different impacts of solar cycle on ozone over different regions.~~plateau. However, ~~detailed~~ details of the mechanism ~~about~~of the solar cycle response of tropospheric and surface ozone over the Tibetan Plateau ~~is unclear and~~ remains to be investigated.

5 Multivariate regression of surface ozone at Waliguan

The above analysis suggests that surface ozone at WLG can be influenced by various factors. Some of these factors mainly disturbed the seasonal variation of ozone and contributed to the inter-annual differences, others contributed also to the observed long-term trends. To quantify the contributions of different factors to surface ozone at WLG, a multivariate regression was performed, with normalized monthly ozone concentration being dependent and time and the potential influencing factors being independent variables. All candidate independent variables, e.g., the QBO index, the NAO index, the SSN, the modelled O_3Strat, the NW trajectory frequency (f(NW)), the SE trajectory frequency (f(SE)),and the calculated direct transport contribution of tropospheric ozone ($O_{3,trop}$),were converted to normalized monthly values. The regression equation takes the form described in Sect. 2.6.

The regression was conducted stepwise to avoid overfitting. The coefficient of determination (R^2) and residual sum of squares (RSS) were calculated after each step of the regression. Correlation coefficients were calculated between the residual and all remaining variables. The variable that correlates best with the residual was chosen as the next independent variable to be included in the model. The regression stopped when the changes in R^2 and RSS were less than 1%. The first step of the regression was to fit the third order harmonic function (6) to the normalized ozone data. Five factors (i.e., O_3Strat, $O_{3,trop}$, SSN, f(NW), and QBO index) were successively included in the regression and became independent variables. Changes of R^2 and RSS after each step are shown in the supplement (Fig. S3). The regression coefficients are listed in ~~Table 6.~~Table 6. An empirical model for normalized monthly ozone at WLG is obtained by integrating the regression coefficients in ~~Table 6~~Table 6 into equations (5)-(7). This empirical model is used for the calculation of normalized monthly ozone at the site.

~~Figure 18~~Figure 18 shows a comparison between the calculated and observed ozone, together with the calculated contributions of the influencing factors to the normalized monthly ozone at the site. It can be seen that the calculated normalized ozone reproduces well the observed one (R^2=0.92). The differences (residual) between the observed and calculated normalized ozone are within ±0.25 and mostly within ±0.10. An ozone trend of 0.25 ppbv year^{-1} is obtained from the observational data, while the calculated ozone data gives a trend of only 0.08 ppbv year^{-1}. The discrepancy can partly be explained by the trend in the residual (0.11 ppbv year^{-1}). The rest should be due to the uncertainties associated with the empirical model as well as the independents.

The regression ~~produced a background signal~~found an annual variation in the normalized ozone, with amplitude of about 0.67 and no trend. The modelled O_3Strat, $O_{3,trop}$, SSN, f(NW) and QBO contribute up to 0.32, 0.17, 0.11, 0.12 and 0.04, respectively, to the calculated normalized ozone. These results indicate that the level of surface ozone at WLG has a basic component (the background signal), which makes the major contribution to the seasonal variation of ozone but has no long-term trend. The background signal is enhanced by varying contributions from STT, tropospheric ozone transport and sunspot number, influenced by changes in the NW trajectory frequencies, and very little by QBO.

6 Conclusions

Through an observational and modelling analysis, we have discussed the key drivers of various periodicities and long-term trends of ozone measured at WLG for the four seasons over the past two decades, previously reported in the companion paper ~~(Xu et al., 2016)~~(Xu et al., 2016). The impact of air mass origin is investigated using backward trajectory analysis combined with PSCF analysis, the influence of STE and increasing anthropogenic emissions in Asia is evaluated using chemistry-climate model hindcasts driven by reanalysis winds (GFDL-AM3; Lin et al., 2017). The impact of direct tropospheric ozone transport on ozone at WLG is examined using 3D tropospheric ozone climatology data (a subset of TOST) combined with the trajectory analysis results.

Our ~~result~~results show that different processes have contributed to the observed increasing ozone trends at WLG during spring versus autumn. Analysis of a stratospheric ozone tracer in GFDL-AM3 indicates that STT can explain ~60% of the simulated and ~70% of the total observed springtime ozone increase over 1994-2013 at WLG (Fig.4a). This interpretation is consistent with an increase in the NW air mass frequency over this period inferred from the trajectory analysis (Fig.3). STT contributes to the observed high-ozone anomalies at WLG during the springs of 1999 and 2012 (Figs 11 and 12), linked to the unusual structure of the jet stream as occurs over the western United States during the same years ~~(Lin et al., 2015a)~~(Lin et al., 2015a). During autumn, observations at WLG are more heavily influenced by polluted air masses originated from Southeast Asia than in the other seasons (Fig.1 and Fig.7). The GFDL-AM3 model captures the observed ozone increase at WLG during autumn (0.26 ± 0.11 ppbv year^{-1}) and simulates a greater ozone increase of 0.38 ± 0.11 ppbv year^{-1} under conditions with strong transport from Southeast Asia (Fig.5c), indicating that rising anthropogenic emissions of ozone precursors in Southeast Asia play a key role in raising ozone observed at WLG during autumn (Fig.6). During summer, WLG is mostly influenced by easterly air masses from the cities to the east of WLG but these trajectories do not extend to the polluted regions of eastern China and have decreased significantly over the last two decades (Fig.2), which likely explains why summertime ozone measured at WLG shows no significant trend despite ozone increases in Eastern China. The direct transport of tropospheric ozone to WLG calculated from the TOST data and trajectory residence time reveals significant increases during autumn mostly coming from the eastern sector (Tab. 2 and Figs. 8 and 9).

The periodicities detected in the HHT analysis of ozone data previously reported by ~~Xu et al. (2016)~~Xu et al. (2016) are linked to various climate indices including EASMI, QBO and sunspot cycle. The 2-3 year periodicity is linked to the QBO and the 3-7 year periodicity could be partly explained by the EASMI, while the 11 year periodicity is well connected to the sunspot cycle.An empirical model is obtained for normalized monthly level of surface ozone at WLG using the multivariate regression technique and used to explain the observed ozone trends. Based on these relationships, an empirical model has been established for normalized monthly ozone through multivariate regression. The regression model reproduces well the observation and can capture about one third of the observed ozone trend.

The results obtained in this work clearly show the complexity of surface ozone in terms of influencing factors. Comprehensive investigations are recommended to understand variations of surface ozone at any sites, in particular the long-term trends. Our work in this paper and the companion paper shows an example of de-convoluting the ozone variations and interpreting those using related dynamical and chemical factors of different scales, which hopefully can inspire similar studies.

Data availability

The ozone data analysed in this work are partly available at the World Data Center for Greenhouse Gases (WDCGG) (http://ds.data.jma.go.jp/gmd/wdcgg/cgi-bin/wdcgg/download.cgi?index=WLG236N00-CMA&param=201405120001&select=inventory). The entire data set can be made available for scientific purposes upon request to the corresponding author (xuxb@camscma.cn). The AM3 global model simulations are archived at GFDL and are available to the public upon request to Meiyun Lin (Meiyun.Lin@noaa.gov).

Acknowledgements

This work is supported by the Natural Science Foundation of China (No.41330422 and 41505107), China Special Fund for Meteorological Research in the Public Interest (No. GYHY201106023), Environmental Protection Public Welfare Scientific Research Project, Ministry of Environmental Protection of the People's Republic of China (No. 201509002), the Key research and development program of the Ministry of Science and Technology (No. 2016YFC0202300) and the Basic Research Fund of CAMS (No. 2016Y006). We thank CMA, NOAA/ESRL and WDCGG for making available the monthly CO data.

References

~~Ara Begum, B., Kim, E., Jeong, C. H., Lee, D. W., and Hopke, P. K.: Evaluation of the potential source contribution function using the 2002 Quebec forest fire episode, Atmospheric Environment, 39, 3719-3724, 10.1016/j.atmosenv.2005.03.008, 2005.~~

~~Baldwin, M. P., Gray, L. J., Dunkerton, T. J., Hamilton, K., Haynes, P. H., Randel, W. J., Holton, J. R., Alexander, M. J., Hirota, I., and Horinouchi, T.: The quasi - biennial oscillation, Reviews of Geophysics, 39, 179-229, 10.1029/1999RG000073, 2001.~~

~~Bonasoni, P., Evangelisti, F., Bonafe, U., Ravegnani, F., Calzolari, F., Stohl, A., Tositti, L., Tubertini, O., and Colombo, T.: Stratospheric ozone intrusion episodes recorded at Mt. Cimone during the VOTALP project: case studies, Atmospheric Environment, 34, 1355-1365, http://dx.doi.org/10.1016/S1352-2310(99)00280-0, 2000.~~

~~Chandra, S., Ziemke, J. R., and Stewart, R. W.: An 11 - year solar cycle in tropospheric ozone from TOMS measurements, Geophysical Research Letters, 26, 185-188, 10.1029/1998GL900272, 1999.~~

~~Creilson, J. K., Fishman, J., and Wozniak, A. E.: Intercontinental transport of tropospheric ozone: a study of its seasonal variability across the North Atlantic utilizing tropospheric ozone residuals and its relationship to the North Atlantic Oscillation, Atmospheric Chemistry and Physics, 3, 2053-2066, 10.5194/acp-3-2053-2003, 2003.~~

~~Derong, Z., Aijun, D., Huiting, M., Congbin, F., Tao, W., Chan, L. Y., Ke, D., Yang, Z., Jane, L., An, L., and Nan, H.: Impacts of the East Asian monsoon on lower tropospheric ozone over coastal South China, Environmental Research Letters, 8, 044011, 2013.~~

~~Ding, A., and Wang, T.: Influence of stratosphere-to-troposphere exchange on the seasonal cycle of surface ozone at Mount Waliguan in western China, Geophysical Research Letters, 33, L03803, 10.1029/2005GL024760, 2006.~~

~~Ding, A. J., Wang, T., Thouret, V., Cammas, J. P., and Nédélec, P.: Tropospheric ozone climatology over Beijing: analysis of aircraft data from the MOZAIC program, Atmospheric Chemistry and Physics, 8, 1-13, 10.5194/acp-8-1-2008, 2008.~~

~~Draxler, R. R., and Hess, G. D.: Description of the HYSPLIT_4 modeling system, NOAA Tech. Memo, ERL ARL-224, NOAA Air Resources Laboratory, Silver Spring, MD, 24 pp., 1997.~~

Draxler, R. R., and Hess, G. D.: An overview of the HYSPLIT_4 modelling system for trajectories, dispersion and deposition, Australian Meteorological Magazine, 47, 295-308, 1998.
Draxler, R. R.: HYSPLIT4 user's guide, NOAA Tech. Memo, ERL ARL-230, NOAA Air Resources Laboratory, Silver Spring, MD, 1999.
Homeyer, C. R.: Chemical and Dynamical Characteristics of Stratosphere-Troposphere Exchange, Atmospheric Sciences, Texas A&M University, 2012.
Huang, F.-X., Liu, N.-Q., and Zhao, M.-X.: Solar Cycle Signal of Tropospheric Ozone over the Tibetan Plateau, Chinese Journal of Geophysics, 52, 913-921, 10.1002/cjg2.1416, 2009.
Hudson, R. D.: Measurements of the movement of the jet streams at mid-latitudes, in the Northern and Southern Hemispheres, 1979 to 2010, Atmospheric Chemistry and Physics, 12, 7797-7808, 10.5194/acp-12-7797-2012, 2011.
Itahashi, S., Uno, I., Irie, H., Kurokawa, J. I., and Ohara, T.: Regional modeling of tropospheric NO2 vertical column density over East Asia during the period 2000–2010: comparison with multisatellite observations, Atmospheric Chemistry and Physics, 14, 3623-3635, 10.5194/acp-14-3623-2014, 2014.
Ji, C. P., Zou, H., and Zhou, L. B.: QBO Signal in Total Ozone Over the Tibet, Climatic and Environmental Research, 6, 416-424, 2001.
Jia, S., Xu, X., Lin, W., Wang, Y., He, X., and Zhang, H.: Increased mixing ratio of surface ozone by nighttime convection process over the North China Plain, Journal of Applied Meteorological Science, 26, 280-290, 2015.
Koumoutsaris, S., Bey, I., Generoso, S., and Thouret, V.: Influence of El Niño–Southern Oscillation on the interannual variability of tropospheric ozone in the northern midlatitudes, Journal of Geophysical Research: Atmospheres, 113, D19301, 10.1029/2007JD009753, 2008.
Kurokawa, J., Ohara, T., Morikawa, T., Hanayama, S., Janssens-Maenhout, G., Fukui, T., Kawashima, K., and Akimoto, H.: Emissions of air pollutants and greenhouse gases over Asian regions during 2000–2008: Regional Emission inventory in ASia (REAS) version 2, Atmospheric Chemistry and Physics, 13, 11019-11058, 10.5194/acp-13-11019-2013, 2013.
Lal, S., Venkataramani, S., Chandra, N., Cooper, O. R., Brioude, J., and Naja, M.: Transport effects on the vertical distribution of tropospheric ozone over western India, Journal of Geophysical Research: Atmospheres, 2014JD021854, 10.1002/2014JD021854, 2014.
Langford, A. O.: Stratosphere-troposphere exchange at the subtropical jet: Contribution to the tropospheric ozone budget at midlatitudes, Geophysical Research Letters, 26, 2449-2452, 10.1029/1999GL900556, 1999.
Langford, A. O., Aikin, K. C., Eubank, C. S., and Williams, E. J.: Stratospheric contribution to high surface ozone in Colorado during springtime, Geophysical Research Letters, 36, L12801, 10.1029/2009GL038367, 2009.
Langford, A. O., Senff, C. J., Alvarez Ii, R. J., Brioude, J., Cooper, O. R., Holloway, J. S., Lin, M. Y., Marchbanks, R. D., Pierce, R. B., Sandberg, S. P., Weickmann, A. M., and Williams, E. J.: An overview of the 2013 Las Vegas Ozone Study (LVOS): Impact of stratospheric intrusions and long-range transport on surface air quality, Atmospheric Environment, 109, 305-322, http://dx.doi.org/10.1016/j.atmosenv.2014.08.040, 2015.
Lee, H. N., Tositti, L., Zheng, X., and Bonasoni, P.: Analyses and comparisons of variations of 7Be, 210Pb, and 7Be/210Pb with ozone observations at two Global Atmosphere Watch stations from high mountains, Journal of Geophysical Research: Atmospheres, 112, D05303, 10.1029/2006JD007421, 2007.
Lefohn, A. S., Wernli, H., Shadwick, D., Oltmans, S. J., and Shapiro, M.: Quantifying the importance of stratospheric-tropospheric transport on surface ozone concentrations at high- and low-elevation monitoring sites in the United States, Atmospheric Environment, 62, 646-656, http://dx.doi.org/10.1016/j.atmosenv.2012.09.004, 2012.
Li, J., and Zeng, Q.: A unified monsoon index, Geophysical Research Letters, 29, 115-111-115-114, 10.1029/2001GL013874, 2002.
Liang, M.-C., Tang, J., Chan, C.-Y., Zheng, X. D., and Yung, Y. L.: Signature of stratospheric air at the Tibetan Plateau, Geophysical Research Letters, 35, L20816, 10.1029/2008GL035246, 2008.
Lin, M., Fiore, A. M., Cooper, O. R., Horowitz, L. W., Langford, A. O., Levy, H., Johnson, B. J., Naik, V., Oltmans, S. J., and Senff, C. J.: Springtime high surface ozone events over the western United States: Quantifying the role of stratospheric intrusions, Journal of Geophysical Research: Atmospheres, 117, D00V22, 10.1029/2012JD018151, 2012a.
Lin, M., Fiore, A. M., Horowitz, L. W., Cooper, O. R., Naik, V., Holloway, J., Johnson, B. J., Middlebrook, A. M., Oltmans, S. J., Pollack, I. B., Ryerson, T. B., Warner, J. X., Wiedinmyer, C., Wilson, J., and Wyman, B.: Transport of Asian ozone pollution into surface air over the western United States in spring, Journal of Geophysical Research: Atmospheres, 117, D00V07, 10.1029/2011JD016961, 2012b.
Lin, M., Horowitz, L. W., Oltmans, S. J., Fiore, A. M., and Fan, S.: Tropospheric ozone trends at Mauna Loa Observatory tied to decadal climate variability, Nature Geoscience, 7, 136-143, 10.1038/ngeo2066, 2014.
Lin, M., Fiore, A. M., Horowitz, L. W., Langford, A. O., Oltmans, S. J., Tarasick, D., and Rieder, H. E.: Climate variability modulates western US ozone air quality in spring via deep stratospheric intrusions, Nature Communications, 6, 10.1038/ncomms8105, 2015a.
Lin, M., Horowitz, L. W., Cooper, O. R., Tarasick, D., Conley, S., Iraci, L. T., Johnson, B., Leblanc, T., Petropavlovskikh, I., and Yates, E. L.: Revisiting the evidence of increasing springtime ozone mixing ratios in the free troposphere over western North America, Geophysical Research Letters, 8719-8728, 10.1002/2015GL065311, 2015b.
Lin, M., Horowitz, L. W., Payton, R., Fiore, A. M., and Tonnesen, G.: US surface ozone trends and extremes from 1980 to 2014: quantifying the roles of rising Asian emissions, domestic controls, wildfires, and climate, Atmospheric Chemistry and Physics, 17, 2943-2970, 10.5194/acp-17-2943-2017, 2017.

Liu, G., Liu, J., Tarasick, D. W., Fioletov, V. E., Jin, J. J., Moeini, O., Liu, X., Sioris, C. E., and Osman, M.: A global tropospheric ozone climatology from trajectory-mapped ozone soundings, Atmospheric Chemistry and Physics, 13, 10659-10675, 10.5194/acp-13-10659-2013, 2013.

Liu, H., Jacob, D. J., Chan, L. Y., Oltmans, S. J., Bey, I., Yantosca, R. M., Harris, J. M., Duncan, B. N., and Martin, R. V.: Sources of tropospheric ozone along the Asian Pacific Rim: An analysis of ozonesonde observations, Journal of Geophysical Research: Atmospheres, 107, 4573, 10.1029/2001JD002005, 2002.

Liu, J. J., Jones, D. B. A., Worden, J. R., Noone, D., Parrington, M., and Kar, J.: Analysis of the summertime buildup of tropospheric ozone abundances over the Middle East and North Africa as observed by the Tropospheric Emission Spectrometer instrument, Journal of Geophysical Research: Atmospheres, 114, D05304, 10.1029/2008JD010993, 2009.

Liu, J. J., Jones, D. B. A., Zhang, S., and Kar, J.: Influence of interannual variations in transport on summertime abundances of ozone over the Middle East, Journal of Geophysical Research: Atmospheres, 116, D20310, 10.1029/2011JD016188, 2011.

Lucey, D., Hadjiiski, L., Hopke, P. K., Scudlark, J. R., and Church, T.: Identification of sources of pollutants in precipitation measured at the mid-Atlantic US coast using potential source contribution function (PSCF), Atmospheric Environment, 35, 3979-3986, 10.1016/s1352-2310(01)00185-6, 2001.

Ma, J., Tang, J., Zhou, X., and Zhang, X.: Estimates of the Chemical Budget for Ozone at Waliguan Observatory, Journal of Atmospheric Chemistry, 41, 21-48, 10.1023/A:1013892308983, 2002.

Ma, J., Zheng, X., and Xu, X.: Comment on "Why does surface ozone peak in summertime at Waliguan?" by Bin Zhu et al, Geophysical Research Letters, 32, L01805, 10.1029/2004GL021683, 2005.

Ma, J., Lin, W. L., Zheng, X. D., Xu, X. B., Li, Z., and Yang, L. L.: Influence of air mass downward transport on the variability of surface ozone at Xianggelila Regional Atmosphere Background Station, southwest China, Atmospheric Chemistry and Physics, 14, 5311-5325, 10.5194/acp-14-5311-2014, 2014.

Ma, Z., Xu, J., Quan, W., Zhang, Z., Lin, W., and Xu, X.: Significant increase of surface ozone at a rural site, north of eastern China, Atmospheric Chemistry and Physics, 16, 3969-3977, 10.5194/acp-16-3969-2016, 2016.

Maycock, A. C., Matthes, K., Tegtmeier, S., Thieblemont, R., and Hood, L. L.: The representation of solar cycle signals in stratospheric ozone – Part 1: A comparison of recently updated satellite observations, Atmospheric Chemistry and Physics, 16, 10021-10043, 10.5194/acp-16-10021-2016, 2016.

Ningombam, S. S.: Variability of sunspot cycle QBO and total ozone over high altitude western Himalayan regions, Journal of Atmospheric and Solar-Terrestrial Physics, 73, 2305-2313, http://dx.doi.org/10.1016/j.jastp.2011.06.015, 2011.

Oman, L. D., Douglass, A. R., Ziemke, J. R., Rodriguez, J. M., Waugh, D. W., and Nielsen, J. E.: The ozone response to ENSO in Aura satellite measurements and a chemistry-climate simulation, Journal of Geophysical Research: Atmospheres, 118, 965-976, 10.1029/2012JD018546, 2013.

Sioris, C. E., McLinden, C. A., Fioletov, V. E., Adams, C., Zawodny, J. M., Bourassa, A. E., Roth, C. Z., and Degenstein, D. A.: Trend and variability in ozone in the tropical lower stratosphere over 2.5 solar cycles observed by SAGE II and OSIRIS, Atmospheric Chemistry and Physics, 14, 3479-3496, 10.5194/acp-14-3479-2014, 2014.

Škerlak, B., Sprenger, M., and Wernli, H.: A global climatology of stratosphere–troposphere exchange using the ERA-Interim data set from 1979 to 2011, Atmospheric Chemistry and Physics, 14, 913-937, 10.5194/acp-14-913-2014, 2014.

Sprenger, M., and Wernli, H.: A northern hemispheric climatology of cross-tropopause exchange for the ERA15 time period (1979–1993), Journal of Geophysical Research: Atmospheres, 108, 8521, 10.1029/2002JD002636, 2003.

Stohl, A., Spichtinger-Rakowsky, N., Bonasoni, P., Feldmann, H., Memmesheimer, M., Scheel, H. E., Trickl, T., Hübener, S., Ringer, W., and Mandl, M.: The influence of stratospheric intrusions on alpine ozone concentrations, Atmospheric Environment, 34, 1323-1354, http://dx.doi.org/10.1016/S1352-2310(99)00320-9, 2000.

Sun, L., Xue, L., Wang, T., Gao, J., Ding, A., Cooper, O. R., Lin, M., Xu, P., Wang, Z., Wang, X., Wen, L., Zhu, Y., Chen, T., Yang, L., Wang, Y., Chen, J., and Wang, W.: Significant increase of summertime ozone at Mount Tai in Central Eastern China, Atmos. Chem. Phys., 16, 10637-10650, 10.5194/acp-16-10637-2016, 2016a.

Sun, L., Xue, L., Wang, T., Gao, J., Ding, A., Cooper, O. R., Lin, M., Xu, P., Wang, Z., Wang, X., Wen, L., Zhu, Y., Chen, T., Yang, L., Wang, Y., Chen, J., and Wang, W.: Significant increase of summertime ozone at Mount Tai in Central Eastern China, Atmospheric Chemistry and Physics, 16, 10637-10650, 10.5194/acp-16-10637-2016, 2016b.

Tang, Q., Prather, M. J., and Hsu, J.: Stratosphere-troposphere exchange ozone flux related to deep convection, Geophysical Research Letters, 38, L03806, 10.1029/2010gl046039, 2011.

van der A, R. J., Peters, D. H. M. U., Eskes, H., Boersma, K. F., Van Roozendael, M., De Smedt, I., and Kelder, H. M.: Detection of the trend and seasonal variation in tropospheric NO2 over China, Journal of Geophysical Research: Atmospheres, 111, D12317, 10.1029/2005JD006594, 2006.

Verstraeten, W. W., Neu, J. L., Williams, J. E., Bowman, K. W., Worden, J. R., and Boersma, K. F.: Rapid increases in tropospheric ozone production and export from China, Nature Geoscience, 8, 690-695, 10.1038/ngeo2493, http://www.nature.com/ngeo/journal/v8/n9/abs/ngeo2493.html#supplementary-information, 2015.

Voulgarakis, A., Hadjinicolaou, P., and Pyle, J. A.: Increases in global tropospheric ozone following an El Niño event: examining stratospheric ozone variability as a potential driver, Atmospheric Science Letters, 12, 228-232, 10.1002/asl.318, 2011.

Wang, R., Xu, X., Jia, S., Ma, R., Ran, L., Deng, Z., Lin, W., Wang, Y., and Ma, Z.: Lower tropospheric distributions of O3 and aerosol over Raoyang, a rural site in the North China Plain, Atmospheric Chemistry and Physics, 17, 3891-3903, 10.5194/acp-17-3891-2017, 2017a.

Wang, T., Ding, A., Gao, J., and Wu, W. S.: Strong ozone production in urban plumes from Beijing, China, Geophysical Research Letters, 33, L21806, 10.1029/2006gl027689, 2006a.

Wang, T., Wong, H. L. A., Tang, J., Ding, A., Wu, W. S., and Zhang, X. C.: On the origin of surface ozone and reactive nitrogen observed at a remote mountain site in the northeastern Qinghai-Tibetan Plateau, western China, Journal of Geophysical Research: Atmospheres, 111, D08303, 10.1029/2005JD006527, 2006b.

Wang, T., Wei, X. L., Ding, A. J., Poon, C. N., Lam, K. S., Li, Y. S., Chan, L. Y., and Anson, M.: Increasing surface ozone concentrations in the background atmosphere of Southern China, 1994–2007, Atmospheric Chemistry and Physics, 9, 6217-6227, 10.5194/acp-9-6217-2009, 2009.

Wang, T., Xue, L., Brimblecombe, P., Lam, Y. F., Li, L., and Zhang, L.: Ozone pollution in China: A review of concentrations, meteorological influences, chemical precursors, and effects, Science of The Total Environment, 575, 1582-1596, https://doi.org/10.1016/j.scitotenv.2016.10.081, 2017b.

Wang, Y., Konopka, P., Liu, Y., Chen, H., Müller, R., Plöger, F., Riese, M., Cai, Z., and Lü, D.: Tropospheric ozone trend over Beijing from 2002–2010: ozonesonde measurements and modeling analysis, Atmospheric Chemistry and Physics, 12, 8389-8399, 10.5194/acp-12-8389-2012, 2012.

Xu, W., Lin, W., Xu, X., Tang, J., Huang, J., Wu, H., and Zhang, X.: Long-term trends of surface ozone and its influencing factors at the Mt Waliguan GAW station, China – Part 1: Overall trends and characteristics, Atmospheric Chemistry and Physics, 16, 6191-6205, 10.5194/acp-16-6191-2016, 2016.

Xu, X., Lin, W., Wang, T., Yan, P., Tang, J., Meng, Z., and Wang, Y.: Long-term trend of surface ozone at a regional background station in eastern China 1991-2006: enhanced variability, Atmospheric Chemistry and Physics, 8, 2595-2607, 10.5194/acp-8-2595-2008, 2008.

Xue, L. K., Wang, T., Zhang, J. M., Zhang, X. C., Deliger, Poon, C. N., Ding, A. J., Zhou, X. H., Wu, W. S., Tang, J., Zhang, Q. Z., and Wang, W. X.: Source of surface ozone and reactive nitrogen speciation at Mount Waliguan in western China: New insights from the 2006 summer study, Jounal of Geophysical Research, 116, D07306, 10.1029/2010jd014735, 2011.

Yang, Y., Liao, H., and Li, J.: Impacts of the East Asian summer monsoon on interannual variations of summertime surface-layer ozone concentrations over China, Atmospheric Chemistry and Physics, 14, 6867-6879, 10.5194/acp-14-6867-2014, 2014.

Zeng, G., and Pyle, J. A.: Influence of El Niño Southern Oscillation on stratosphere/troposphere exchange and the global tropospheric ozone budget, Geophysical Research Letters, 32, L01814, 10.1029/2004GL021353, 2005.

Zeng, Y., and Hopke, P. K.: A studyof the sources of acid precipitation in Ontario, Canada, Atmospheric Environment, 23, 1499-1509, 1989.

Zhang, F., Zhou, L. X., Novelli, P. C., Worthy, D. E. J., Zellweger, C., Klausen, J., Ernst, M., Steinbacher, M., Cai, Y. X., Xu, L., Fang, S. X., and Yao, B.: Evaluation of in situ measurements of atmospheric carbon monoxide at Mount Waliguan, China, Atmospheric Chemistry and Physics, 11, 5195-5206, 10.5194/acp-11-5195-2011, 2011.

Zheng, X. D., Shen, C. D., Wan, G. J., Liu, K. X., Tang, J., and Xu, X. B.: ~(10)Be/~7Be implies the contribution of stratosphere-troposphere transport to the winter-spring surface O_3 variation observed on the Tibetan Plateau, Chin. Sci. Bull., 56, 84-88, 2011.

Zhou, L., Hopke, P. K., and Liu, W.: Comparison of two trajectory based models for locating particle sources for two rural New York sites, Atmospheric Environment, 38, 1955-1963, 10.1016/j.atmosenv.2003.12.034, 2004.

Zhu, B., Akimoto, H., Wang, Z., Sudo, K., Tang, J., and Uno, I.: Why does surface ozone peak in summertime at Waliguan?, Geophysical Research Letters, 31, L17104, 10.1029/2004GL020609, 2004.

Ziemke, J. R., Chandra, S., and Bhartia, P. K.: A 25-year data record of atmospheric ozone in the Pacific from Total Ozone Mapping Spectrometer (TOMS) cloud slicing: Implications for ozone trends in the stratosphere and troposphere, Journal of Geophysical Research: Atmospheres, 110, D15105, 10.1029/2004JD005687, 2005.

Ziemke, J. R., Chandra, S., Oman, L. D., and Bhartia, P. K.: A new ENSO index derived from satellite measurements of column ozone, Atmospheric Chemistry and Physics, 10, 3711-3721, 10.5194/acp-10-3711-2010, 2010.

Zou, H., Ji, C. P., Zhou, L. B., Wang, W., and Jiang, Y. X.: ENSO Signal in Total Ozone over Tibet, Climatic and Environmental Research, 6, 267-272, 2001.

Ara Begum, B., Kim, E., Jeong, C.-H., Lee, D.-W., and Hopke, P. K.: Evaluation of the potential source contribution function using the 2002 Quebec forest fire episode, Atmospheric Environment, 39, 3719-3724, 10.1016/j.atmosenv.2005.03.008, 2005.

Baldwin, M. P., Gray, L. J., Dunkerton, T. J., Hamilton, K., Haynes, P. H., Randel, W. J., Holton, J. R., Alexander, M. J., Hirota, I., and Horinouchi, T.: The quasi‐biennial oscillation, Reviews of Geophysics, 39, 179-229, 10.1029/1999RG000073, 2001.

Bonasoni, P., Evangelisti, F., Bonafe, U., Ravegnani, F., Calzolari, F., Stohl, A., Tositti, L., Tubertini, O., and Colombo, T.: Stratospheric ozone intrusion episodes recorded at Mt. Cimone during the VOTALP project: case studies, Atmospheric Environment, 34, 1355-1365, http://dx.doi.org/10.1016/S1352-2310(99)00280-0, 2000.

Chandra, S., Ziemke, J. R., and Stewart, R. W.: An 11‐year solar cycle in tropospheric ozone from TOMS measurements, Geophysical Research Letters, 26, 185-188, 10.1029/1998GL900272, 1999.

Collimore, C. C., Martin, D. W., Hitchman, M. H., Huesmann, A., and Waliser, D. E.: On The Relationship between the QBO and Tropical Deep Convection, Journal of Climate, 16, 2552-2568, 10.1175/1520-0442(2003)016<2552:otrbtq>2.0.co;2, 2003.

Creilson, J. K., Fishman, J., and Wozniak, A. E.: Intercontinental transport of tropospheric ozone: a study of its seasonal variability across the North Atlantic utilizing tropospheric ozone residuals and its relationship to the North Atlantic Oscillation, Atmospheric Chemistry and Physics, 3, 2053-2066, 10.5194/acp-3-2053-2003, 2003.

Derong, Z., Aijun, D., Huiting, M., Congbin, F., Tao, W., Chan, L. Y., Ke, D., Yang, Z., Jane, L., An, L., and Nan, H.: Impacts of the East Asian monsoon on lower tropospheric ozone over coastal South China, Environmental Research Letters, 8, 044011, 2013.

Ding, A., and Wang, T.: Influence of stratosphere-to-troposphere exchange on the seasonal cycle of surface ozone at Mount Waliguan in western China, Geophysical Research Letters, 33, L03803, 10.1029/2005GL024760, 2006.

Ding, A. J., Wang, T., Thouret, V., Cammas, J. P., and Nédélec, P.: Tropospheric ozone climatology over Beijing: analysis of aircraft data from the MOZAIC program, Atmospheric Chemistry and Physics, 8, 1-13, 10.5194/acp-8-1-2008, 2008.

Draxler, R. R., and Hess, G. D.: Description of the HYSPLIT_4 modeling system, NOAA Tech. Memo, ERL ARL-224, NOAA Air Resources Laboratory, Silver Spring, MD, 24 pp., 1997.

Draxler, R. R., and Hess, G. D.: An overview of the HYSPLIT_4 modelling system for trajectories, dispersion and deposition, Australian Meteorological Magazine, 47, 295-308, 1998.

Draxler, R. R.: HYSPLIT4 user's guide, NOAA Tech. Memo, ERL ARL-230, NOAA Air Resources Laboratory, Silver Spring, MD, 1999.

Homeyer, C. R.: Chemical and Dynamical Characteristics of Stratosphere-Troposphere Exchange, Atmospheric Sciences, Texas A&M University, 2012.

Huang, F.-X., Liu, N.-Q., and Zhao, M.-X.: Solar Cycle Signal of Tropospheric Ozone over the Tibetan Plateau, Chinese Journal of Geophysics, 52, 913-921, 10.1002/cjg2.1416, 2009.

Hudson, R. D.: Measurements of the movement of the jet streams at mid-latitudes, in the Northern and Southern Hemispheres, 1979 to 2010, Atmospheric Chemistry and Physics, 12, 7797-7808, 10.5194/acp-12-7797-2012, 2011.

Itahashi, S., Uno, I., Irie, H., Kurokawa, J. I., and Ohara, T.: Regional modeling of tropospheric NO2 vertical column density over East Asia during the period 2000–2010: comparison with multisatellite observations, Atmospheric Chemistry and Physics, 14, 3623-3635, 10.5194/acp-14-3623-2014, 2014.

Ji, C. P., Zou, H., and Zhou, L. B.: QBO Signal in Total Ozone Over the Tibet, Climatic and Environmental Research, 6, 416-424, 2001.

Jia, S., Xu, X., Lin, W., Wang, Y., He, X., and Zhang, H.: Increased mixing ratio of surface ozone by nighttime convection process over the North China Plain, Journal of Applied Meteorological Science, 26, 280-290, 2015.

Koumoutsaris, S., Bey, I., Generoso, S., and Thouret, V.: Influence of El Niño–Southern Oscillation on the interannual variability of tropospheric ozone in the northern midlatitudes, Journal of Geophysical Research: Atmospheres, 113, D19301, 10.1029/2007JD009753, 2008.

Kurokawa, J., Ohara, T., Morikawa, T., Hanayama, S., Janssens-Maenhout, G., Fukui, T., Kawashima, K., and Akimoto, H.: Emissions of air pollutants and greenhouse gases over Asian regions during 2000–2008: Regional Emission inventory in ASia (REAS) version 2, Atmospheric Chemistry and Physics, 13, 11019-11058, 10.5194/acp-13-11019-2013, 2013.

Kwan, K. F., and Samah, A. A.: A conceptual model relating the quasi-biennial oscillation and the tropospheric biennial oscillation, International Journal of Climatology, 23, 347-362, 10.1002/joc.876, 2003.

Lal, S., Venkataramani, S., Chandra, N., Cooper, O. R., Brioude, J., and Naja, M.: Transport effects on the vertical distribution of tropospheric ozone over western India, Journal of Geophysical Research: Atmospheres, 2014JD021854, 10.1002/2014JD021854, 2014.

Langford, A. O.: Stratosphere-troposphere exchange at the subtropical jet: Contribution to the tropospheric ozone budget at midlatitudes, Geophysical Research Letters, 26, 2449-2452, 10.1029/1999GL900556, 1999.

Langford, A. O., Aikin, K. C., Eubank, C. S., and Williams, E. J.: Stratospheric contribution to high surface ozone in Colorado during springtime, Geophysical Research Letters, 36, L12801, 10.1029/2009GL038367, 2009.

Langford, A. O., Senff, C. J., Alvarez Ii, R. J., Brioude, J., Cooper, O. R., Holloway, J. S., Lin, M. Y., Marchbanks, R. D., Pierce, R. B., Sandberg, S. P., Weickmann, A. M., and Williams, E. J.: An overview of the 2013 Las Vegas Ozone Study (LVOS): Impact of stratospheric intrusions and long-range transport on surface air quality, Atmospheric Environment, 109, 305-322, http://dx.doi.org/10.1016/j.atmosenv.2014.08.040, 2015.

Lee, H. N., Tositti, L., Zheng, X., and Bonasoni, P.: Analyses and comparisons of variations of 7Be, 210Pb, and 7Be/210Pb with ozone observations at two Global Atmosphere Watch stations from high mountains, Journal of Geophysical Research: Atmospheres, 112, D05303, 10.1029/2006JD007421, 2007.

Lefohn, A. S., Wernli, H., Shadwick, D., Oltmans, S. J., and Shapiro, M.: Quantifying the importance of stratospheric-tropospheric transport on surface ozone concentrations at high- and low-elevation monitoring sites in the United States, Atmospheric Environment, 62, 646-656, http://dx.doi.org/10.1016/j.atmosenv.2012.09.004, 2012.

Li, J., and Zeng, Q.: A unified monsoon index, Geophysical Research Letters, 29, 115-111-115-114, 10.1029/2001GL013874, 2002.

Liang, M.-C., Tang, J., Chan, C.-Y., Zheng, X. D., and Yung, Y. L.: Signature of stratospheric air at the Tibetan Plateau, Geophysical Research Letters, 35, L20816, 10.1029/2008GL035246, 2008.

Lin, M., Fiore, A. M., Cooper, O. R., Horowitz, L. W., Langford, A. O., Levy, H., Johnson, B. J., Naik, V., Oltmans, S. J., and Senff, C. J.: Springtime high surface ozone events over the western United States: Quantifying the role of stratospheric intrusions, Journal of Geophysical Research: Atmospheres, 117, D00V22, 10.1029/2012JD018151, 2012a.

Lin, M., Fiore, A. M., Horowitz, L. W., Cooper, O. R., Naik, V., Holloway, J., Johnson, B. J., Middlebrook, A. M., Oltmans, S. J., Pollack, I. B., Ryerson, T. B., Warner, J. X., Wiedinmyer, C., Wilson, J., and Wyman, B.: Transport of Asian ozone pollution into surface air over the western United States in spring, Journal of Geophysical Research: Atmospheres, 117, D00V07, 10.1029/2011JD016961, 2012b.

Lin, M., Horowitz, L. W., Oltmans, S. J., Fiore, A. M., and Fan, S.: Tropospheric ozone trends at Mauna Loa Observatory tied to decadal climate variability, Nature Geoscience, 7, 136-143, 10.1038/ngeo2066, 2014.

Lin, M., Fiore, A. M., Horowitz, L. W., Langford, A. O., Oltmans, S. J., Tarasick, D., and Rieder, H. E.: Climate variability modulates western US ozone air quality in spring via deep stratospheric intrusions, Nature Communications, 6, 10.1038/ncomms8105, 2015a.

Lin, M., Horowitz, L. W., Cooper, O. R., Tarasick, D., Conley, S., Iraci, L. T., Johnson, B., Leblanc, T., Petropavlovskikh, I., and Yates, E. L.: Revisiting the evidence of increasing springtime ozone mixing ratios in the free troposphere over western North America, Geophysical Research Letters, 8719-8728, 10.1002/2015GL065311, 2015b.

Lin, M., Horowitz, L. W., Payton, R., Fiore, A. M., and Tonnesen, G.: US surface ozone trends and extremes from 1980 to 2014: quantifying the roles of rising Asian emissions, domestic controls, wildfires, and climate, Atmospheric Chemistry and Physics, 17, 2943-2970, 10.5194/acp-17-2943-2017, 2017.

Liu, G., Liu, J., Tarasick, D. W., Fioletov, V. E., Jin, J. J., Moeini, O., Liu, X., Sioris, C. E., and Osman, M.: A global tropospheric ozone climatology from trajectory-mapped ozone soundings, Atmospheric Chemistry and Physics, 13, 10659-10675, 10.5194/acp-13-10659-2013, 2013.

Liu, H., Jacob, D. J., Chan, L. Y., Oltmans, S. J., Bey, I., Yantosca, R. M., Harris, J. M., Duncan, B. N., and Martin, R. V.: Sources of tropospheric ozone along the Asian Pacific Rim: An analysis of ozonesonde observations, Journal of Geophysical Research: Atmospheres, 107, 4573, 10.1029/2001JD002005, 2002.

Liu, J. J., Jones, D. B. A., Worden, J. R., Noone, D., Parrington, M., and Kar, J.: Analysis of the summertime buildup of tropospheric ozone abundances over the Middle East and North Africa as observed by the Tropospheric Emission Spectrometer instrument, Journal of Geophysical Research: Atmospheres, 114, D05304, 10.1029/2008JD010993, 2009.

Liu, J. J., Jones, D. B. A., Zhang, S., and Kar, J.: Influence of interannual variations in transport on summertime abundances of ozone over the Middle East, Journal of Geophysical Research: Atmospheres, 116, D20310, 10.1029/2011JD016188, 2011.

Lucey, D., Hadjiiski, L., Hopke, P. K., Scudlark, J. R., and Church, T.: Identification of sources of pollutants in precipitation measured at the mid-Atlantic US coast using potential source contribution function (PSCF), Atmospheric Environment, 35, 3979-3986, 10.1016/s1352-2310(01)00185-6, 2001.

Ma, J., Tang, J., Zhou, X., and Zhang, X.: Estimates of the Chemical Budget for Ozone at Waliguan Observatory, Journal of Atmospheric Chemistry, 41, 21-48, 10.1023/A:1013892308983, 2002.

Ma, J., Zheng, X., and Xu, X.: Comment on "Why does surface ozone peak in summertime at Waliguan?" by Bin Zhu et al, Geophysical Research Letters, 32, L01805, 10.1029/2004GL021683, 2005.

Ma, J., Lin, W. L., Zheng, X. D., Xu, X. B., Li, Z., and Yang, L. L.: Influence of air mass downward transport on the variability of surface ozone at Xianggelila Regional Atmosphere Background Station, southwest China, Atmospheric Chemistry and Physics, 14, 5311-5325, 10.5194/acp-14-5311-2014, 2014.

Ma, Z., Xu, J., Quan, W., Zhang, Z., Lin, W., and Xu, X.: Significant increase of surface ozone at a rural site, north of eastern China, Atmospheric Chemistry and Physics, 16, 3969-3977, 10.5194/acp-16-3969-2016, 2016.

Maycock, A. C., Matthes, K., Tegtmeier, S., Thieblemont, R., and Hood, L. L.: The representation of solar cycle signals in stratospheric ozone – Part 1: A comparison of recently updated satellite observations, Atmospheric Chemistry and Physics, 16, 10021-10043, 10.5194/acp-16-10021-2016, 2016.

Ningombam, S. S.: Variability of sunspot cycle QBO and total ozone over high altitude western Himalayan regions, Journal of Atmospheric and Solar-Terrestrial Physics, 73, 2305-2313, http://dx.doi.org/10.1016/j.jastp.2011.06.015, 2011.

Oman, L. D., Douglass, A. R., Ziemke, J. R., Rodriguez, J. M., Waugh, D. W., and Nielsen, J. E.: The ozone response to ENSO in Aura satellite measurements and a chemistry-climate simulation, Journal of Geophysical Research: Atmospheres, 118, 965-976, 10.1029/2012JD018546, 2013.

Sioris, C. E., McLinden, C. A., Fioletov, V. E., Adams, C., Zawodny, J. M., Bourassa, A. E., Roth, C. Z., and Degenstein, D. A.: Trend and variability in ozone in the tropical lower stratosphere over 2.5 solar cycles observed by SAGE II and OSIRIS, Atmospheric Chemistry and Physics, 14, 3479-3496, 10.5194/acp-14-3479-2014, 2014.

Škerlak, B., Sprenger, M., and Wernli, H.: A global climatology of stratosphere–troposphere exchange using the ERA-Interim data set from 1979 to 2011, Atmospheric Chemistry and Physics, 14, 913-937, 10.5194/acp-14-913-2014, 2014.

Sprenger, M., and Wernli, H.: A northern hemispheric climatology of cross-tropopause exchange for the ERA15 time period (1979–1993), Journal of Geophysical Research: Atmospheres, 108, 8521, 10.1029/2002JD002636, 2003.

Stohl, A., Spichtinger-Rakowsky, N., Bonasoni, P., Feldmann, H., Memmesheimer, M., Scheel, H. E., Trickl, T., Hübener, S., Ringer, W., and Mandl, M.: The influence of stratospheric intrusions on alpine ozone concentrations, Atmospheric Environment, 34, 1323-1354, http://dx.doi.org/10.1016/S1352-2310(99)00320-9, 2000.

Sun, L., Xue, L., Wang, T., Gao, J., Ding, A., Cooper, O. R., Lin, M., Xu, P., Wang, Z., Wang, X., Wen, L., Zhu, Y., Chen, T., Yang, L., Wang, Y., Chen, J., and Wang, W.: Significant increase of summertime ozone at Mount Tai in Central Eastern China, Atmospheric Chemistry and Physics, 16, 10637-10650, 10.5194/acp-16-10637-2016, 2016.

Tang, Q., Prather, M. J., and Hsu, J.: Stratosphere-troposphere exchange ozone flux related to deep convection, Geophysical Research Letters, 38, L03806, 10.1029/2010gl046039, 2011.

van der A, R. J., Peters, D. H. M. U., Eskes, H., Boersma, K. F., Van Roozendael, M., De Smedt, I., and Kelder, H. M.: Detection of the trend and seasonal variation in tropospheric NO2 over China, Journal of Geophysical Research: Atmospheres, 111, D12317, 10.1029/2005JD006594, 2006.

Verstraeten, W. W., Neu, J. L., Williams, J. E., Bowman, K. W., Worden, J. R., and Boersma, K. F.: Rapid increases in tropospheric ozone production and export from China, Nature Geoscience, 8, 690-695, 10.1038/ngeo2493, http://www.nature.com/ngeo/journal/v8/n9/abs/ngeo2493.html#supplementary-information, 2015.

Voulgarakis, A., Hadjinicolaou, P., and Pyle, J. A.: Increases in global tropospheric ozone following an El Niño event: examining stratospheric ozone variability as a potential driver, Atmospheric Science Letters, 12, 228-232, 10.1002/asl.318, 2011.

Wang, R., Xu, X., Jia, S., Ma, R., Ran, L., Deng, Z., Lin, W., Wang, Y., and Ma, Z.: Lower tropospheric distributions of O3 and aerosol over Raoyang, a rural site in the North China Plain, Atmospheric Chemistry and Physics, 17, 3891-3903, 10.5194/acp-17-3891-2017, 2017.

Wang, T., Ding, A., Gao, J., and Wu, W. S.: Strong ozone production in urban plumes from Beijing, China, Geophysical Research Letters, 33, L21806, 10.1029/2006gl027689, 2006a.

Wang, T., Wong, H. L. A., Tang, J., Ding, A., Wu, W. S., and Zhang, X. C.: On the origin of surface ozone and reactive nitrogen observed at a remote mountain site in the northeastern Qinghai-Tibetan Plateau, western China, Journal of Geophysical Research: Atmospheres, 111, D08303, 10.1029/2005JD006527, 2006b.

Wang, T., Wei, X. L., Ding, A. J., Poon, C. N., Lam, K. S., Li, Y. S., Chan, L. Y., and Anson, M.: Increasing surface ozone concentrations in the background atmosphere of Southern China, 1994–2007, Atmospheric Chemistry and Physics, 9, 6217-6227, 10.5194/acp-9-6217-2009, 2009.

Wang, Y., Konopka, P., Liu, Y., Chen, H., Müller, R., Plöger, F., Riese, M., Cai, Z., and Lü, D.: Tropospheric ozone trend over Beijing from 2002–2010: ozonesonde measurements and modeling analysis, Atmospheric Chemistry and Physics, 12, 8389-8399, 10.5194/acp-12-8389-2012, 2012.

Xu, W., Lin, W., Xu, X., Tang, J., Huang, J., Wu, H., and Zhang, X.: Long-term trends of surface ozone and its influencing factors at the Mt Waliguan GAW station, China – Part 1: Overall trends and characteristics, Atmospheric Chemistry and Physics, 16, 6191-6205, 10.5194/acp-16-6191-2016, 2016.

Xu, X., Lin, W., Wang, T., Yan, P., Tang, J., Meng, Z., and Wang, Y.: Long-term trend of surface ozone at a regional background station in eastern China 1991-2006: enhanced variability, Atmospheric Chemistry and Physics, 8, 2595-2607, 10.5194/acp-8-2595-2008, 2008.

Xue, L. K., Wang, T., Zhang, J. M., Zhang, X. C., Deliger, Poon, C. N., Ding, A. J., Zhou, X. H., Wu, W. S., Tang, J., Zhang, Q. Z., and Wang, W. X.: Source of surface ozone and reactive nitrogen speciation at Mount Waliguan in western China: New insights from the 2006 summer study, Jounal of Geophysical Research, 116, D07306, 10.1029/2010jd014735, 2011.

Yang, Y., Liao, H., and Li, J.: Impacts of the East Asian summer monsoon on interannual variations of summertime surface-layer ozone concentrations over China, Atmospheric Chemistry and Physics, 14, 6867-6879, 10.5194/acp-14-6867-2014, 2014.

Zeng, G., and Pyle, J. A.: Influence of El Niño Southern Oscillation on stratosphere/troposphere exchange and the global tropospheric ozone budget, Geophysical Research Letters, 32, L01814, 10.1029/2004GL021353, 2005.

Zeng, Y., and Hopke, P. K.: A studyof the sources of acid precipitation in Ontario, Canada, Atmospheric Environment, 23, 1499-1509, 1989.

Zhang, F., Zhou, L. X., Novelli, P. C., Worthy, D. E. J., Zellweger, C., Klausen, J., Ernst, M., Steinbacher, M., Cai, Y. X., Xu, L., Fang, S. X., and Yao, B.: Evaluation of in situ measurements of atmospheric carbon monoxide at Mount Waliguan, China, Atmospheric Chemistry and Physics, 11, 5195-5206, 10.5194/acp-11-5195-2011, 2011.

Zheng, X. D., Shen, C. D., Wan, G. J., Liu, K. X., Tang, J., and Xu, X. B.: ~(10)Be/~7Be implies the contribution of stratosphere-troposphere transport to the winter-spring surface O_3 variation observed on the Tibetan Plateau, Chin. Sci. Bull., 56, 84-88, 2011.

Zhou, L., Hopke, P. K., and Liu, W.: Comparison of two trajectory based models for locating particle sources for two rural New York sites, Atmospheric Environment, 38, 1955-1963, 10.1016/j.atmosenv.2003.12.034, 2004.

Zhu, B., Akimoto, H., Wang, Z., Sudo, K., Tang, J., and Uno, I.: Why does surface ozone peak in summertime at Waliguan?, Geophysical Research Letters, 31, L17104, 10.1029/2004GL020609, 2004.

Ziemke, J. R., Chandra, S., and Bhartia, P. K.: A 25-year data record of atmospheric ozone in the Pacific from Total Ozone Mapping Spectrometer (TOMS) cloud slicing: Implications for ozone trends in the stratosphere and troposphere, Journal of Geophysical Research: Atmospheres, 110, D15105, 10.1029/2004JD005687, 2005.

Ziemke, J. R., Chandra, S., Oman, L. D., and Bhartia, P. K.: A new ENSO index derived from satellite measurements of column ozone, Atmospheric Chemistry and Physics, 10, 3711-3721, 10.5194/acp-10-3711-2010, 2010.

Zou, H., Ji, C. P., Zhou, L. B., Wang, W., and Jiang, Y. X.: ENSO Signal in Total Ozone over Tibet, Climatic and Environmental Research, 6, 267-272, 2001.

Table 1 The linear variation slope (k) of 24h and 168h average trajectory direction occurrence frequency (in % $year^{-1}$, numbers in bold are significant under a confidence level of 95%).

k (% a^{-1})	Season	Trajectory direction							
		S	SW	W	NW	N	NE	E	SE
t=≤24h	MAM	**-0.17**	**-0.19**	0.39	-0.32	-0.11	**-0.30**	**1.38**	**-0.69**
	JJA	**-0.42**	**-0.20**	0.04	-0.13	-0.01	-0.23	**2.75**	**-1.80**
	SON	-0.16	-0.24	0.60	-0.41	**-0.17**	**-0.32**	**1.39**	**-0.69**
	DJF	0.08	-0.17	-0.30	-0.22	**-0.09**	**-0.17**	**0.84**	0.05
t=≤168h	MAM	-0.01	0.01	-0.27	**1.34**	-0.01	-0.01	**-0.38**	**-0.67**
	JJA	**-0.10**	0.02	**0.42**	0.57	0.31	**0.50**	0.15	**-1.87**
	SON	**-0.14**	**-0.32**	0.05	**0.91**	0.03	0.13	0.04	**-0.71**
	DJF	0.01	-0.09	-0.67	0.54	0.17	0.11	-0.05	-0.02

Table 2 Trend of total contribution of direct ozone transport on WLG ozone concentration (ppbv $year^{-1}$), confidence intervals are given for $p<0.1$

Season	all-year	Spring	Summer	Autumn	Winter
Slope	0.28±0.30	0.27±0.30	0.16±1.11	**0.56±0.54**	0.01±0.32
P-value	0.12	0.13	0.80	**0.09**	0.98

Table 3 The Kendall's variation slope (k, ppbv $year^{-1}$) of ozone concentrations associated with different trajectory directions, the according confidence interval and p-values.

Variable	Time of day	Trajectory direction			
		SW	NW	NE	SE
k (ppbv $year^{-1}$)	all day	0.18	0.13	0.20	0.26
	day	0.17	0.14	0.28	0.35
	night	0.13	0.11	0.20	0.28
95% Confidence Interval (ppbv $year^{-1}$)	all day	0.11-0.23	0.08-0.19	0.12-0.31	0.19-0.34
	day	0.13-0.23	0.07-0.19	0.15-0.41	0.26-0.44
	night	0.06-0.19	0.06-0.19	0.11-0.29	0.21-0.35
p	all day	<0.01	<0.01	<0.01	<0.01
	day	<0.01	<0.01	<0.01	<0.01
	night	0.01	<0.01	<0.01	<0.01

Table 4 Correlation between the surface ozone (1994-2013), the NCEP Reanalysis Precipitation (1990-2015) and the EASMI (1990-2015)

r (p-value)	**June**	**July**	**August**
Precipitation & EASMI	-0.12 (0.15)	**-0.47 (0.02)**	0.21 (0.12)
O_3 & EASMI	-0.08 (0.76)	**-0.59 (0.01)**	-0.32 (0.20)
O_3& Precipitation	**0.30 (0.10)**	-0.01 (0.20)	**-0.51(0.03)**

Table 5 The changes in stratospheric ozone input and in ozone concentration associated with East Asian, European and North American transport (%) introduced by the East Asian Monsoon. The average ozone values associated with the EACOt≥67th, EUCOt≥67th, NACOt≥67th are used to represent the ozone transported from East Asia ($O_{3,ea}$), Europe ($O_{3,eu}$), and North America ($O_{3,na}$). The East Asian Summer Monsoon Index (EASMI) to filter out those $O_{3,ea}$, $O_{3,eu}$ and $O_{3,na}$ associated with the lower and upper 15 percentile of EASMI. The relative change induced by the East Asian Monsoon is then calculated with the equation ($O_{3, EASMI}$<=15th-$O_{3,EASMI}$>=85th)/$\bar{O}_3$.

Month	($O_{3, EASMI<=15th}$-$O_{3,EASMI>=85th}$)/$\bar{O}_3$ (%)					
	O_3Strat	$O_{3,ea}$	$O_{3,eu}$	$O_{3,na}$	Mean	$O_{3,WLG}$
June	10.4	-6.2	1.3	-3.8	0.4	-0.5
July	18.9	6.2	0.1	4.3	7.4	8.7
August	26.6	-0.4	-3.2	-3.2	4.9	4.5

Table 6 Multivariate regression coefficients (Eq. 6-7) of the surface ozone at WLG

factor	Regression Coefficients						
	t_0						
t	1.003						
	a_0	$a_{1,1}$	$a_{2,1}$	$a_{1,2}$	$a_{2,2}$	$a_{1,3}$	$a_{2,3}$
BKG	0.190	-0.250	0.229	0.028	-0.007	-0.005	-0.012
	$b_{i,0}$	$b_{i,1}$	$b_{i,2}$				
O_3Strat	0.336	-0.135	-0.109				
$O_{3,trop}$	0.100	0.042	-0.112				
SSN	0.057	-0.031	-0.055				
NW_{freq}	0.111	-0.048	-0.100				
QBO	0.021	-0.006	-0.018				

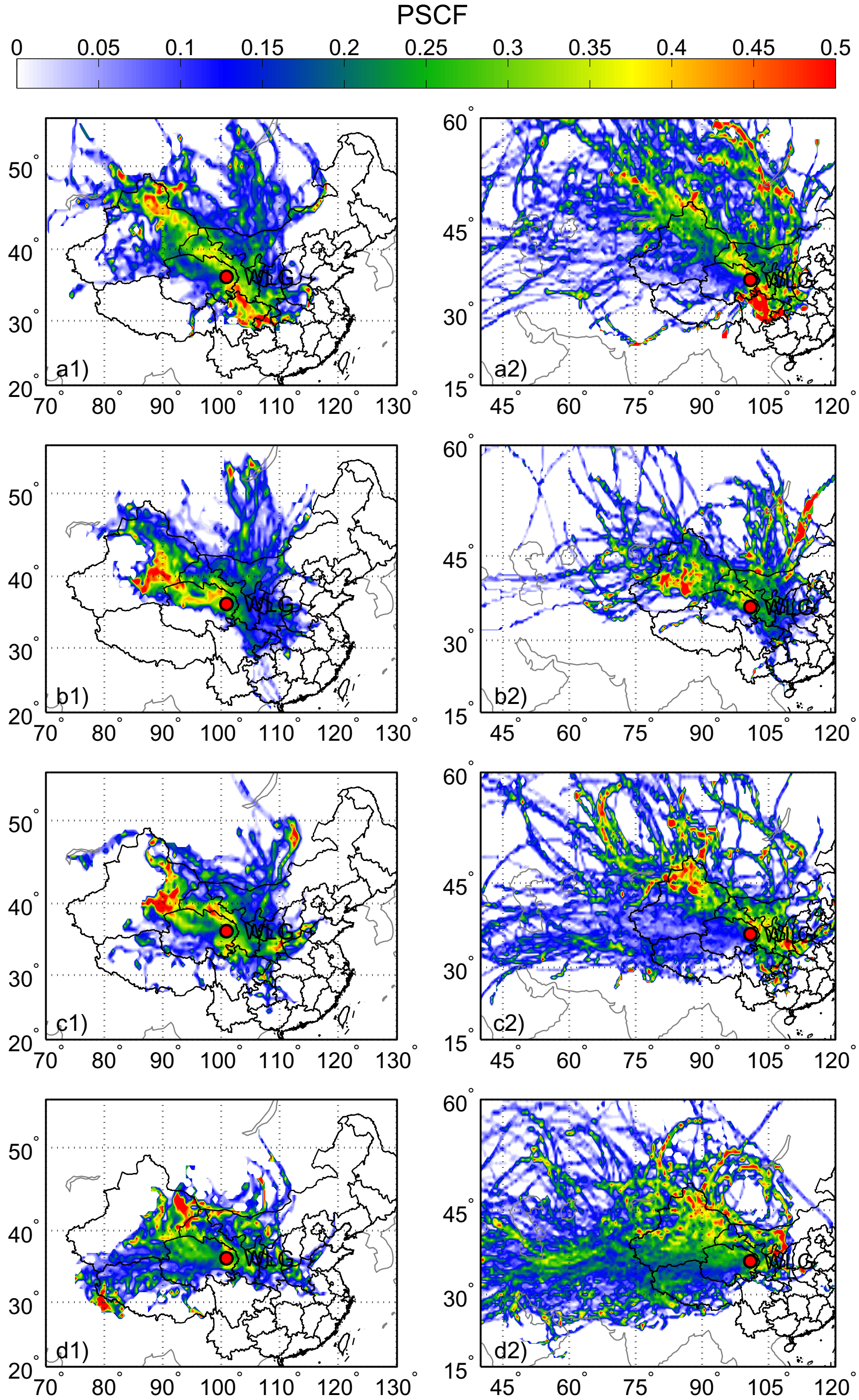

Figure 1 The 1994-2013 climatology of air mass origins at WLG inthein the PBL (left) and FT (right) for spring (a), summer (b), autumn (c) and winter (d), based on the PSCF analysis (Sect. 2.3).

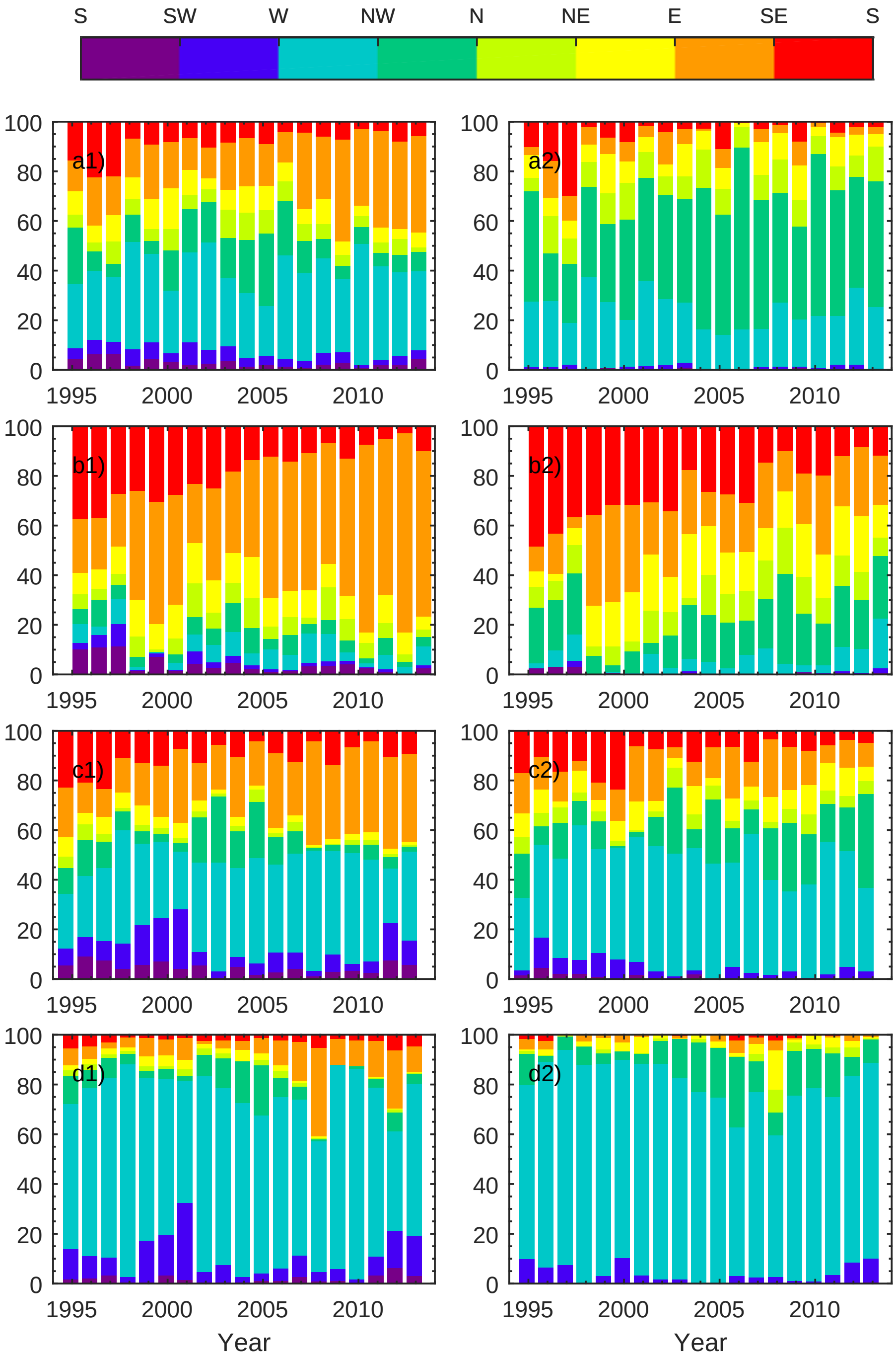

Figure 2 The average trajectory direction occurrence frequencies in a) spring, b) summer, c) autumn and d) winter of1) t<24h and 2) t<168h.

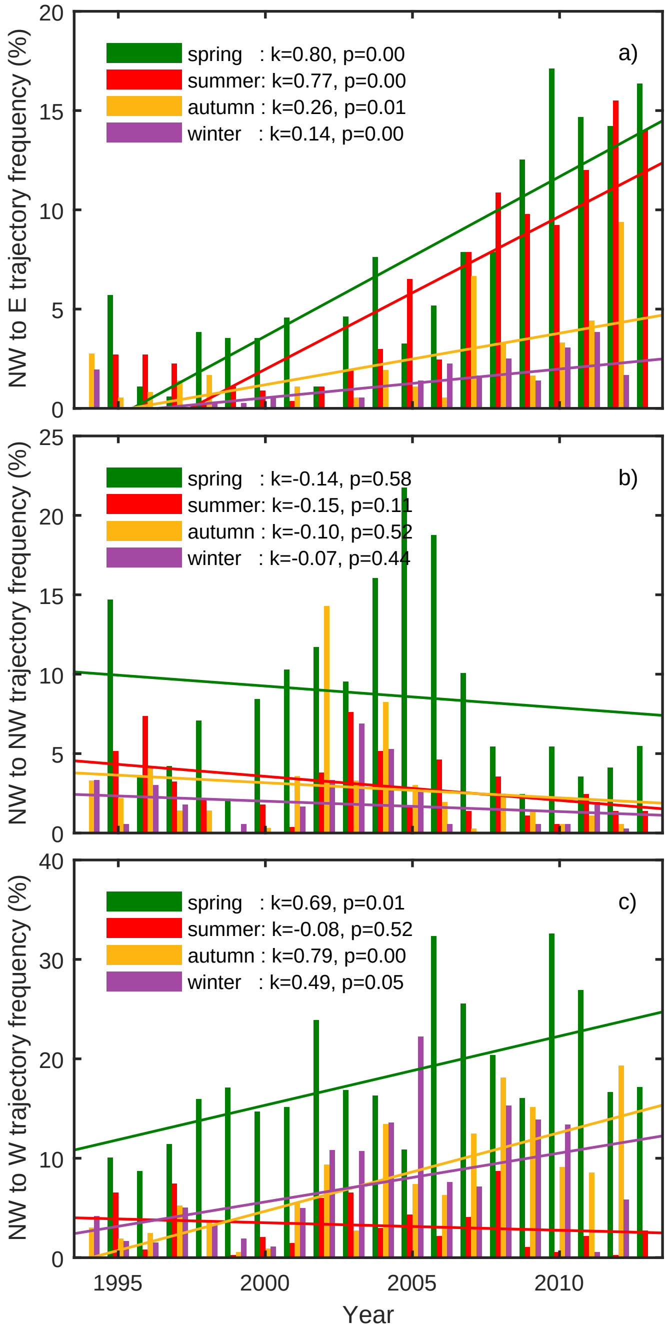

Figure 3 The occurrence frequency of trajectories ~~that originate from the NW at t=-~~whose average 168h direction are NW and ~~turn to the~~24h direction are E (a), NW (b) and W(c) ~~at t=-24h~~ in spring (green), summer (red), autumn (orange) and winter (purple). Bars stand for the occurrence frequencies, while lines are their corresponding linear trends.

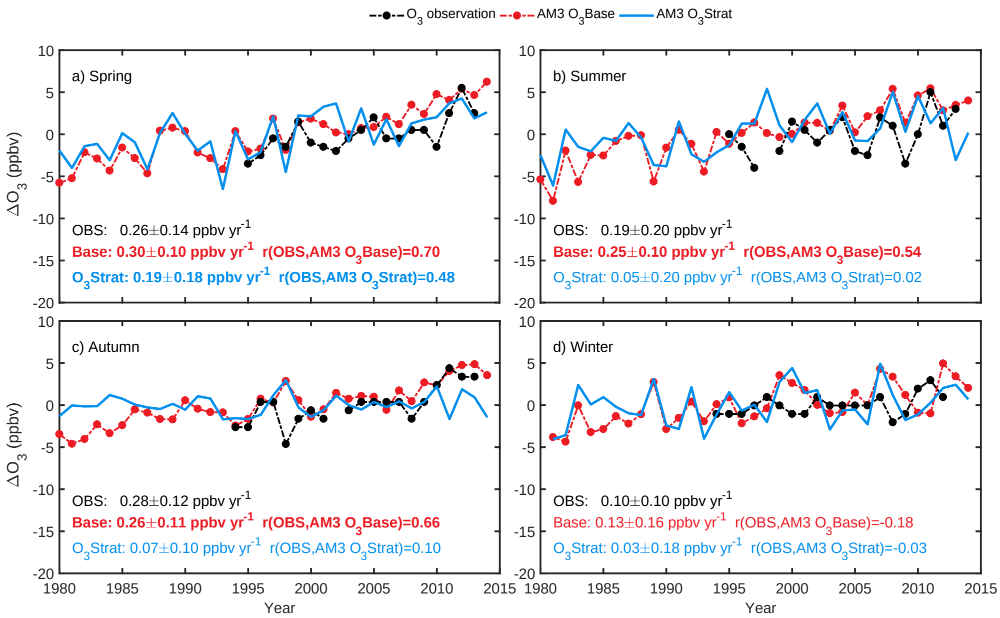

Figure 4 Comparison of seasonal median ozone anomalies at Mt. Waliguan over the period 1980-2014from available observations (black), GFDL-AM3 BASE simulations (red) and AM3 stratospheric ozone tracer (O_3Strat, blue) for a) spring, b) summer, c) autumn and d) winter. The linear trends (with the 95% confidence intervals) over the period 1994-2013 and correlations between observations and models are shown.

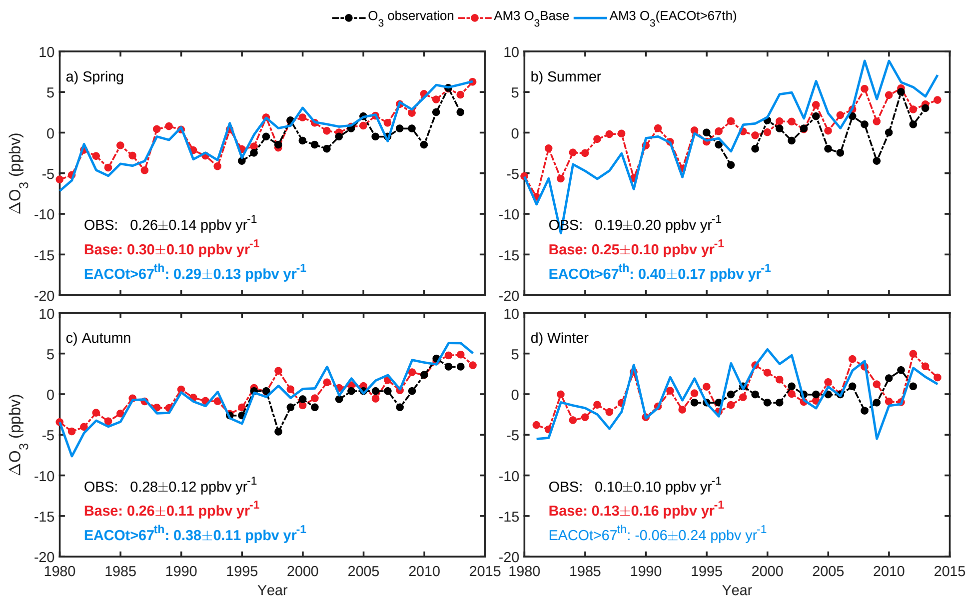

Figure 5 Comparison of seasonal median ozone anomalies at Mt. Waliguan over the period 1980-2014 from available observations (black), GFDL-AM3 BASE simulations (red) and under conditions with strong transport from East Asia (EACOt> 67th, blue) for a) spring, b) summer, c) autumn and d) winter. The linear trends (with the 95% confidence intervals) over the period 1994-2013 and correlations between observations and models are shown.

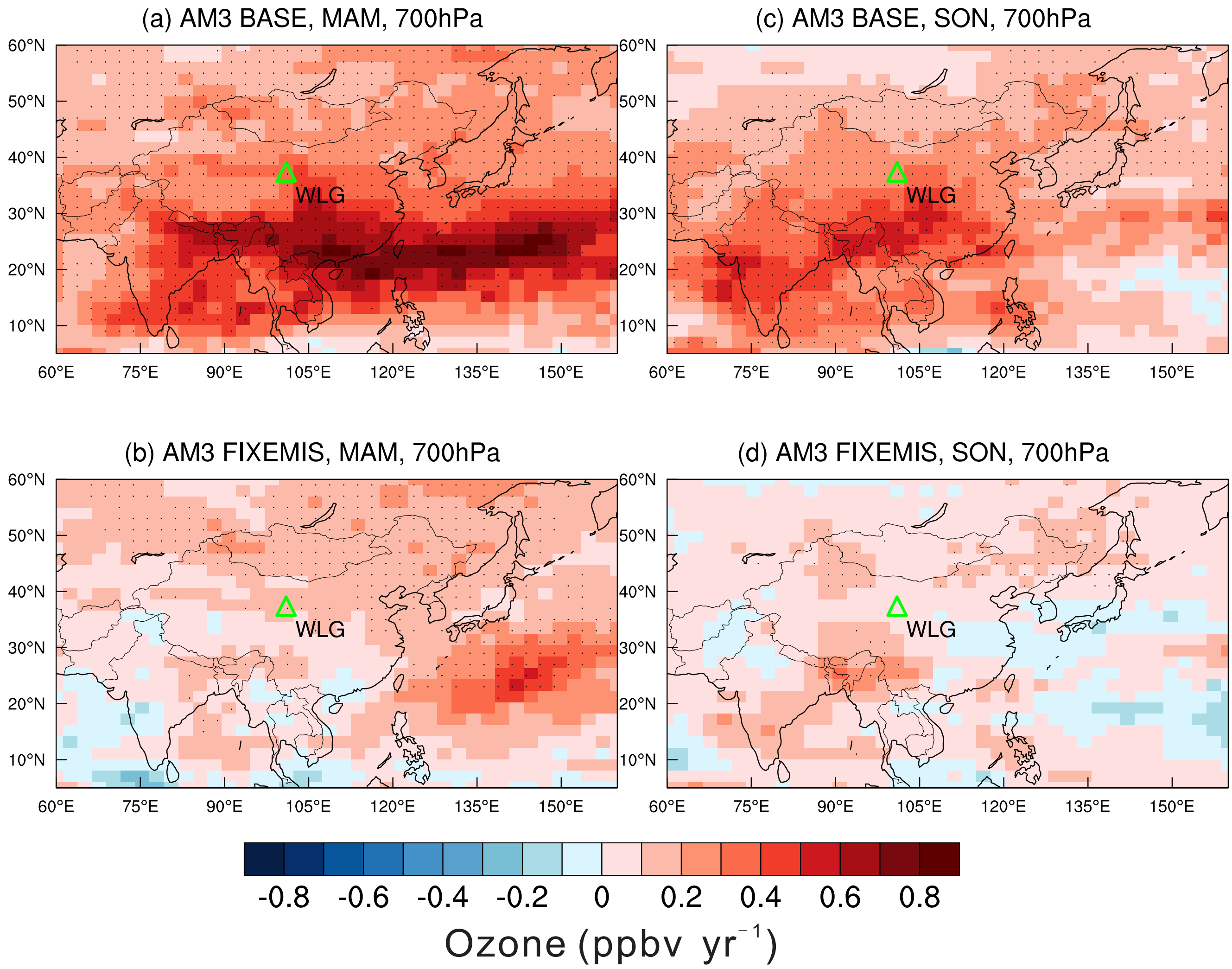

Figure 6 (a-b) The 1995-2014 trends of springtime average ozone sampled at 700 hPa as simulated by theGFDL-AM3 model with time-varying (BASE) and constant anthropogenic emissions (FIXEMIS). (c-d)Same as (a-b) but for autumn. Triangle denote the location of WLG. Stippling indicates areas where the trend is statistically significant at the 95% confidence level.

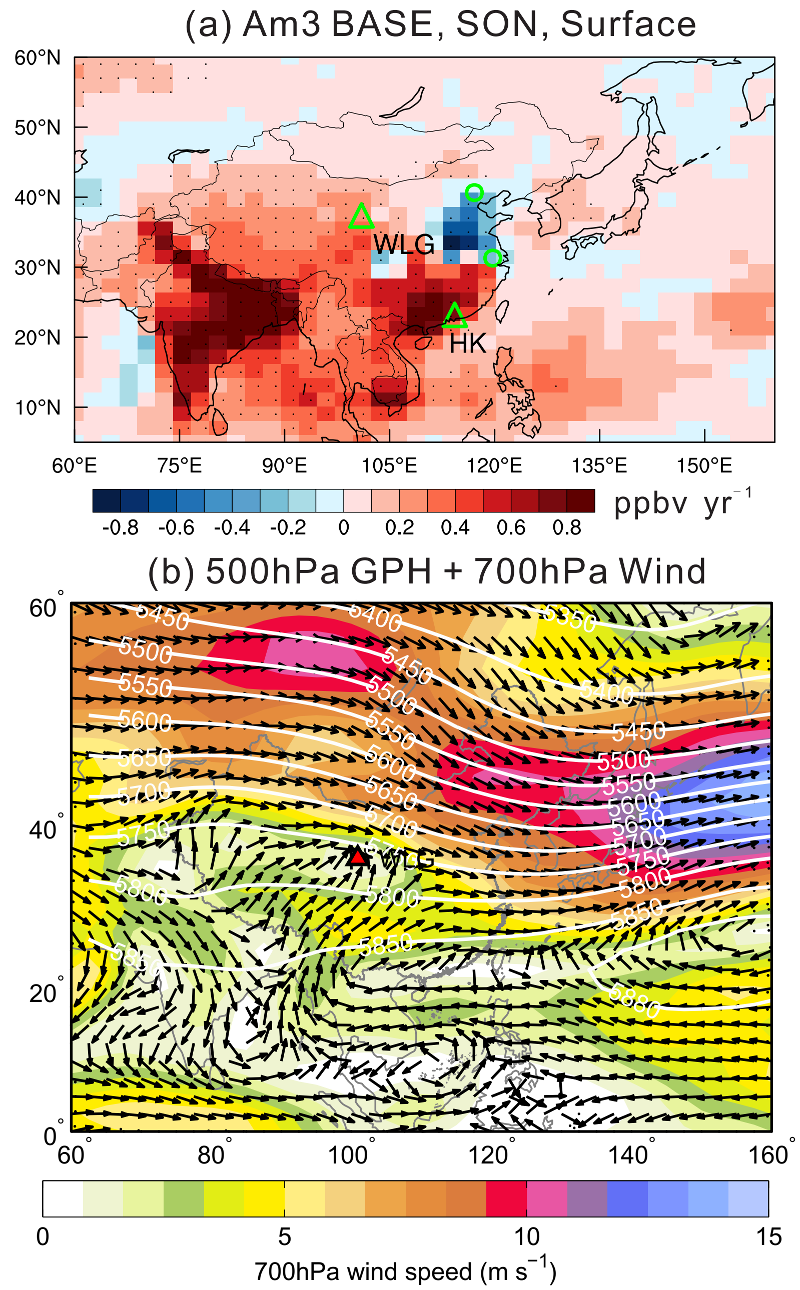

Figure 7 (a) The 1995-2014 trends of autumn average daily maximum 8-hour average ozone sampled in the surface level from the GFDL-AM3 model with time-varying anthropogenic emissions (BASE). Stippling indicates areas where the trend is statistically significant at the 95% confidence level. Green symbols denote the locations of WLG, Hong Kong, Shangdianzi and LinAn. (b) Mean 700hPa wind speed (colorshading), direction (black arrows) and 500hPa geopotential height (contours) in autumn averaged over the 1994-2013 period.

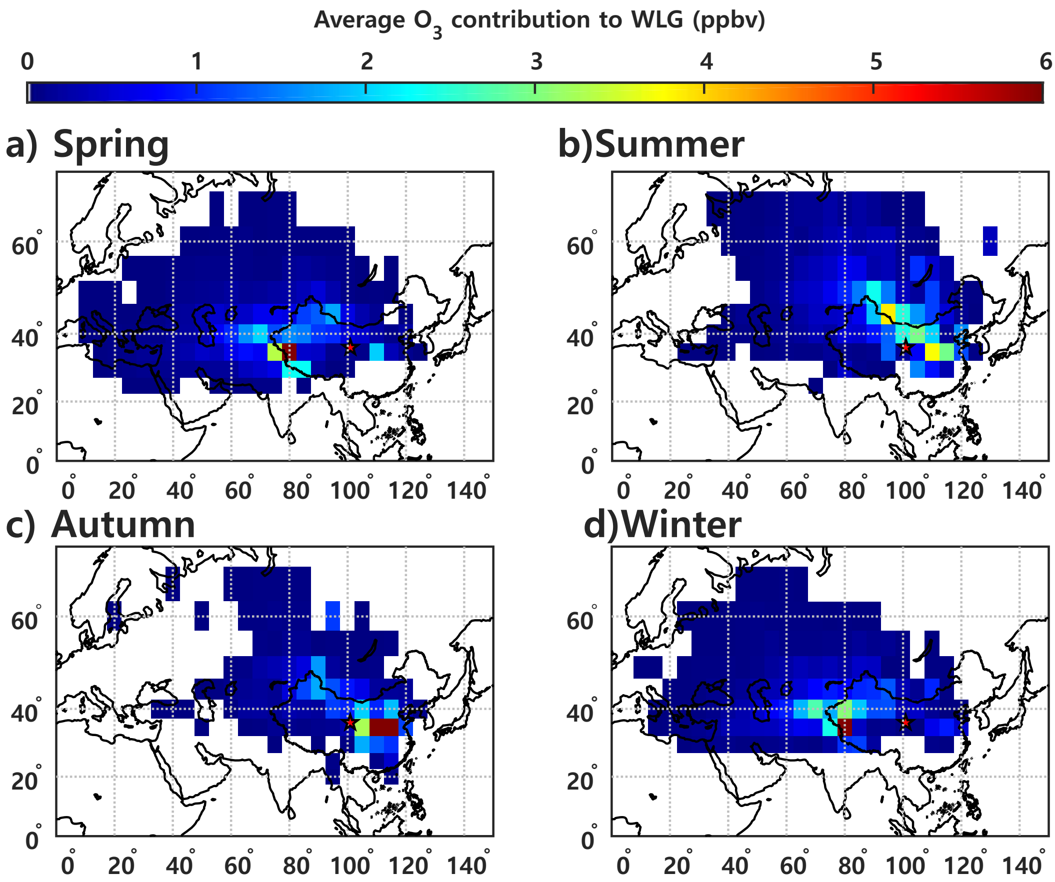

Figure 8 Average seasonal distributions of ozone contribution to WLG through direct transport of ozone during 1994-2013

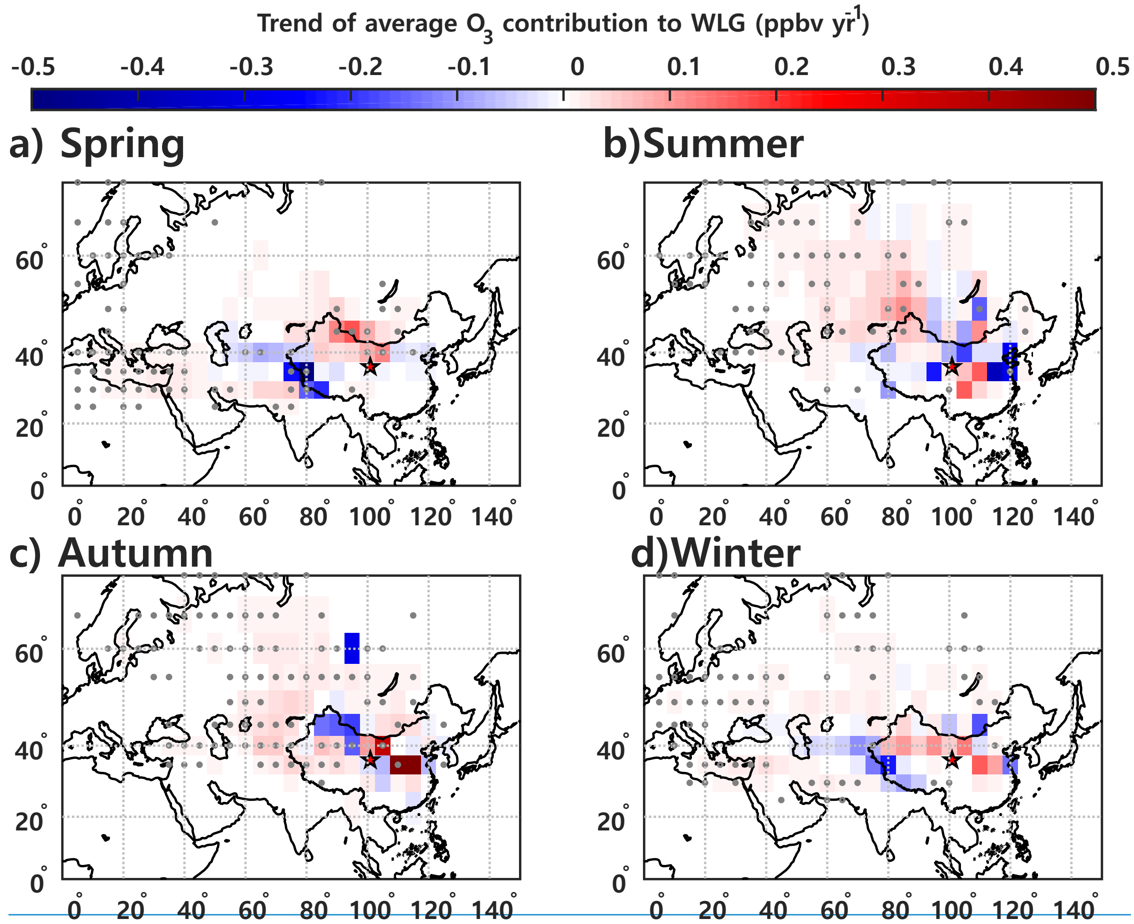

Trend of average O_3 contribution to WLG (ppbv yr^{-1})
-0.5
-0.4
-0.3
-0.2
-0.1
0
0.1
0.2
0.3
0.4
0.5
a) Spring
b)Summer
c) Autumn
d)Winter
0°
20°
40°
60°
80°
100°
120°
140°

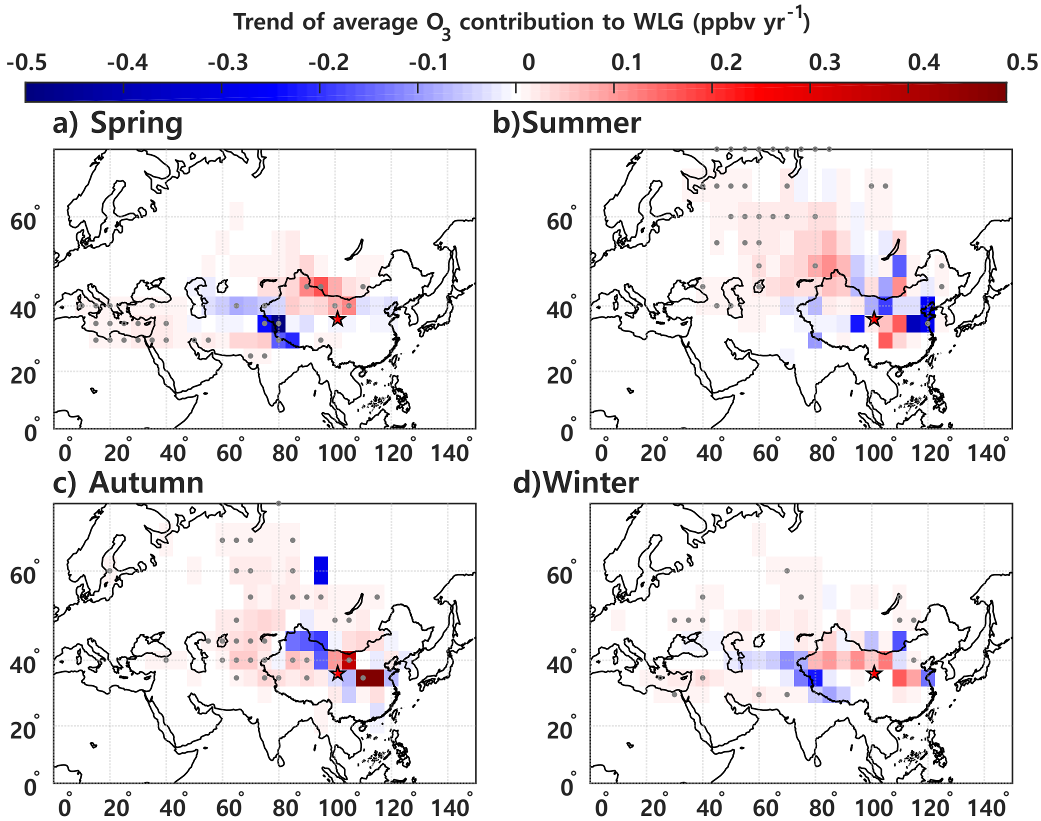

Figure 9 Average seasonal distributions of the trend of ozone contribution to WLG through direct transport of ozone during 1994-2013, grey dots stand for the ~~grids passing the 95% confidence test~~grid cells with $p<0.05$.

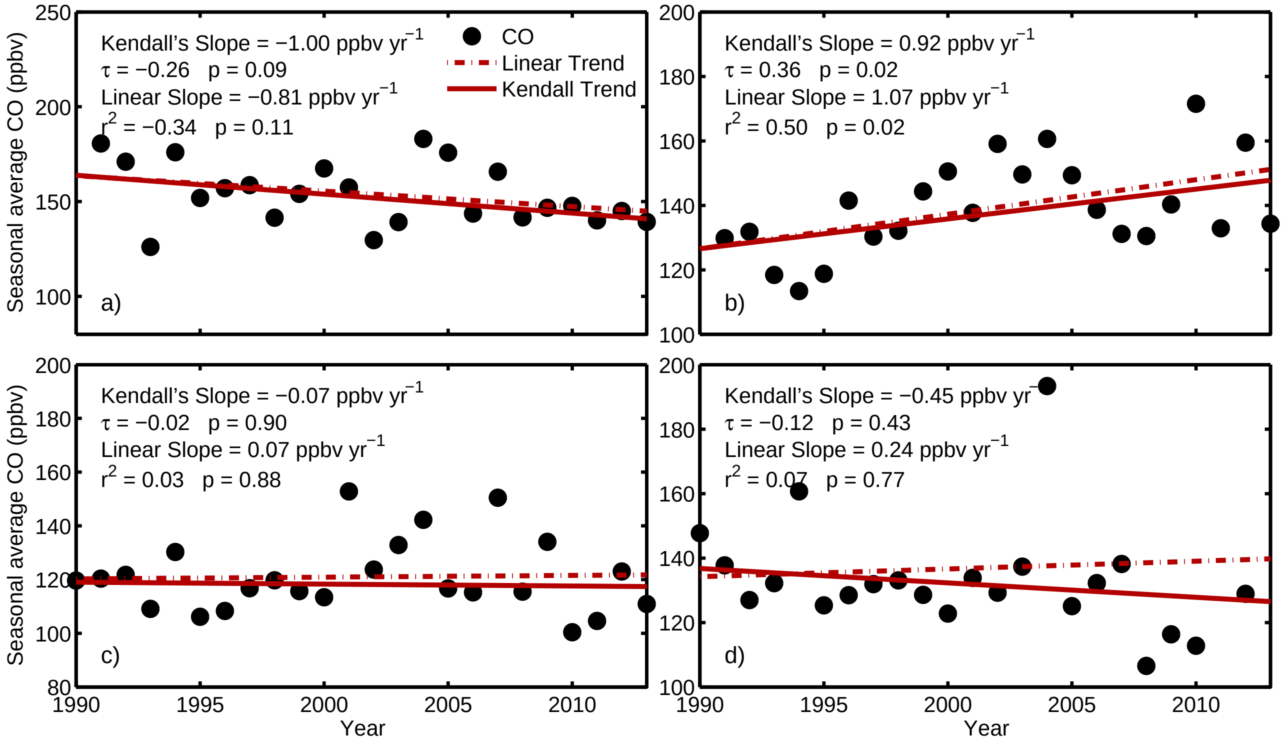

Figure 10 Mann-Kendall and linear trends of seasonal average CO observed during a) spring, b) summer, d) autumn and d) winter from 1990-2013 at WLG

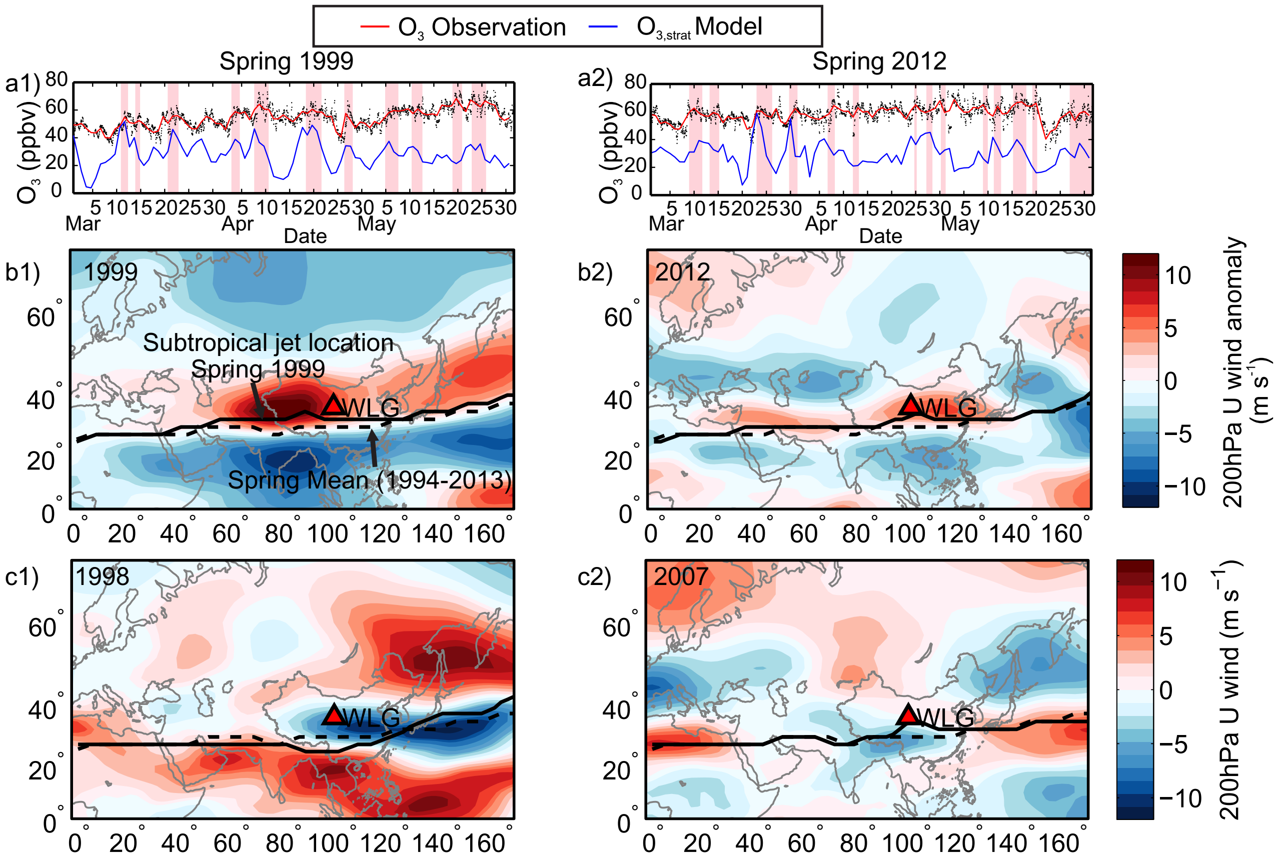

Figure 11 Temporal variations of a) hourly (black dots) and daily (red line) mean surface ozone observations and modelled O_3Strat (blue line) from March to May in 1999 and 2012; b) 200hPa zonal wind anomaly in the springs of 1999 and 2012 with the strong stratospheric influence; c) Same as (a) but for the springs of 1998 and 2007 with weak stratospheric influence.

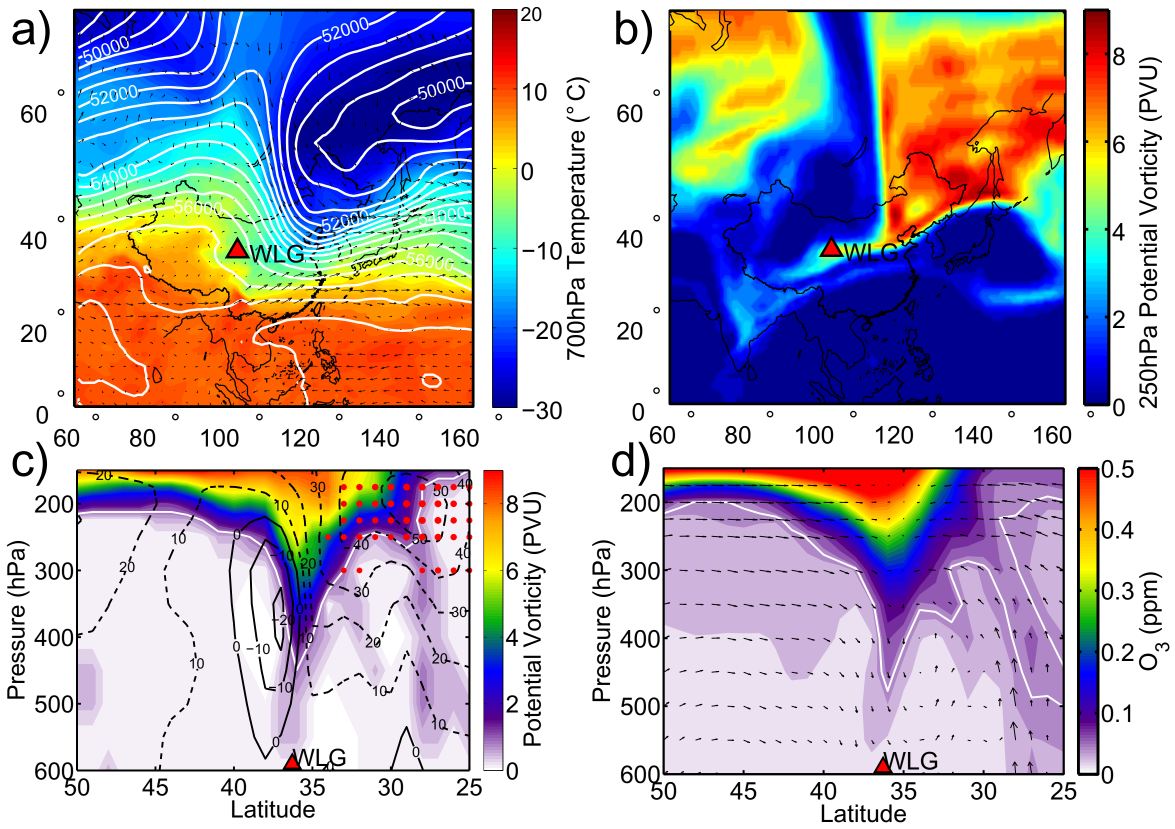

Figure 12a) Map of 500hPa geopotential height (white contours), 700hPa temperature (shading) and wind field (black arrows); b) Map of 250hPa potential vorticity; c) the cross-section of potential vorticity along the 101.0E longitude line. The white line denotes the 1 PVU isoline, the black lines are U wind isolines (dashed lines for westerly winds and solid lines for easterly winds) and the red dots indicate the location of the subtropical jet stream (U wind>35m s^{-1}); d) The cross-section of ozone mixing ratios, V wind and W wind vector along the 101.0E longitude line from the ECMWF reanalysis during an STT transport event on 30 Mar 2012.The while line denotes the 50-ppbv ozone contour.

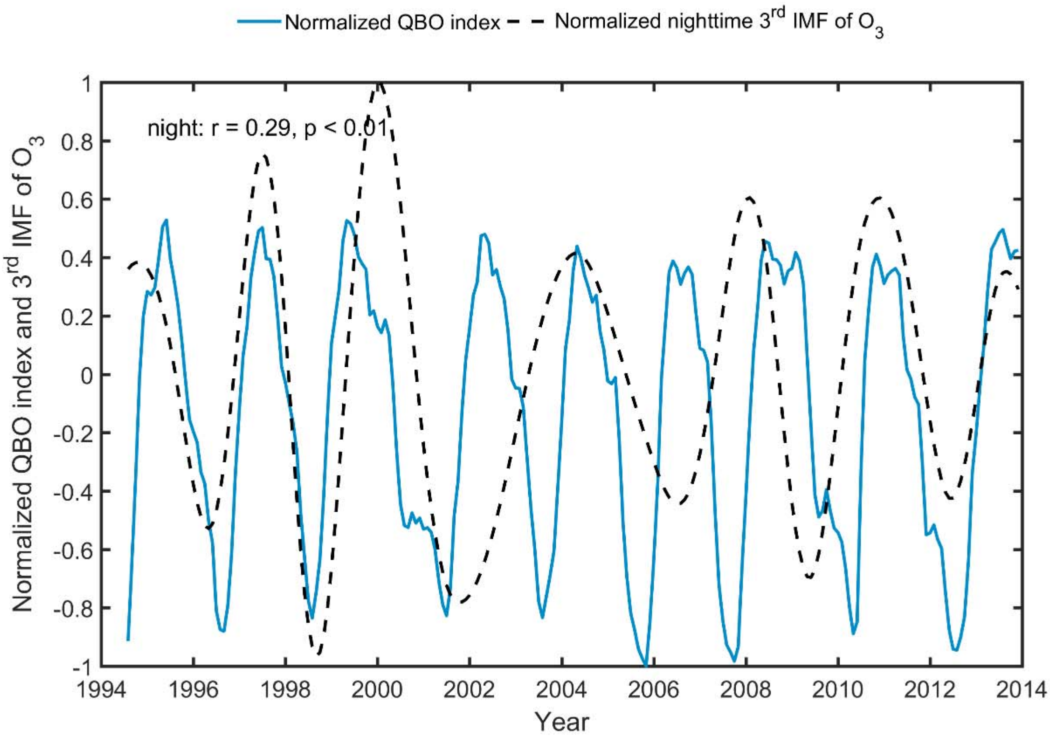

Figure 13 Comparison between the normalized nighttime (dashed black line) 3rd IMF and the normalized 30hPa QBO index (solid blue line) during 1994-2013.

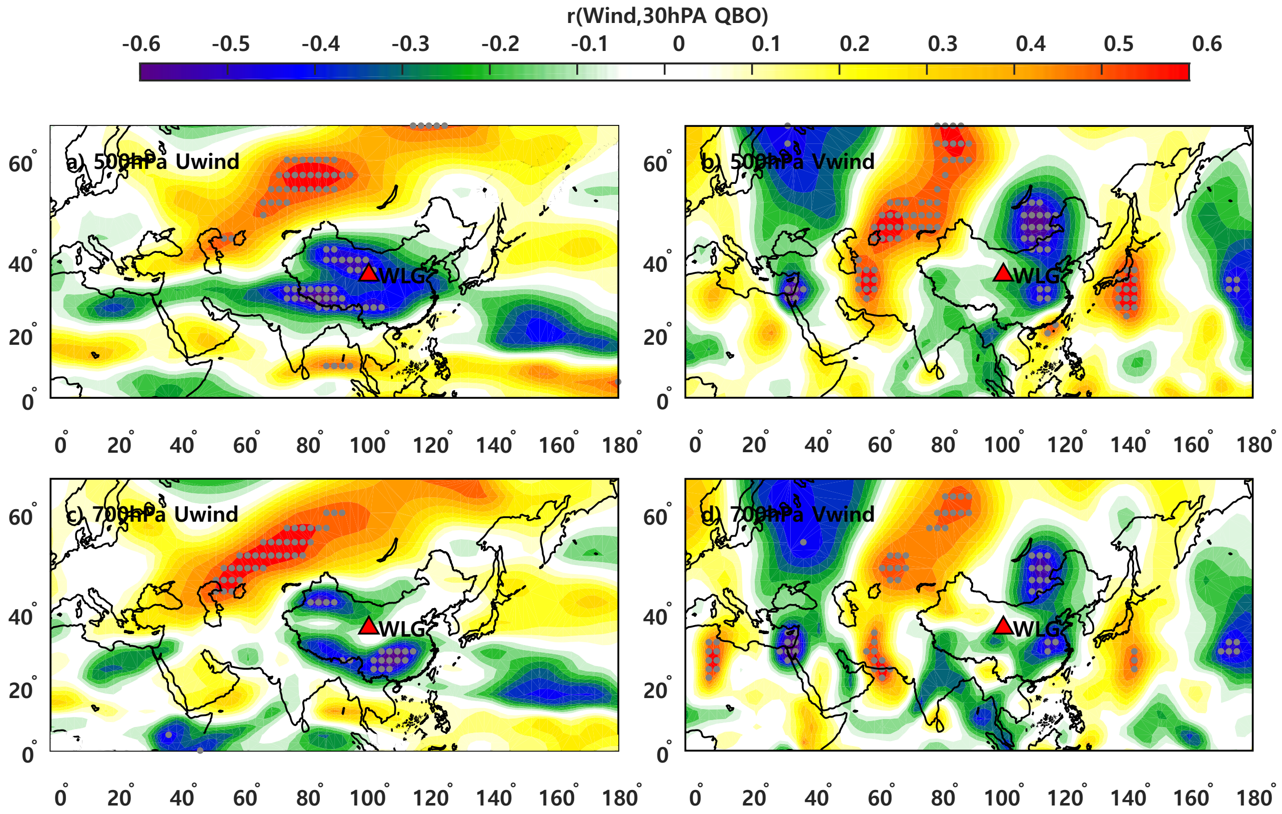

Figure ~~14~~14 Correlation coefficients between the QBO index and zonal (a, c) and meridional (b, d) wind at 500 hPa and 700 hPa with grey dots indicating those that are significant ($p<0.05$). The red triangles indicate the position of WLG.

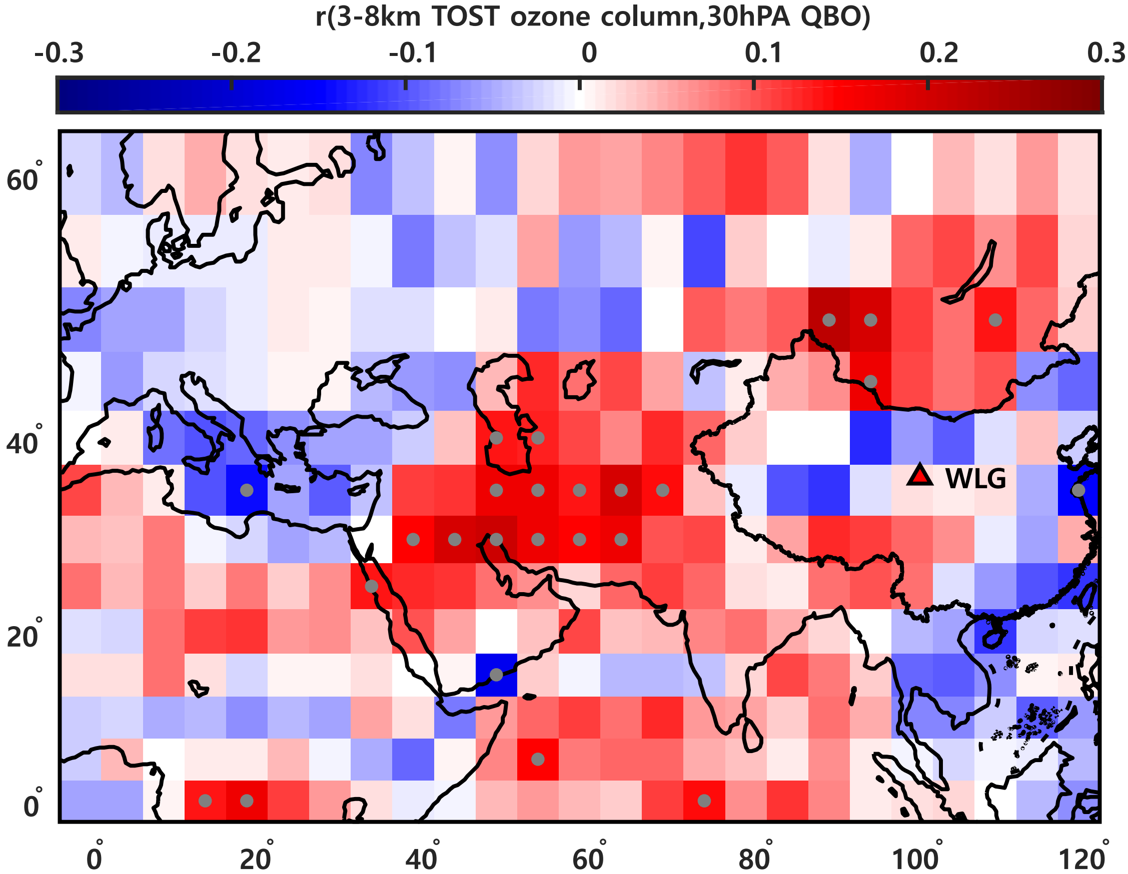

Figure ~~15~~15 Correlation coefficients between the QBO index and the 3-8 km TOST ozone columns. Correlations for the grids with grey dots indicating those that are significant ($p<0.05$)

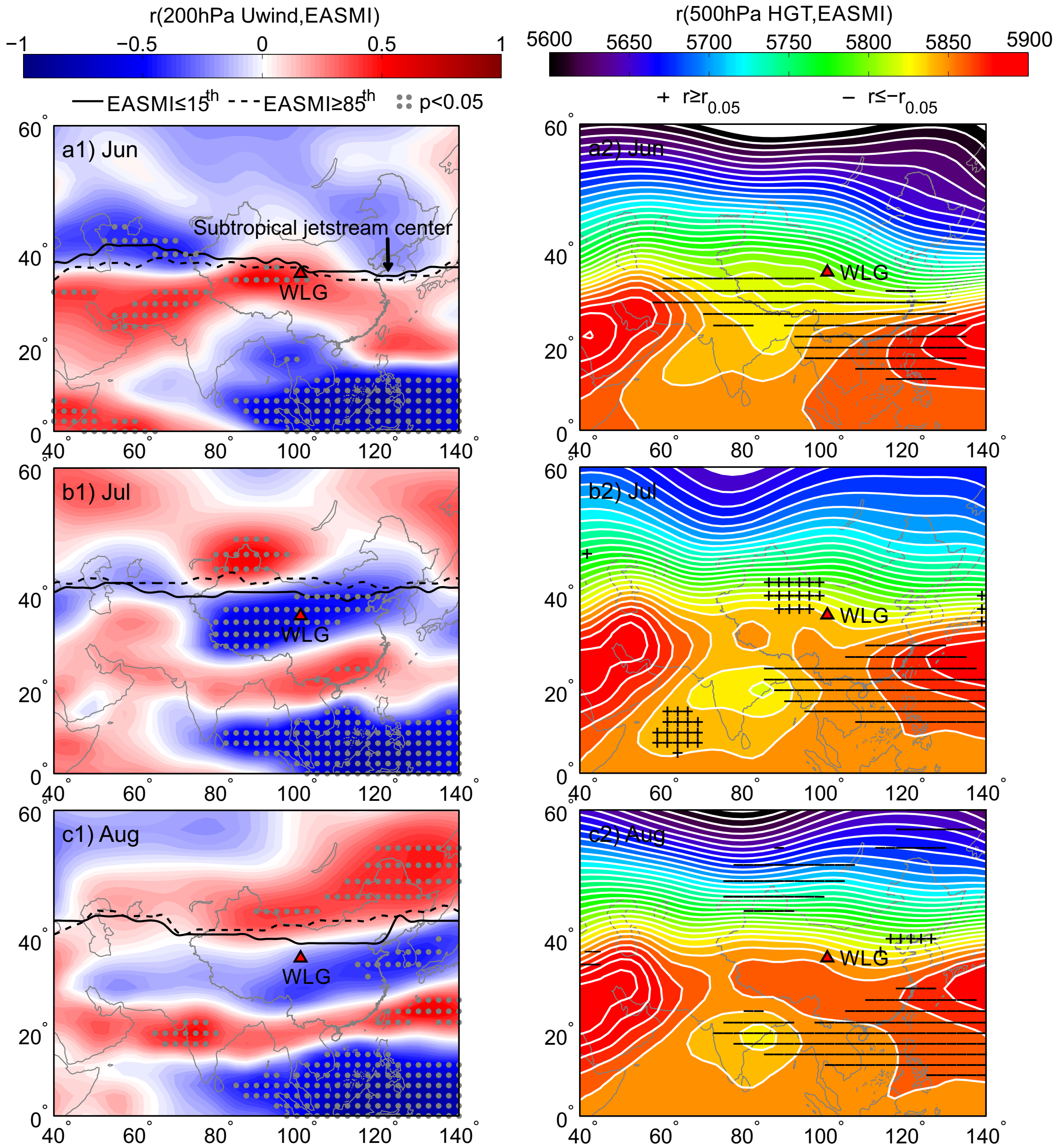

Figure 16 1) The correlation coefficient between the 200hPa zonal wind and the EASMI and the average location of the subtropical jetstream center for the EASMI≤15th and EASMI≥85th cases and 2) the average 500hPa geopotential height and the location of significant positive(+)/negative(-) correlation ($p<0.05$) between 500hPa geopotential height and the EASMI in a) Jun, b) Jul and c) Aug during 1990 to 2015.

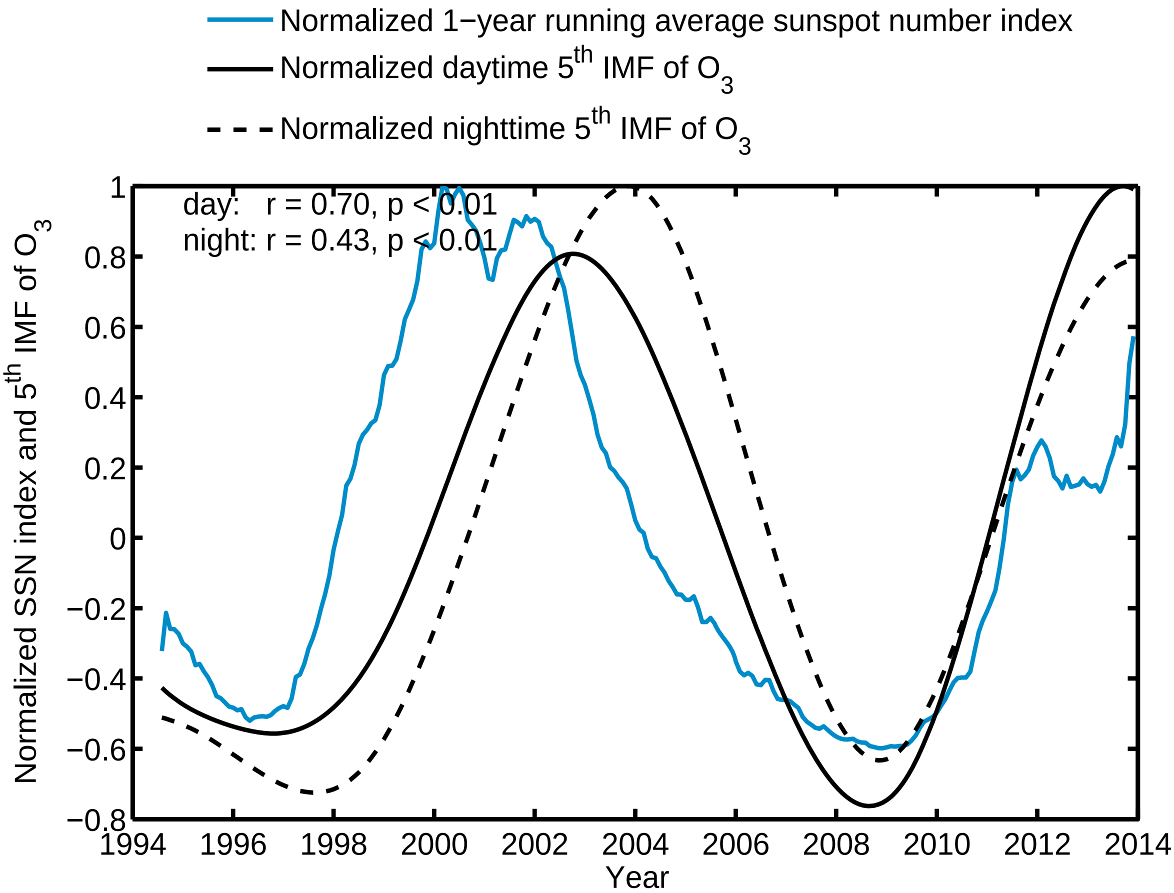

Figure 17 Comparison between the 5th IMF and the 1-year running average SSN during 1994-2013.

5

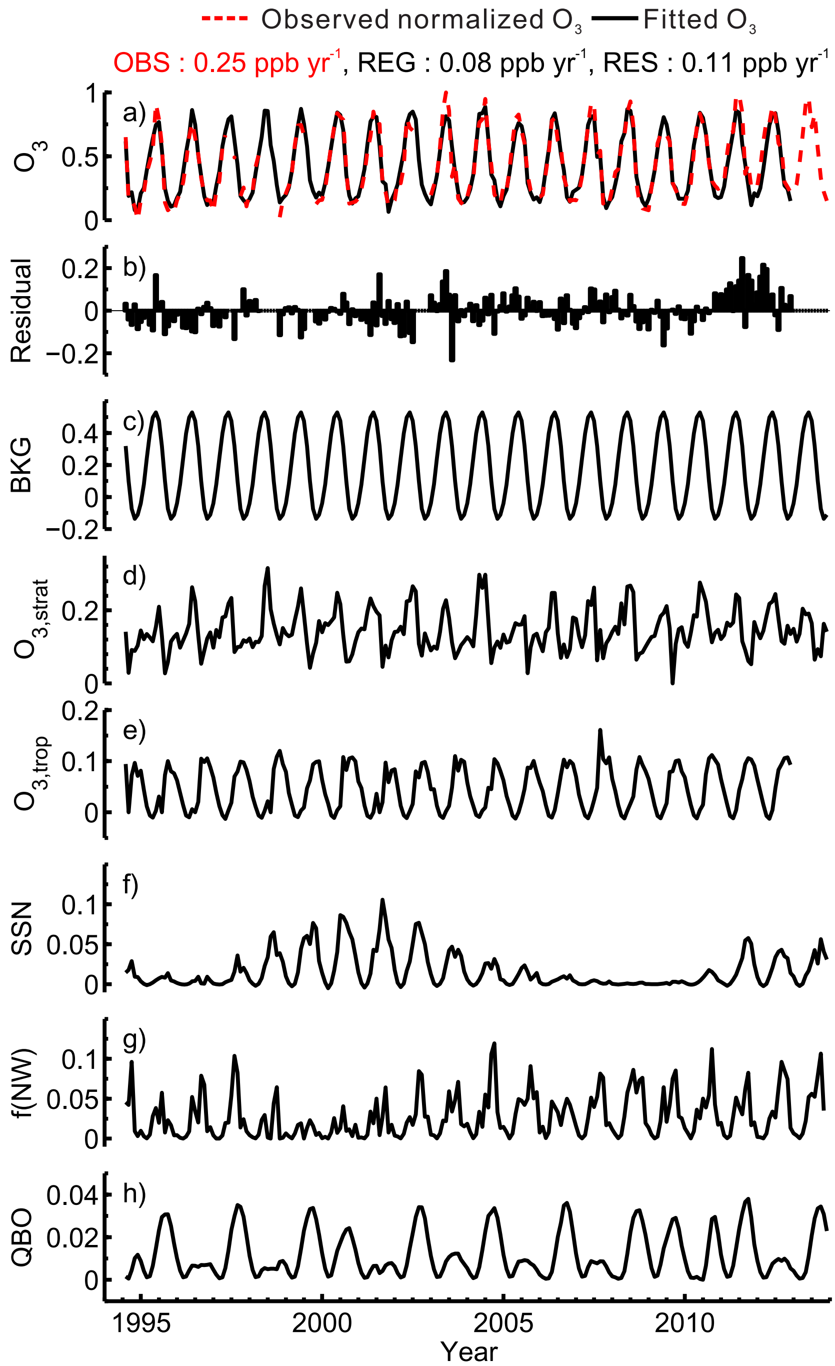

Figure 18 Temporal variation of the a) normalized observed and fitted ozone concentration, b) the residual of the regression, the contribution of c) a background factor and 5 influencing factors to the ozone regression: d) the modelled O_3Strat, e) the contribution of tropospheric ozone transport $O_{3,trop}$, f) the sunspot number, g) the frequency of northwesterly trajectories and h) the QBO index

Supplement

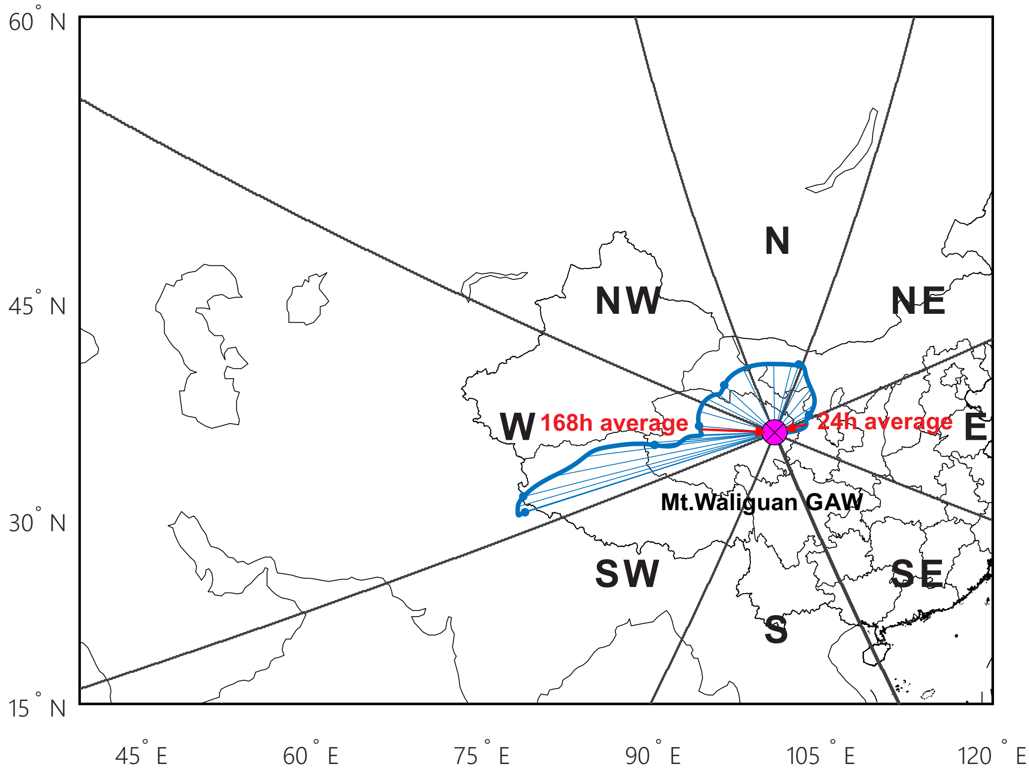

5 Figure S1 Schematic showing an example of the calculation process of 24h and 168h average trajectory directions and the 45-bins the trajectories were clustered into. The blue line shows a 7day trajectory example that bends from W to E, accounting for all the 168 hours, the average direction is westerly, while accounting only for the first 24 hours, the direction is easterly.

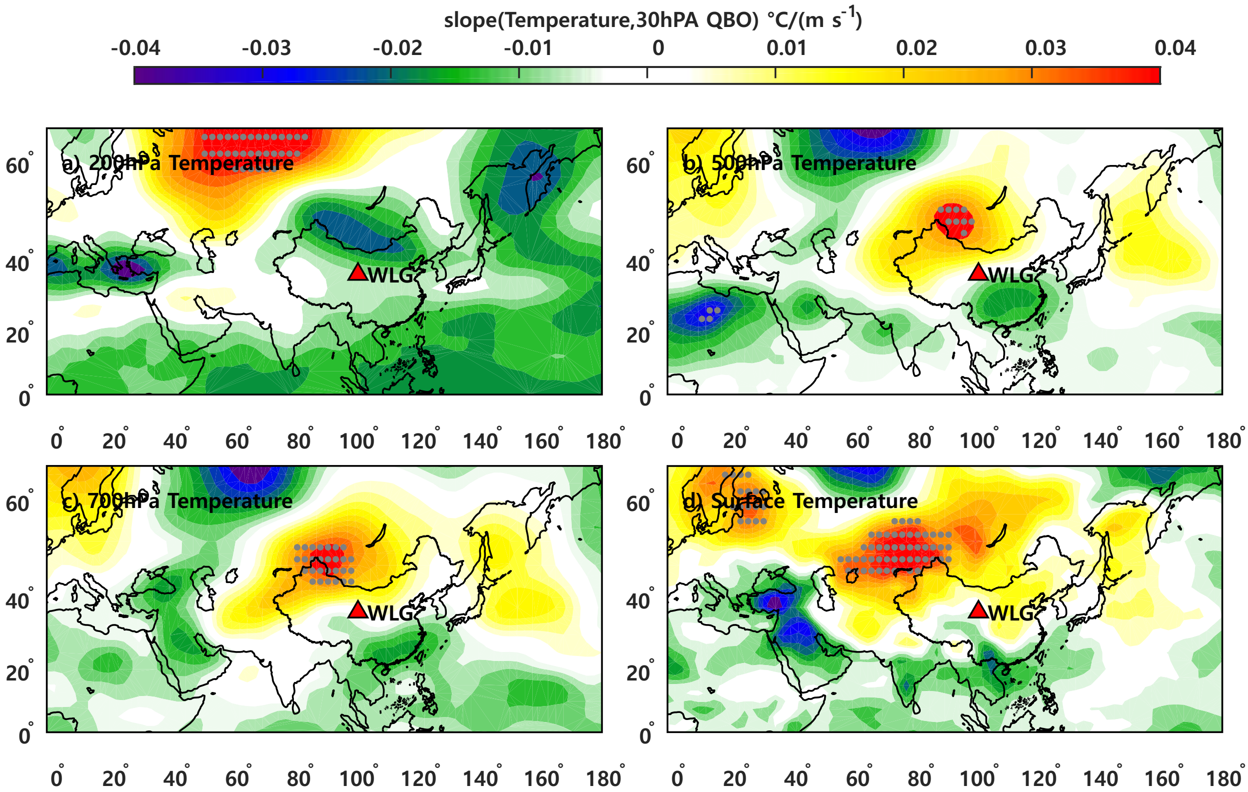

Figure S2 Regression slopes for the correlations between the QBO index and air temperatures at 200 hPa (a), 500 hPa (b), 700 hPa (c) and surface (d), with grey dots indicating the that are significantly correlated ($p<0.05$). The red triangles indicate the position of WLG.

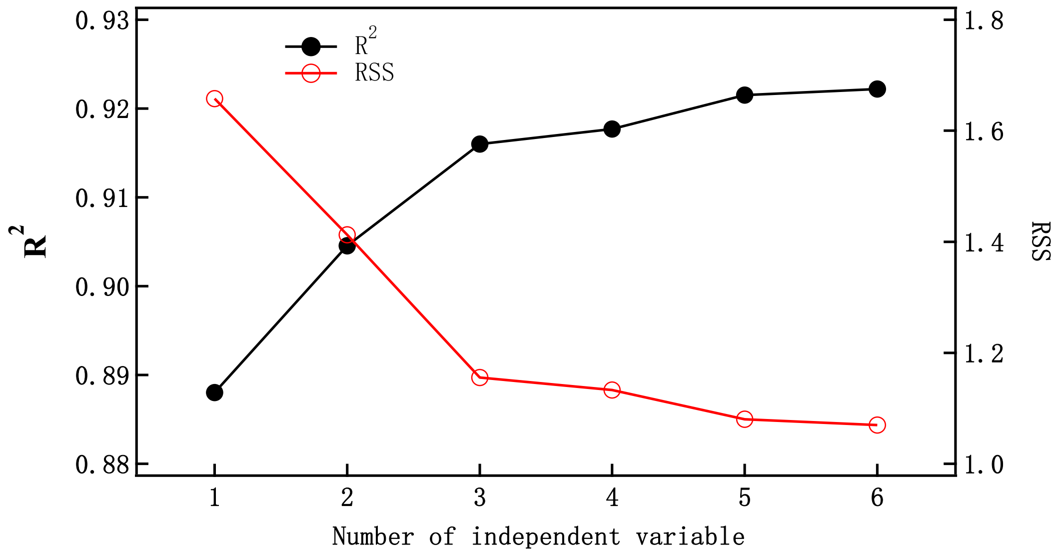

Figure S3 Changes of the coefficient of determination (R^2) and residual sum of squares (RSS) after each step of the multivariate regression.

5